



# PREDIS

## PREDIS – Proceedings of April Workshop 2022

Date 30.9.2022 version Final

Dissemination level Public

**Editors Maria Oksa and Erika Holt**

VTT Technical Research Centre of Finland  
Kivimiehentie 3, Espoo, Finland

[maria.oksa@vtt.fi](mailto:maria.oksa@vtt.fi)

[erika.holt@vtt.fi](mailto:erika.holt@vtt.fi)



This project has received funding from the European Union's Euratom research and training programme 2019-2020 under grant agreement No 945098.



## TABLE OF CONTENTS

1	FOREWORD .....	5
2	OVERVIEW OF STRATEGIC IMPLEMENTATION (WP2).....	7
3	OVERVIEW OF KNOWLEDGE MANAGEMENT (WP3).....	10
4	SCIENTIFIC PROGRESS IN INNOVATIONS IN METALLIC TREATMENT AND CONDITIONING (WP4) .....	13
4.1	Defining Europe-wide Needs and Opportunities for Management of Metallic Waste Streams (Task 4.3.).....	13
4.2	Development and optimisation of decontamination processes (Task 4.4) .....	14
4.2.1	Metallic waste surrogates preparation .....	14
4.2.2	Decontamination of metallic waste using chemical solutions.....	15
4.2.3	Decontamination of metallic samples using a gel technology avoiding secondary liquid waste.....	16
4.2.4	Secondary waste treatment.....	17
4.3	Optimisation of metallic waste characterisation and procedures for waste minimisation and recycling (Task 4.5).....	18
4.3.1	Classification of the metallic waste streams of the different types of reactors .....	18
4.3.2	Characterization and sorting of metallic waste in different management routes .....	19
4.3.3	Development of new radiochemical procedures for DTM radionuclides.....	20
4.4	Encapsulation of reactive metals in magnesium phosphate cement-based matrices (Task 4.6) ..	22
4.4.1	Development of magnesium phosphate cement formulations .....	22
4.4.2	Magnesium phosphate cement cost optimization .....	22
4.4.3	Leaching behaviour of magnesium phosphate cement pastes .....	23
4.4.4	Al corrosion in magnesium phosphate cements.....	23
4.4.5	Steel corrosion in magnesium phosphate cements.....	24
4.4.6	Be corrosion in magnesium phosphate cements.....	25
5	SCIENTIFIC PROGRESS INNOVATIONS IN LIQUID ORGANIC WASTE TREATMENT AND CONDITIONING (WP5).....	26
5.1	Innovations in liquid organic waste treatment and conditioning – overview (WP5) .....	26
5.2	Reference Formulations and Robustness Study Plan (Task 5.3) .....	28
5.3	Study of conditioning matrix performances – Status Update (Task 5.4).....	30
6	SCIENTIFIC PROGRESS IN INNOVATIONS IN SOLID ORGANIC WASTE TREATMENT AND CONDITIONING (WP6).....	32
6.1	Physical and chemical characterization of thermally-treated IERs surrogates .....	32
6.2	Characterization, densification and encapsulation of ashes from incineration of RSOW by IRIS process .....	35
6.3	Synthesis, Stability and Physico-Chemical Characterisation of a Reconditioned Waste Form Relevant to Radioactive Wastes .....	39
6.4	Immobilization of the treated wastes by geopolymer or cement-based materials encapsulation .....	42
6.5	Immobilization of spent salt from MSO process .....	46

6.6	Treatment of surrogate ion exchange resin and conditioning of residues in a novel geopolymer matrix .....	49
6.7	Immobilization of molten salt in alkali-activated and cement-based materials.....	53
6.8	Thermal treatment & wasteform durability at the University of Sheffield (USFD) .....	61
6.9	Physico-Chemical characterisation of reconditioned waste form and stability testing .....	63
6.10	Leaching tests with HIPed ashes .....	66
<b>7</b>	<b>SCIENTIFIC PROGRESS OF INNOVATIONS IN CEMENTED WASTE HANDLING AND PREDISPOSAL STORAGE (WP7) .....</b>	<b>68</b>
7.1	Radiation detection tools for radwaste characterization & monitoring .....	68
7.2	First test of the detection of metal bodies in concrete matrix using the INFN Padova Muon Tomography apparatus.....	74
7.3	Demonstration and implementation of monitoring technologies .....	76

# 1 Foreword

*Maria Oksa and Erika Holt (VTT), maria.oksa@vtt.fi, erika.holt@vtt.fi*

**Keywords:** waste, treatment, predisposal, safety, radioactive, nuclear, science and technology, monitoring, packages, material science

## Status of PREDIS project

The “PREDIS – Pre-disposal management of radioactive waste” project, which started in September 2020, focuses on innovations for new treatments, conditioning, monitoring, characterisation and modelling of low and intermediate level radioactive waste, also making environmental and economic evaluations of them. With 47 seven partners and 25 End User Group members, the PREDIS project has proceeded as planned, supporting the development of the predisposal strategic research and innovation agenda, providing mobility actions to PREDIS partners, advancing the knowledge management and trainings, and making excellent progress in the technical work packages on metallic waste, liquid and solid organic waste as well as cemented waste. After 20 months of project work, the PREDIS community gathered for the Annual Workshop 2022 to share the progress and plan ahead. This report introduces the extended abstracts of presentations given on on Wednesday 27 April, 2022, which was an open day for all interested stakeholders beyond the project consortium.

## PRE-DISPOSAL MANAGEMENT OF RADIOACTIVE WASTE



*Figure 1. PREDIS project in a nutshell.*

## April 2022 Annual PREDIS Workshop

The PREDIS project’s annual workshop was held in April 2022 in Espoo, Finland. This was the first time since the project started in September 2020 when partners could meet physically. This four-day event included a half-day overview session from management and dissemination, strategic implementation and knowledge management points-of-views, one full-day of specific technological work package meetings, one full-day Stakeholder Day open for all and a half-day of excursions. As all partners and interested parties were not able to attend in-person due to the corona pandemic, the workshop was organised as a hybrid event. Almost 150 PREDIS members, of which over 80 were in-person, joined us to present the scientific progress so far, share experiences and meet each other. All members of the PREDIS End User Group were invited to attend the Work Package dedicated sessions and almost 20 external persons participated to these meetings. The open Stakeholder Day gathered and additional twenty interested persons to listen to status updates and the scientific presentations of the technical work packages as well as discuss focus topics within the predisposal strategic research and innovation agenda. At the end of the Stakeholder Day a lively panel discussion took place, where the audience was able to listen in to the views of Finnish and international actors, including waste management experts from nuclear energy companies Teollisuuden Voima Oyj (TVO) and Fortum Oyj, the Finnish Radiation and Nuclear Safety Authority STUK, University of Helsinki and the International Atomic Energy Agency (IAEA).

The annual workshop celebrated the accomplishments of the first year, including the EC's periodic review, the initial set of deliverable reports and the first exchanges of data, samples and researchers between institutes. Collaboration with other parties, including the EURAD project were noted. The event also included time for partners to share about their experiences and network, including preparations for further knowledge management activities of training and mobility. There were special sessions dedicated to the younger and next generation engagement. The tragic situation in Ukraine due to the attack of Russia touches PREDIS project, as two of our partners are Ukrainian (KIPT in Kharkiv and SIIEG NASU in Kiev) in addition to the End User Group member Chornobyl NPP. Viktor Dolin from SIIEG NASU gave a presentation on the very difficult situation of the people and the nuclear energy facilities in Ukraine.

Three optional site-visit excursions were organised to explore facilities relevant to PREDIS, including: 1) the VTT Materials Underground Research Hall with a focus on waste immobilization, geopolymers, monitoring systems, 2) VTT's FiR1 Triga Research reactor decommissioning site focusing on waste characterisation, metallic and concrete waste treatment, digital optimisation, and 3) VTT's Bioruukki Facility to see the waste reduction pilot plant utilising thermal gasification treatment alongside waste characterisation facilities.

This report is the second in the series of *Deliverable 1.5 Technical proceedings of Annual workshops*. The next workshop is scheduled for May 2023, including open public sessions for all interested stakeholders.

More information of the project and its activities can be found in the PREDIS website: <https://predis-h2020.eu/>.

## Acknowledgements

This project has received funding from the Euratom research and training programme 2019-2020 under grant agreement No 945098.

## 2 Overview of Strategic Implementation (WP2)

*Anthony Banford, Aaron Ellis, Linda Fowler, Alan Wareing, NNL, United Kingdom,  
[anthony.w.banford@uknnl.com](mailto:anthony.w.banford@uknnl.com), [alan.s.wareing@uknnl.com](mailto:alan.s.wareing@uknnl.com)*

**Keywords:** Strategic Research Agenda, SRA, End User, Stakeholder Engagement, Predisposal Waste Management

### 1. Introduction

Work Package 2 of PREDIS encompasses a range of strategic activities, including establishing predisposal end user and stakeholder groups, developing a predisposal strategic research agenda, preparing guidance on waste acceptance criteria/systems, lifecycle analysis and project governance. Updates were presented on all tasks within WP2, however the major focus for activity was the development of the PREDIS Strategic Research Agenda (SRA) specific to the needs of predisposal activities. The project intent was to build on available existing research agendas developed by European and worldwide nuclear waste management organisations, fora and governing bodies, identifying topics and themes pertinent to PREDIS. This would then be developed through extensive stakeholder engagement to form the final PREDIS SRA of Predisposal Waste Management before the end of year 4 of the project.

### 2. Ongoing Development of the SRA

In Year 1 – the WP team focused on the consolidation of existing SRAs. A baseline SRA was produced in Month 12 of the project [1]. Year 2 has seen further development of the PREDIS SRA through interactions with the PREDIS End User Group and wider stakeholders. The initial work during year 2 of the project found the project team considering the best engagement approach and the subsequent development of a survey/questionnaire to collate the needs and priorities from the stakeholder community. The engagement approach was devised with the WP2 PREDIS delivery team between December 2021 and February 2022. The aim of the survey was to develop an understanding of the stakeholder priorities for research and the drivers behind these priorities.

The end users were asked to rank their five most important technical topics, and in addition to identify the three most significant drivers; the survey template is shown in Figure 1 with the technical topics on the vertical axis and the drivers on the horizontal axis. The survey was launched on the 23<sup>rd</sup> of March at an online meeting with the end user group.

The initial results were reported back to the end users in a preliminary results session held on 12th April – but the survey remained open. At this point in time the highest ranked technical topics, were:

- Characterisation,
- Waste acceptance Criteria,
- Conditioning and Packaging, and
- (Waste) Treatment/processing.

**Note:** *The survey remained open beyond the workshop to allow other end users to participate, and the ranking is therefore subject to change.*

			DRIVER											
			Societal			Actor Specific				Scientific		Financial		
	Technical Topic	Priority Topics (1- 5)	Economic renewal & growth	Protect citizens & environment	Public trust & confidence	Processes, products & services	Improved performance	Contributes to competences and skills	Improve networks	Science quality and TRL	Innovation	Revenue, turnover	Investment	Sub-areas of key interest
Planning	Inventory	5		X	X		X							Understanding waste inventories from new fuel types.
	Waste Acceptance Criteria			X	X		X							
	Technology Selection					X	X				X			
	Cost Estimating		X									X	X	
	Funding		X									X	X	
Implementation	Waste Hierarchy	2		X	X		X							Waste tracking strategies. Waste segregation techniques.
	Characterisation	1			X		X				X			Remote characterisation. Physico-chemical characteristics
	Treatment Processing	4		X		X				X				Decontamination best practice.
	Conditioning & Packaging			X		X				X				
	Storage			X			X						X	
Operations	Transport				X	X			X					
	Deployment Options		X	X				X						
	Quality & Management Systems				X		X			X				
	Commissioning			X			X	X						
	Optimisation	3				X	X					X		Synergy between new and existing technologies
	Secondary Waste Management			X	X		X							
	R&D		X								X		X	
	Knowledge Management						X	X	X					
	Stakeholder Engagement				X		X		X					

**Figure 1. Illustration of the topic and driver matrix used in the survey**

Table 1 shows the key themes emerging from the survey at this early stage alongside the key themes identified in the consolidated baseline SRA [1]. There is some commonality between the two although differences in language and specificity are recognised and were to be expected.

During the April workshop, breakout sessions were held on these four topic areas: Characterisation, WAC, Conditioning & Packaging, and Treatment/Processing. The focus of these sessions was on exploring the following questions:

- What is the key research issue beneath the main topic area that is of high interest and importance?
- Why is it important / what is its impact?
- When does this need to happen (urgency)?

The outputs of these sessions will feed forward into the draft SRA. However, the process of user engagement remains ongoing with further user input anticipated through the survey/questionnaire and a series of facilitated 'virtual end user workshops' on the technical themes. This will form the basis of the PREDIS SRA, with a draft to be produced in 2023 and final version in 2024.

**Table 1. Key themes from the early questionnaire responses with those from the baseline SRA**

Topic	Key themes from questionnaire responses	Key themes in Baseline SRA
Characterisation	<ul style="list-style-type: none"> <li>• Material/physical/chemical/non-radiological characterisation</li> <li>• Economic aspects - economically viable approaches, simplification of processes to optimise cost/time, optimise number of samples</li> <li>• Radiological characterisation - New radiological characterisation approaches, characterise nuclides in the waste</li> <li>• Assurance - Robustness and fitness for purpose of characterisation methods, representativeness</li> <li>• Data handling, statistical methods (sampling), dealing with uncertainties</li> </ul>	<ul style="list-style-type: none"> <li>• Characterisation of chemical components of waste inventory and associated wastefoms (chemotoxic, physico-chemical properties, including organics)</li> <li>• Characterisation of wastes from advanced fuels and fuel cycles</li> <li>• Effective plant characterisation and tools for analysis and visualisation</li> <li>• Characterisation of legacy and problematic wastes</li> <li>• Cost-effective technologies for radiological characterisation of wastes for countries with small amounts of waste</li> </ul>



Waste Acceptance Criteria	<ul style="list-style-type: none"> <li>• Implications for long-term safety - input to long-term safety assessments, waste evolution, gas generation, long-term safety of innovative matrices</li> <li>• Specific waste types - reactive metals, heavy metals</li> <li>• Establishing WAC - generic criteria without a facility, adapting existing WAC for different/new types of wastes</li> </ul>	<ul style="list-style-type: none"> <li>• Good practice guides for derivation of WAC</li> <li>• WAC for thermally treated products (characterisation requirements, context-specific criteria)</li> </ul>
Conditioning Packaging	<ul style="list-style-type: none"> <li>• New and alternative options - new matrices, package development, new waste streams, reversible packaging, green packaging, re-conditioning</li> <li>• Cement materials and encapsulation techniques</li> <li>• Resins, PVC, aluminium, organic liquids</li> </ul>	<ul style="list-style-type: none"> <li>• Novel conditioning technologies to address problematic wastes (ion exchange resins, tritiated wastes, I-129, sealed sources, Pu residues, bitumen sludges)</li> <li>• New materials as conditioning matrices (e.g. geopolymers)</li> <li>• New materials and components for containers</li> <li>• Optimisation of containers (safety, handling, costs, robustness)</li> <li>• Demonstration of container fabrication and operation at full-scale/industrial scale</li> <li>• Long-term performance of container materials</li> <li>• Knowledge exchange regarding management of damaged or degraded waste packages</li> </ul>
Treatment Processing	<ul style="list-style-type: none"> <li>• New treatment technologies</li> <li>• Technologies for complex wastes (e.g. organic, reactive wastes)</li> <li>• De-categorisation, recycling</li> <li>• Waste volume optimisation</li> </ul>	<ul style="list-style-type: none"> <li>• Need for a variety of treatment processes (flexibility/adaptability)</li> <li>• Understanding best practice in decontamination technologies</li> <li>• Alternative and novel treatment technologies</li> <li>• Optimisation of treatment processes</li> <li>• Knowledge exchange and transfer</li> </ul>

### 3. Way forward

Work on the PREDIS SRA will continue with extensive End User engagement, with the aim of producing a comprehensive draft Predisposal SRA in Spring 2023 for peer review. Beyond the SRA, work continues in PREDIS WP2 on developing guidance on waste acceptance systems/criteria which will be published later in 2022 and on the development of bases for the life cycle assessment case studies for WP4-7.

### Acknowledgements

This project has received funding from the Euratom research and training programme 2019-2020 under grant agreement No 945098.

The authors would like to acknowledge the contributions made by all PREDIS Work Package 2 participants and all who have contributed as Partners, End Users or Stakeholders.

### References

- [1] A. Wareing, L. Fowler, A.W. Banford, Baseline Strategic Research Agenda, [https://predis-h2020.eu/wp-content/uploads/2021/08/PREDIS-T2.2\\_Baseline-SRA\\_M2.3\\_August-2021.pdf](https://predis-h2020.eu/wp-content/uploads/2021/08/PREDIS-T2.2_Baseline-SRA_M2.3_August-2021.pdf), 2021

### 3 Overview of Knowledge Management (WP3)

#### 1. Introduction

The identification, assessment, structuring and dissemination of past and present knowledge of predisposal R&D activities accumulated within the European Commission R&D programmes as well as international and national radioactive waste management organisations, is of vital importance for early-stage radioactive waste management programmes, advanced programs and future generations. It is the objective of this work package to provide access to this knowledge in a systematic and structured way to the participants of the PREDIS beneficiaries and later to the European predisposal community. The knowledge management (KM) work performed within this work package is aligned with the KM activities in the Joint Programme on Radioactive Waste Management (EURAD). The KM WP will make use of the vast amount of knowledge and expertise existing in the PREDIS R&D WPs. The PREDIS KM work package is divided into four tasks to meet its objective.

1. Development of Knowledge management programme
2. State of knowledge
3. Developing and implementing training programme
4. Implementing a mobility programme

#### 2. Description of work and main findings

**State-of-Knowledge Task** is namely focused to develop Domain Insight (DI) documents to populate the PREDIS roadmap. It was identified that the DI documents contain a part that requires from the DI author to identify needs for further R&D. This part could be used as an input to the PREDIS strategic research agenda (SRA) that is in preparation by WP2 'Strategic Implementation'. A streamlining will be necessary to have coherence on these two PREDIS outputs. Unfortunately, the timing is off as the DI production will be finalised after the discussion of the SRA. Nevertheless, WP2 and WP3 will start to align the identifications of these future R&D needs, for predisposal activities, with those DI produced before the final SRA.

It was also clear from the discussions that the response rate on the end-users feedback on SRA was only 26%. WP3 identified a similar problem when getting response from end-users engagement for DI document authoring. Since the persons answering WP2 SRA questionnaire and authoring the DI has the similar expert knowledge in the end-user organisation it was proposed to make an effort to identify these persons in each end-user and PREDIS partner organisation. Having such a list would make it easier to send targeted questionnaires, receive one answer per organisation and coordinate the number of questionnaires sent from PREDIS to the end-user organisations. It was proposed to work along the following lines:

- To work on the authoring list. To find the strategic person for each topic.
- Same author could collaborate on the DI, SRA and Gap Analysis
- End-user engagement webinar to handle all: PREDIS, DI, SRA, EURAD
- Timing is off, SRA comes before the DI
- Course on LCA will be organized by 2023

**Training of young professionals** (including PhD/PostDocs and trainees) is crucial for the PREDIS project. The implementation of training activities allows newcomers and new generations to acquire the level of knowledge needed to develop a professional career in the different subjects related to the predisposal of radioactive waste.

**Training in PREDIS** included 11 webinars by April 2022, including 8 EURAD webinars. Mean registered number was 170, mean attendee number was 120. The ranking of interest (n° of att.) is following:

1. Waste Acceptance Criteria (WAC) 1 – 177 att.
2. Innovations in liquid organic waste treatment and conditioning – 124 att.
3. Waste Acceptance Criteria (WAC) 2 – 119 att.
4. Innovations in solid organic waste treatment and conditioning – 113 att.

The planned EURAD Lunch&Learn since April 2022 sessions were proposed as following

2. **27th April:** Knowledge Management in the German NWMO (BGE) – Origin, approach and practical implementation
3. **19th May:** Deep Borehole Repository of high-level radioactive waste – State of knowledge and pros&cons
4. **28th September:** A pluralistic tool of dialogue on RWM: the Pathway Evaluation Process (PEP)

Next announce PREDIS courses were Overview of PREDIS, held online on June 9 -10 2022; then LLW/ILW course, held in UJV Rez on September 8- 9 2022 in joint effort with the Student meeting, and Course of Waste characterisation, prepared in CIEAMAT for November 2022.

As a part of educational activities WP3 launched games dedicated to PREDIS content and goals (see the example on Figure 1 below). The games will be published periodically on the PREDIS web site.

### Wordle by PREDIS

*Try to guess the word!*



**Figure 1.** An example of PREDIS Games.

WP3 launched **PREDIS Student group** where 35 students from all WPs were organised (KPI being 20 students).

The Student group organised an individual meeting where students made a basis to organise themselves. The following main issues were discussed and decided upon:

- Communication with the WP leaders via email
- The students will provide more feedback when they know better each other, and could talk through this within their complete student group
- Training requests:
  - o Regulatory issues at a high level
  - o Shipping of radioactive material (DI on transport lecture)
  - o How data management is being done?
- The students do not want to connect their network directly with the EURAD student network, but would like to be able to attend EURAD training events
- They also tried the games and found them quite ok
- They will communicate through WhatsApp network
- WP3 would like to engage students to their activities
- Students might contribute to the newsletter; they can have one column for their purposes

**The PREDIS mobility programme** aims at facilitating cooperation between partners and Member States, and the acquisition of knowledge needed to develop a professional career in the different subjects related to the predisposal of radioactive waste. **Mobility portal** is available on <https://pro.evalato.com/3346> and has been opened since September 1, 2021. Mobility programme is framed by Mobility manual that is available on the following [link](#). Until April 2022, 14 mobilities has been submitted, including 2 large mobilities for 3 Ukrainian partner persons – see the Figure 2. All the submitted mobilities has been approved by General assembly.

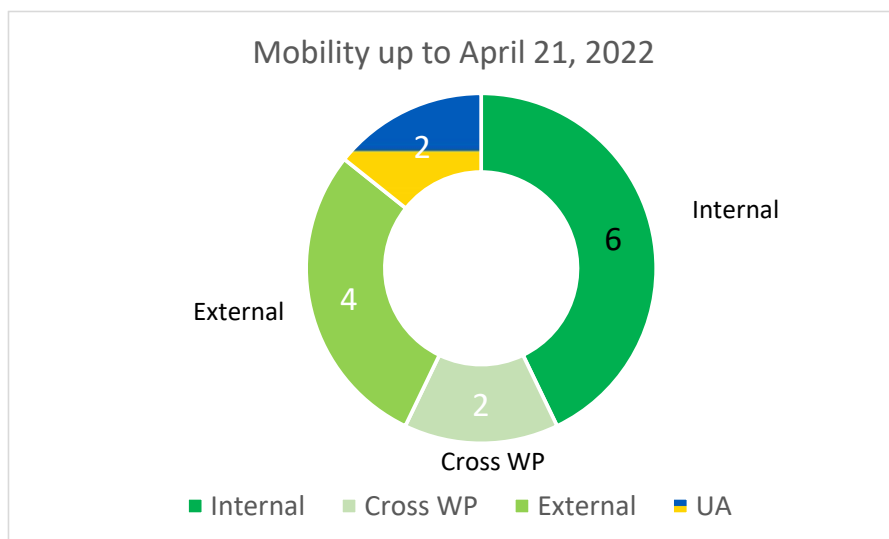


**Figure 2.** PREDIS Mobility approved by April 2022.

WP3 cooperates closely with both Management team and WP leader and representatives of young generation in order to organise and lead WP3 content toward planned goals and general effectiveness.

## 4 Scientific progress in Innovations in metallic treatment and conditioning (WP4)

PREDIS project is developing technologies for treatment and conditioning of radioactive waste such as metallic waste as well as radioactive organic waste whether liquid (RLOW) or solid (RSOW). In WP4 we focus our effort on steel and Ni-alloys radioactive metallic waste, which are major components in nuclear installations. These metallic wastes are often surface-contaminated in the form of corrosion layers of a few tens of micrometers retaining radionuclides including but not limited to activation corrosion products (Co-60, Ni-63, Fe-55) and fission products such as Cs-137.

### 4.1 Defining Europe-wide Needs and Opportunities for Management of Metallic Waste Streams (Task 4.3.)

*Jenny Kent, Adam Fuller, Tim Harrison (Galson Sciences Ltd, UK)*

#### 1. Introduction

Task 4.3 is focused on understanding needs and opportunities for managing metallic radioactive waste. Decommissioning of the current fleet of European civil nuclear power plants is expected to generate thousands of tonnes of radioactive metallic waste. Therefore, we need to develop more effective decontamination and remediation processes for metallic wastes, as well as optimising routes for recycling and reuse.

The presentation summarised work completed to date, including:

- An inventory of metallic waste streams in Europe [1].
- Technology datasheets for metallic waste decontamination processes [2].
- Identification, measurement and management approaches for secondary wastes to inform optimisation of metal decontamination processes [3].

#### 2. Description of work and main findings

An inventory of metallic waste streams has been completed [1]. This found steel to be the dominant metallic waste with an even distribution between current and future arisings. Activated waste represented around 70% of the total volume produced.

WP4 is aiming to develop and optimise decontamination technologies for treatment of metallic waste. A series of datasheets have been created for different metal treatment and decontamination technologies, including jet washing, chemical washing, laser decontamination, plasma melting, induction melting, electrochemical decontamination, Chemical Oxidation Reduction Decontamination (CORD) and Metal Decontamination by Oxidation with Cerium (MEDOC) [2].

An important component of the optimisation process is increasing the process efficiency and reducing secondary waste arisings (including direct and indirect contamination). It is important that all secondary wastes are measured accurately during the experimental programme. To help judge whether a technique is optimal, it is necessary to measure the types, volumes and activities of secondary waste generated, any need for further treatment and the management routes available for these wastes [3].

In future, once experimental work has been completed within WP4, information on secondary wastes and the economic and environmental impacts of these technologies will be gathered to feed into future work on Task 4.3.5 (Economic and environmental impacts of decontamination and metal melting) and interactions with Lifecycle Analysis (LCA) work being undertaken in WP2.

## 4.2 Development and optimisation of decontamination processes (Task 4.4)

### 1. Introduction

Task 4.4.2 is focused on understanding optimization techniques for the decontamination of metallic radioactive waste. Decommissioning of the current fleet of European civil nuclear power plants is expected to generate very large quantities of radioactive metallic waste. Therefore, there is a need to improve the decontamination processes for metallic wastes, and the associated secondary effluents with a goal to be able to recycle the metals in order to promote the concept of circular economy through LCA routes, whilst accounting for the Waste Acceptance Criteria (WAC).

The presentation summarised work completed to date, including:

- Decontamination strategy to be used as a guideline.
- Characterization of surrogate samples used for testing of decontamination techniques.
- Identification of decontamination techniques selected for testing and the parameters which can affect efficiencies.
- Demonstrated the efficacies of different conditions, which show promise in decontamination of such metals.
- Demonstrated the associated treatment techniques for the secondary liquid effluents generated.

### 2. Description of work and main findings

#### 4.2.1 Metallic waste surrogates preparation

*Richard Katona (SORC, Hungary), Thomas Carey (NNL, UK)*

Different types of Ni-alloys are the main structural materials in pressurized water reactors (PWR). Austenitic stainless steels are typically used in the structure of the reactor, the pressurized boundary piping and Inconel alloys are applied in steam generator tubing. Under normal conditions of a nuclear reactor the surfaces of these metals oxidize and form a radioactive corrosion layer [1-2]. From radiation protection issues, safe, effective, easy feasible and low-waste decontamination technology is fundamental [3]. In this part of PREDIS Project representative non-radioactive metal samples with corrosion layers are produced in the laboratory. Thanks to it, a lot of optimisation tests of decontamination technologies can be carried out without having radiation protection issues. The samples are used by IMT Atlantique Subatech Laboratory and CEA. Furthermore, the electrochemical behaviour of oxide-layer was investigated too by SORC.

To form a representative, non-radioactive corrosion layer in the laboratory the metal samples are heated up to high-temperature and oxidised in water vapour. The schematic flow diagram of the equipment can be seen on Figure 1. The surface of carbon steel, stainless steel 1.4571, inconel 690 and 600 were oxidised. Before the oxidation process the surfaces of the metal samples were cleaned by sand-blasting technology, water - and acetone washes. The structures of the formed oxide-layer were analysed in the IMT Atlantique Subatech Laboratory.

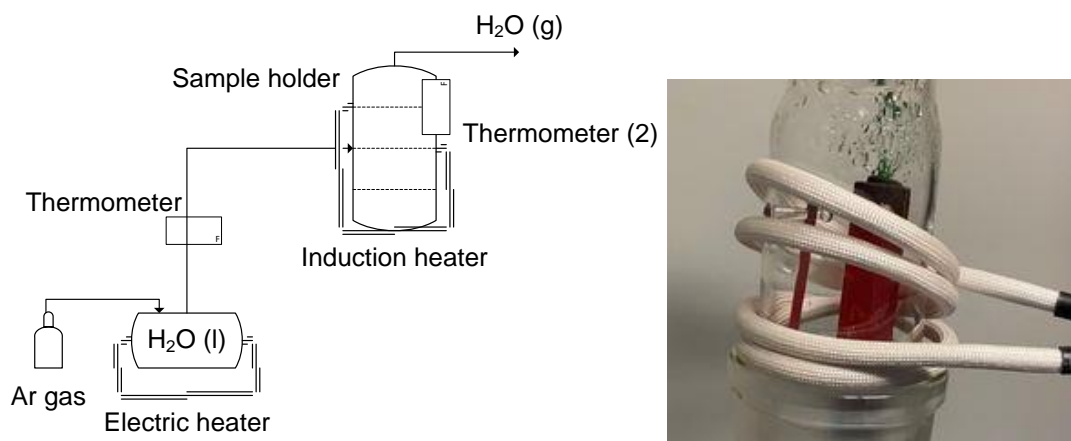


**Figure 1:** Schematic flow diagram and picture of the laboratory equipment.

Figure 2 shows the oxidised and the clear metal samples.





**Figure 2:** The picture of the oxidised – and pristine samples.

As a second step, electrochemical test were carried out with the clear- and oxidised metal samples in a standard three-electrode cell, which consists of RADELKIS OP-0830P saturated calomel reference electrode (SCE), stainless steel counter electrode, the metal samples as working electrode. The electrolyte was 5 g/dm<sup>3</sup> KMnO<sub>4</sub> and 10 g/dm<sup>3</sup> NaOH solution (alkaline treatment of AP-CITROX decontamination technology). The reaction rate was determined by TAFEL-analysis. The results are shown in Figures 3-4.

#### 4.2.2 Decontamination of metallic waste using chemical solutions

*Aditya Rivonkar, Tomo Suzuki-Muresan, Abdessalam Abdelouas, Marcel Mokili, (IMT Atlantique, France), Alban Gossard (CEA, France), Richard Katona (SORC, Hungary), Thomas Carey (NNL, UK)*

A thorough study of some of the existing decontamination techniques was carried out and after considering different parameters with a special emphasis on WAC, two techniques were chosen for further study and testing, with some parameters identified which could play a significant role in the efficiency of these processes and the secondary wastes they generate. The selected processes were Chemical Oxidation Reduction Decontamination (CORD) and Metal Decontamination by Oxidation with Cerium (MEDOC).

Surrogate samples are being prepared by SORC (Hungary) for testing the efficiencies of these processes under the various parameters. A thorough characterization of these samples using various techniques such as X-Ray Diffraction (XRD) and Scanning Electron Microscopy (SEM) to ensure the samples on which tests are being carried out are an accurate representation of the metals being utilized in NPPs (Figure 3). A series of tests using the CORD process at different concentrations and the process showed great potential at high concentrations but also at low concentration albeit at the expense of increased number of cycles. A second round of characterization was carried out after the treatment to verify the efficiency of these processes in dissolving the corrosion layer, wherein would lie the majority of the radioactivity.

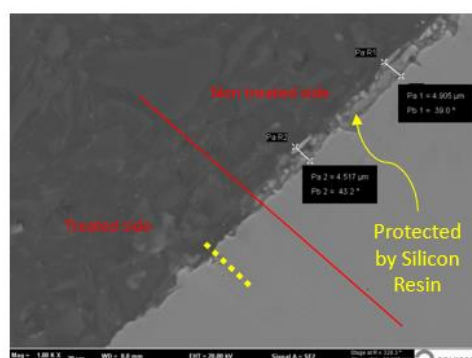


**Figure 3:** SEM image of a treated sample showing the effects of treatment on the contaminated oxide layer as compared to without treatment.

It is not only important for the optimisation to increase the process efficiency but also to reduce the secondary waste arisings (including direct and indirect contamination). A detailed plan was put forward to treat the effluents of the CORD process using precipitation and co-precipitation to extract the dissolved metallic ions in the form of hydroxide precipitates, which can be conditioned, thereby reducing the volumes of resins utilized.

The methods are following the guidelines proposed through the WAC, but also discussions are taking place with WP2 members on the Life Cycle Analysis (LCA), to estimate the environmental impact of these processes. It is utmost importance to not only reduce the amount of waste sent to waste repositories but also to reduce the environmental footprint of all the process being utilized.

## Acknowledgements

Thanks to Richard Katona (SORC) for providing the surrogate samples for the tests and Marion Allart (IMN) for all her support and guidance for the SEM characterization of the samples.

### 4.2.3 Decontamination of metallic samples using a gel technology avoiding secondary liquid waste

*Alban Gossard (CEA, France)*

Inorganic self-drying gels is a decontamination technology developed at the CEA, France [1]. Such gels are composed of mineral colloidal particles (typically silica or alumina) dispersed in a decontaminating solution. The gel adheres to surfaces, which induces a prolonged contact between the surface and the decontaminating solution. This solution is specifically chosen to attack the substrate down to few microns and then release incrustated contaminants, which are then absorbed into the gel. Finally, the gel dries and fractures into a non-powdery solid trapping the contamination that is readily removable by brushing or vacuuming. The main advantage of this process is that only an inorganic solid is produced as secondary waste.

In this study, different acidic-based gel formulations, containing silica as a viscosing agent, were tested on stainless steel coupons (see Figure 4, left). After deposition of a gel layer on the coupon, drying and elimination of the solid residues, the corrosion efficiency was determined by gravimetric measurement. The best formulation, containing nitric acid and Ce(IV), proved to corrode around 0.24  $\mu\text{m}$  of the stainless steel surface.

This operation was also performed on a complex geometry item (in stainless steel) by dipping it in a bath of gel (Figure 4, right). Noteworthy the gel formulation was modified to present adapted rheological properties for a perfect cover of the complex geometry by the gel, especially in the tiny interstices. The corrosion efficiency was also evaluated between 0.2 and 0.3  $\mu\text{m}$ .



**Figure 4:** Corrosion of a stainless steel plan coupon by gel deposition (left) and a stainless steel complex geometry item using a bath of gel (right).

As a perspective, this gel technology is going to be tested on simulated oxidized metallic samples developed by SORC, Hungary. Corrosion of oxidized stainless steel, carbon steel and Inconel Alloy 600 coupons will be performed using inorganic gels containing nitric acid and Ce(IV). The coupons will be finely characterized using XRD and SEM measurement and the corrosion efficiency of the gel will be compared with other decontamination technologies developed at IMT Atlantique, France.

## References

- [1] A. Gossard, A. Lilin, S. Faure, "Gels, coatings and foams for radioactive surface decontamination: State of the art and challenges for the nuclear industry", **Progress in Nuclear Energy** 149 (2022) 104255



## 4.2.4 Secondary waste treatment

*Martin Straka (UJV-Rez, Czech Republic), Mathurin Robin, Tomo Suzuki-Muresan, Abdessalam Abdelouas, Marcel Mokili, (IMT Atlantique, France)*

UJV's activity within the Task 4.4 was focused on experimental study of electrochemical behavior of several elements in so-called 2<sup>nd</sup> generation ionic liquids (defined especially by hydrophobicity, usable under normal atmosphere). In particular, uranium, cobalt, europium and several other lanthanides were studied in ionic liquids (IL) with bis(trifluoromethanesulfonyl)imide anion (TSFI).

For all main elements (U, Co, Eu), electrochemical potentials of their reduction to the basic state were defined (see Figure 5). It was found that TSFI anion has electrochemical window wide enough to reduce these elements to the metallic state and electrolytic experiments were successfully conducted leading to compact deposits (Figure 6).

These results can be further used in drafting both primary and secondary waste decontamination flow-sheets.

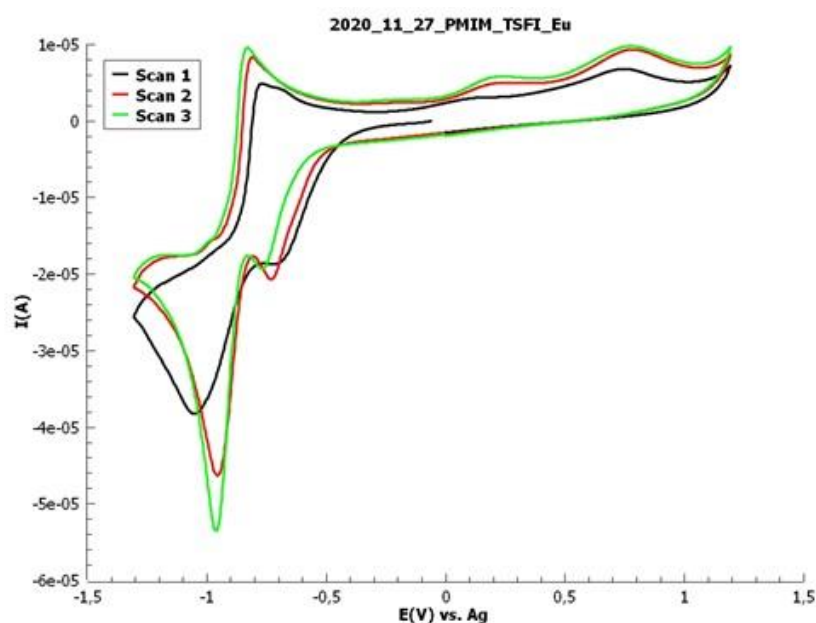


**Figure 5:** Cyclic voltammogram of Eu in bis(trifluoromethanesulfonyl)imide based ionic liquid, platinum working electrode, Ag reference electrode, scan rate 50 mV/s.

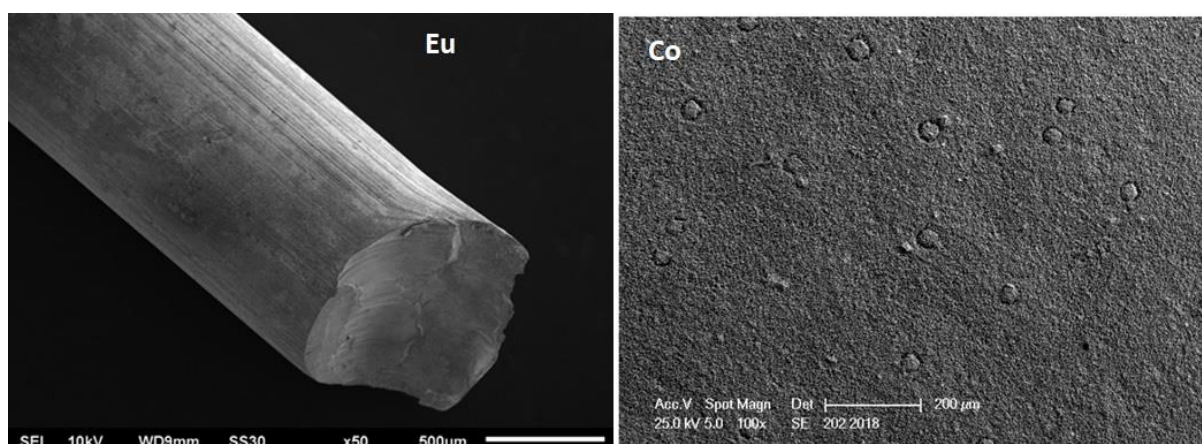


**Figure 6:** Deposited layer of Eu and detail of compact deposit of Co on Pt electrode.

## 4.3 Optimisation of metallic waste characterisation and procedures for waste minimisation and recycling (Task 4.5)

### 4.3.1 Classification of the metallic waste streams of the different types of reactors

*Rita Plukiene, Artūras Plukis, Elena Lagzdina, Marina Konstantinova (FTMC), Anastasia Savidou (NCSR), Marie Charlotte Bornhöft (DMT)*

#### 1. Introduction

Metallic radioactive waste (MRW) with a wide list of radionuclides of different concentrations is one of the important issues for every nuclear power plant under decommissioning dealing with the radioactive waste management and final disposal. The best practice is needed for optimized waste classification including the quantification of specified radionuclides but also for assessment of activity reduction and declassification possibilities in the waste materials before placement in the specific disposal sites. The classification of the metallic radioactive waste (MRW) streams is changing together with MRW activity: the higher activity RW (HLW, ILW) needs classification related to radioprotection and best packaging concept, LLW and VLLW needs decontamination and clearance or declassification afterwards to meet the WAC of the disposal site.

#### 2. Description of work and main findings

In a pre-dismantling stage, the classification of MRW using modelling by obtaining neutron activation map in the 3D of reactor core and peripheral hardware is overviewed and analysed. The different complicity 2D-3D models of the reactors are used for assessment of radioactive metals activation by the neutron flux in the different Nuclear Power Plants (NPP) [1,2]. The deterministic and Monte Carlo modelling methods and code packages are chosen depending on the research needs and the goal of the particular investigation. In all cases the modelling should be validated by the actual experimental data, to ensure that the considered model is an accurate representation of the real reactor construction. The validated calculation models serve as a guiding tool for pre-dismantling characterization of the metallic waste without costly and complicated experiments. Overview of simulation models used for the neutron flux distribution in a 3D reactor core calculation with presentation of real examples of activation of the reactor materials (RBMK, PWR, BWR).

In a second stage, detailed characterization of MRW during dismantling via experimental measurements applying non-destructive and destructive measurement techniques (analysis of measurement results of the samples) should be performed. Study of surface and volume activity discrimination by non-destructive gamma measurement in metallic waste was performed according to peak shape/intensity and Compton/peak ratios.

The determination of Nuclide Vectors (NV) for MRW stream is performed by combining of modelling and measurements for separation of activation zones and identification of key and difficult to measure (DTM) nuclides. Optimized NV is obtained by analysing and systemizing the information about radioactive metallic waste streams, identifying the optimal list of relevant radionuclides, describing inter-correlations between key nuclides and difficult to measure nuclides including multivariate analysis of the already measured data at the sites and numerical analysis of activation and contamination parts for the waste streams.

#### 3. Conclusions

In the frame of PREDIS project in the WP4 4.5.1 subtask we are developing an optimized scheme for classification of the reactor metallic materials regarding the level of activation and contamination. As the methodology for characterization of the metallic waste is similar to all reactors and is based on nuclide vector (NV) determination our main attention is paid to optimized separation of neutron activation and surface contamination activity parts by applying both modelling and measurement techniques (WP4 4.5.2 subtask) and by analysing and systemizing the information about radioactive metallic waste streams. Especially it is important to take into account the possibility of clearance after implementation of a specific decontamination process (e.g. a sand blasting, melting, radiochemical treatment (WP4 4.5.3 subtask.)). NV optimization could serve also for improvement of WAC for specific landfill if taking into account MRW activation and surface contamination terms, peculiarities of nuclides (waste form/matrix/radiotoxicity etc.) and also merging/separating different reactor systems according to measurements results and analysis. At the end of the project recommendation for optimized classification of the metallic waste including assessment activation and surface contamination activity terms, estimation of possibility of decontamination: clear or declassify the waste stream will be assessed.

## References

- [1] Remeikis V., Grineviciute J., Duškesas G., Juodis L., Plukienė R., Plukis A., Review of modeling experience during operation and decommissioning of RBMK-1500 reactors. II. Radioactive waste management, Nucl. Eng. Des. 380 (2021) 111242.
- [2] Schlömer L., Philippen P-W, Lukas B., Activation calculation for the dismantling and decommissioning of a light water reactor using MCNP™ with ADVANTG and ORIGEN-S. EPJ Web of Conferences 153, (2017) 05020.

### 4.3.2 Characterization and sorting of metallic waste in different management routes

*Fabiana Gentile, Filippo Gagliardi, Giulia Colavolpe (NUCLECO), Joerg Feinhals, Marie-Charlotte Bornhoeft (DMT), José Luis Leganés Nieto, Diego Espejo Hernando (ENRESA), Rita Plukiene, Elena Lagzdina (FTMC)*

#### 1. Introduction

The characterization of metallic waste from nuclear facilities aims to help decision whether decontamination is needed (clearance criteria haven't been met and can be met after decontamination) as well as to select the most efficient decontamination process. The main management routes for metallic waste are: 1) general clearance; 2) specific clearance for disposal at a landfill; 3) specific clearance for melting; 4) melt inside a controlled area and clear; 5) controlled reuse for other purpose; 6) controlled melting for shielding or cask production; 7) wait and clear; 8) disposal as radioactive waste. For characterization the scaling factors should be determined by sampling and then measurement by a non-destructive technique is carried out. In the frame of this subtask the scaling factor approaches in different countries is discussed and a new non-destructive  $\gamma$ -spectrometry set up is proposed for reduction of the measurement uncertainties. Furthermore, spectrums are produced by MCNP simulations and compared with experimental spectrums. The information we get from the comparison of the spectrums will be used for better characterization of the metallic waste.

#### 2. Description of work

For the non-destructive gamma spectrometry measurements, the metallic segments are put in a shallow box 1.2m x 1.2m. The box is divided in four squares and four detectors are put above each square at the middle at 0.6 to 0.8 m from the bottom of the box.

In addition to the previous work done the following is investigated: 1) the measurement of convex pipes and convex surfaces; 2) the degree to which the thickness of the sections affects the result of the measurement; 3) the degree to which the orientation of the sections inside the box affects the result of the measurement; 4) the degree to which a half-full box (i.e. if some segments are missing) would affect the measurement result. Moreover, spectrums of Co-60 and Cs-137 point sources as well as Sr-90/Y-90 surface source were produced by simulations and compared with the corresponding experimental spectrums.

#### 3. Conclusions

So far the significant reduction in measurement uncertainty, i.e. uncertainty less than 30%, can be generally achieved, while the sensitivity is sufficient for acceptable measuring time (i.e. less than 20min for 1Mg of metallic waste). Furthermore, simplified geometries could replace the real geometries of the source, making the non-destructive gamma spectrometry measurements more user friendly. Regarding the comparison of spectrums, the qualitative agreement between the simulated and experimental spectrums was achieved. Quantitative comparison of spectrums of simulated and real spectra in case of complex geometries of the sources with multiple radionuclides will be carried out.

## References

- Havenith (2019) Atw. Internat. Zeitsch. fuer Kernn, vol. 6, no. 3, pp. 160-166
- Savidou and Stamatelatos (2010), vol. 25, no. 2, pp. 133-137
- Metwally et al. (2004) "Gaussian broadening of MCNP pulse height spectra," Transaction of the American Nuclear Society

IAEA (2003), "MCNP - A General Monte Carlo N-Particles Transport Code, Version 5," Vol. 1 LA-CP-03-0245, vol. II: User's Guide

Shiba et al. (2017) Energy Procedia, vol. 131, pp. 250-257

### 4.3.3 Development of new radiochemical procedures for DTM radionuclides

*Anumaija Leskinen, Tommi Kekki (VTT), Mojmír Němec, Kateřina Čubová (CTU), Tomo Suzuki, Nicolas Bessagnet, Marcel Mokili, Abdesselam Abdelouas (IMTA)*

## 1. Introduction

Radionuclides of very low energy emission may be found in certain metallic radioactive waste as surface contaminants or neutron activated radionuclides in the base metal. The radionuclides are divided to easy-to-measure (ETM) and difficult-to-measure (DTM) radionuclides. These radionuclides have to be accurately quantified with a robust and validated radiochemical procedure. Four radionuclides have been selected: Ni-59 ( $7.6 \times 10^5$  y,  $\beta^+$ , EC,  $E_{X-K\alpha 1} = 6.93$  keV (20%),  $E_{X-K\alpha 2} = 6.91$  keV (10%),  $E_{\gamma\pm} = 511$  keV), Ni-63 (98.7 y,  $\beta^-$ ,  $E_{\max} = 66.98$  keV (100%)), Ca-41 ( $7.6 \times 10^4$  y, EC,  $E_{EC} = 421.64$  keV (100%)), Zr-93 ( $1.61 \times 10^6$  y,  $\beta^-$ ,  $E_{\max} = 60.0$  keV (73%) and 90.8 keV (27%)). The targets of the study is to provide a highly selective and efficient separation and purification, and to develop a sensitive to ultra-sensitive method of measurement, depending on the radionuclide. The utilised technologies are gamma spectrometry, liquid scintillation counting (LSC), and Inductively Coupled Plasma Mass spectrometry (ICP-MS).

## 2. Description of work and main findings

The general methodology is based on the separation-purification of sample (synthetic, or a solid containing the radionuclide source, or a surrogate), the conditioning to obtain the most suitable form for measurements (liquid form or deposition on filters), and the selection of an adapted analytical technique and the optimization of the detection efficiency prior to the measurement.

Ni-59 / Ni-63: To prepare the Ni-59 samples at VTT, Fe-55 standard was used and the sample was prepared using DMG precipitation method. The effect of the film to protect the detector from the radionuclide and the distance to the detector were evaluated. However, difficulties were found with uneven precipitate distribution on filter, significant amount of Fe-55 in waste, and inconsistent spectrometry results, mainly. So called sourceless samples (i.e. without mass) were therefore prepared by directly drying the eluted sample on either a Petri dish or a filter. The results showed that Fe-55 in 1mL 3M HnO<sub>3</sub> without DMG-precipitate provided a good consistency of results even tough crystallisation was seen on top of the samples.

Concerning the measurements, two techniques are currently optimized. The measurement by broad energy HPGe detector provide very good results with low detection limit (100 Bq/sample) based on Fe-55 standard. Another technique based on annihilation is investigated based on the  $\beta^+$  decay mode of Ni-59. The advantage of this technique is the analysis of Ni-59 in the whole liquid fraction containing both Ni-59 and Ni-63. After the Ni-59 analysis, a LSC sample for Ni-63 measurement can be prepared (i.e., mixing of sample with liquid scintillation cocktail).

To overcome the difficulty of the sample preparation and to provide an additional separation and concentration step against non-depositing radionuclides, a simplified preparation is in development at CTU. It is based on the electrodeposition of Ni on a thin stainless steel planchette, and the measurement of the planchette for the X-ray contribution of Ni-59 at low-energy gamma spectrometer, and then the soft beta from Ni-63 with LSC.

Zr-93: The evaluation of Zr-93 requires the development of a purification and a separation procedure to remove the contribution of Fe, Ni, Cr, Nb, and Mo coming from the digestion of the metallic sample during the sample preparation. Several series of samples of Zr are prepared at IMTA to evaluate this effect during the analysis of Zr by ICP-MS. Chromatographic separation on resins (UTEVA, TK400) are used with non radioactive solutions and Inconel metal. Stable Zr-90 is used for this evaluation that will be used as the tracer of separation and purification efficiency when in contact with Zr-93. The efficiency of Zr recovering is between 30-80%.

As Zr-93 will be analysed by LSC, evaluation of liquid scintillation cocktail stability is started based on the last elution conditions (acid concentration) after the chromatographic separation resin. Effect of acid concentration and type of cocktail is evaluating combined with the effect of time. The results showed that Ultima Gold AB remains stable in HCl 1M up to 54h. Ni-63 will be used as a surrogate of Zr-93 due to the close energy range and the limited supply of Zr-93 standard source.

### 3. Conclusions

The sample preparation and purification, the analytical method and the optimisation of the limit of detection are ongoing. Surrogate is used to replace targeted radionuclides due to lack of production or availability. Fe-55 is used to simulate Ni-59, and Ni-63 to simulate Zr-93.

### References

- Leskinen et al. (2020) JRNC 323:399-413
- Taddei et al. (2013) Appl Rad Isot 77:50-55
- Fisera et al. (2010) JRNC 586:713-717
- Lee et al. (2013) JRNC 298:1221-1226
- Taddei et al. (2013) JRNC 295:2267-2272
- Junqueira et al (2019) ISBN: 978-85-99141-08-3
- T. C. Oliveira et al. (2011) J Radioanal Nucl Chem 289:497–501
- S. Osvath et al. (2017) J Radioanal Nucl Chem 314:31–38



## 4.4 Encapsulation of reactive metals in magnesium phosphate cement-based matrices (Task 4.6)

Magnesium phosphate cements (MPC) are based on the acid-base chemical reaction between a soluble phosphate salt (mostly potassium dihydrogen phosphate), magnesium oxide and water to produce K-struvite ( $\text{MgKPO}_4 \cdot 6\text{H}_2\text{O}$ ). A MPC formulation was proposed as a reference to begin the studies of this task.

### 4.4.1 Development of magnesium phosphate cement formulations

*Raúl Fernández, Mikel Dieguez, Ana Isabel Ruiz, Jaime Cuevas, Universidad Autónoma de Madrid, (UAM)  
María Cruz Alonso, Inés García-Lodeiro (CSIC)*

The work was mainly focused on the influence of fillers in MPC formulations. Si-rich earth-materials, pumice, wollastonite, metakaolin and volcanic ash have demonstrated to be potential alternatives to substitute fly ash as filler, exhibit similar and even higher compressive strength than the MPC prepared with fly ash. However, the incorporation of these fillers can only reach a 40% compared to fly ash. Wollastonite and volcanic ash allow larger incorporation in the formulation, which is preferred because reduced costs. The filler has negligible effect on the formation of K-struvite. XRD results show the main reflections of major phases present in the initial samples, mostly dominated by the mineralogy of the filler. Quartz is present, while feldspars and micas are also present, inherited from the mineralogical composition of the fillers. After 7 days K-struvite becomes the main reaction product, and a better crystallised K-struvite is observed with the increasing curing time. Unreacted periclase is also observed. No new formed mineral phases have been identified. The fillers should not react with the cement, avoiding the alteration of the physical and chemical properties. Chemical compositions determined by SEM-EDX in MPC prepared with the 5 fillers indicate that both, Mg/P and K/P ratios are close to 1, as in the K-struvite (Figures 7 and 8).

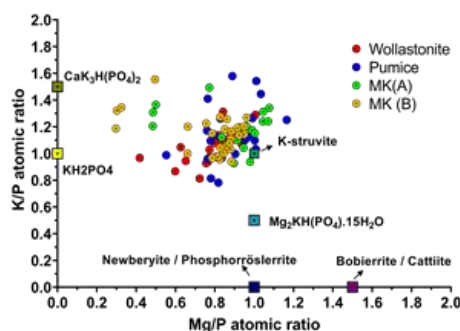


**Figure 7:** Chemical compositions of MPC pastes using pumite, wollastonite and both MKs.

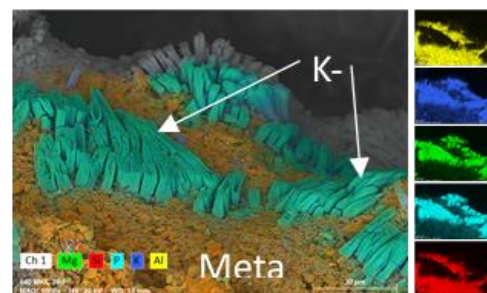


**Figure 8:** SEM photograph of K-struvite nucleation on the surface of MK, after 28 d of curing in sealed plastic bags.

The physical stability of MPC was also studied as a function of the curing conditions. For a  $\text{MgO}/\text{KH}_2\text{PO}_4$  molar ratio of 1, samples are very unstable and efflorescence is observed. For ratio higher than 2, the structural and chemical stability is guaranteed in any hydration conditions, but the pH also increases from 7 (ratio 1) to 7.8 (ratio 2) and 8.7 (ratio 3) after 7 d curing at 100% R.H. Long-term curing are needed to demonstrate the effect of the pH increase on the Al corrosion.

### 4.4.2 Magnesium phosphate cement cost optimization

*Lavinia Stefan (Orano),  
Kim Le, Sylvie Delpech, Davide Rodrigues, Céline Cannes (CNRS)*

The nature of the magnesium oxide and the phosphate source were studied. Using reactive  $\text{MgO}$ , cheaper than dead burnt  $\text{MgO}$ , is possible with new retarder, Na or K-thiosulfate (Figure 9). MPC can also be prepared with calcium phosphate. However preliminary results show that more work on retarder must be made to keep the water/cement ratio at 0.51. Moreover, the type of filler on the MPC properties and cost was examined (Figure 10). The compressive strength is improved by adding blast furnace slag (BFS), which is in huge amount on the territory of Ukraine. MPC with filler present a weight stabilization higher (650 – 700 °C) than without the additives (300 °C) and MPC with BFS present similar leaching behavior than the MPC with fly ash.

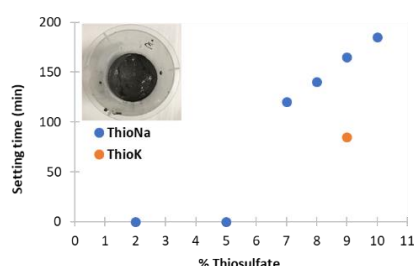


**Figure 9:** Setting time of MPC prepared with reactive MgO and thiosulfate.

Filler	Density (g/cm <sup>3</sup> )	Compressive strength (MPa)			
		7 d	14 d	28 d	90 d
FA	1.9	8	10	16	16.2
BFS	2.1	16.5	18.8	21.6	22.4
1/2FA+1/2BFS	2.0	9.6	12.8	17.2	17.4

**Figure 10:** Density and compressive strength of MPC as a function of the filler and time.

#### 4.4.3 Leaching behaviour of magnesium phosphate cement pastes

Laura Diaz Caselles, Céline Cau Dit Coumes, P. Antonucci, A. Rousselet (CEA),  
A. Mesbah (Univ. Lyon, IRCELYON)

Leaching behavior of MPC paste were investigated for 90 d by using a semi-dynamic leaching test and demineralized water as the leaching solution. Leaching solution was controlled over time by HNO<sub>3</sub> titration and pH was set at 7. The leaching solution was periodically renewed to limit accumulation of dissolved species. Chemical analyses of the leachates, recovered after each renewal, indicated that leaching was kinetically controlled by the diffusion of dissolved species through the pore network of the cement paste. The flux of dissolved K exceeded that of Mg and P by factors of 3.15 and 1.8, respectively. Several processes might explain why the leaching flux of K exceeded those of P and Mg: (i) release of K from fly ash, (ii) incongruent dissolution of K-struvite, and/or (iii) reprecipitation of K-free and Mg-rich phosphate phases. This later hypothesis seemed to be supported by SEM/EDS analyses performed on a polished section of the cement paste after the leaching test (Figures 11 and 12). A transition zone seemed to be present near the corroded layer (analyses were performed in a thickness of c.a. 1 mm). This zone contained K-struvite, but also magnesium phosphate minerals having a much lower K content. Further analyses will be performed to verify the mineralogical evolution through the sample, and thus, the distance between the corroded layer and the sound core. As for the corroded layer, it had a thickness of c.a. 200 μm and exhibited poor cohesion as well as lower K, P and Mg concentrations. Future work will be focused on the characterization of the phase assemblage in the different zones of the leached cement paste.

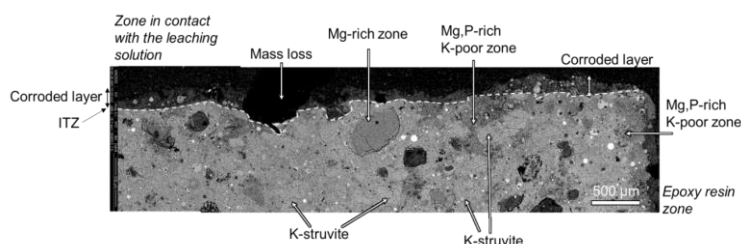


**Figure 11:** Reconstruction of SEM images obtained from a polished MPC paste section after leaching.

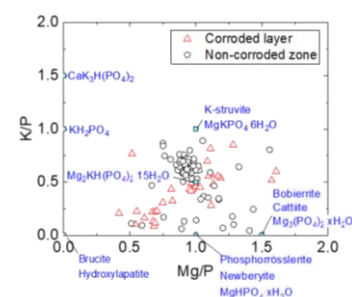


**Figure 12:** EDS mixing diagram of Mg/P vs K/P atomic ratios of the sample after leaching test. Data from the corroded layer and the non-corroded zone analyzed (c.a. 1 mm).

#### 4.4.4 Al corrosion in magnesium phosphate cements

María Cruz Alonso, Carla Fernandez (CSIC)

The Al and Al-Mg alloy corrosion was studied in simulated MPC and OPC pore media. At high pH, 12.5, Al is highly corroded during 6 months ( $E_{\text{corr}} < -1.3\text{V/SHE}$  and  $i_{\text{corr}} \geq 10\mu\text{A/cm}^2$ ). In simulated MPC pore media, containing phosphates and borates, Al and Al-Mg alloy are initially corroded and after one week, the reactivity decreases with time ( $E_{\text{corr}} > -0.8\text{V/SHE}$ ,  $i_{\text{corr}} \sim 1\text{--}0.1\mu\text{A/cm}^2$ ). With phosphates,  $i_{\text{corr}}$  is higher than with borates. Although the presence of borates initially induces more negative  $E_{\text{corr}}$  and higher  $i_{\text{corr}}$ , the Al alloy is rapidly less

corroded ( $i_{\text{corr}} < 0.01 \mu\text{A}/\text{cm}^2$ ) showing a positive effect of borates to the Al passivation. The Al and Al-Mg alloy corrosion was also studied in mortars of MPC and OPC (CEM I, CEM IV and CEM I +50%SF) under water immersion. In the MPC mortar, the pH is smaller than 7.5 for at least 50 d, and increases above 9 after 300 d of immersion (Figure 13). This was attributed to the MPC leaching with release of phosphates and borates. In the CEM I and IV mortars, the pH is always higher than 12.5, while in the CEM I+50%SF a decrease up to around 10.5 is measured. The corrosion potential in the MPC overpass the line of  $\text{H}_2$  evolution ( $E_{\text{corr}} > -0.4\text{V}/\text{SHE}$ ) while in OPC binders, it is smaller than  $-1.2\text{V}/\text{SHE}$  (Figure 14). The corrosion current depends strongly on the type of mortar:  $i_{\text{corr}} \leq 0.001 \mu\text{A}/\text{cm}^2$  for MPC,  $\leq 0.01 \mu\text{A}/\text{cm}^2$  for low-pH binder and  $\leq 0.1 \mu\text{A}/\text{cm}^2$  for CEM I and IV. The volume of  $\text{H}_2$  generated by aqueous corrosion was calculated by electrochemistry. The maximum  $\text{H}_2$  evolution is observed during the first 50 d ( $< 1\text{L}/\text{m}^2$  in MPC,  $5\text{L}/\text{m}^2$  in low-pH and  $15\text{--}20\text{L}/\text{m}^2$  for CEM I and IV). At longer exposure period a stabilisation occurs, with negligible  $\text{H}_2$  evolution in the MPC and low-pH binders (Figure 15). The Al-Mg alloy shows higher risk of corrosion than Al.

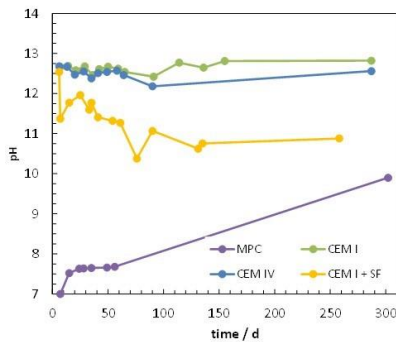


**Figure 13:** pH evolution of MPC, CEM I, CEM IV and CEMI+50%SF.

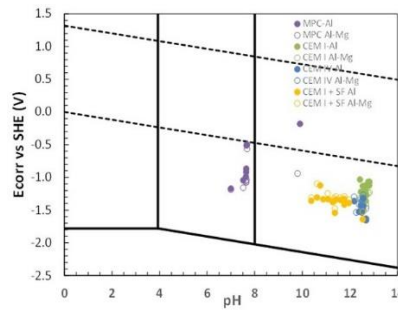


**Figure 14:** Pourbaix diagram of Al in water and corrosion potential of Al and Al-Mg in different binders.

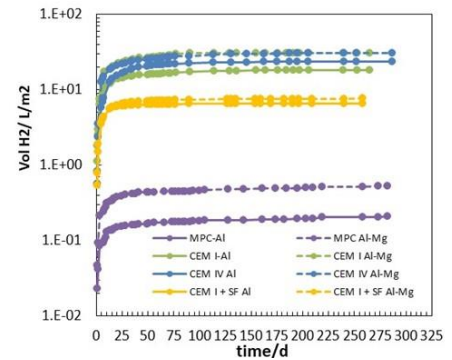


**Figure 15:** Volume of  $\text{H}_2$  produced by Al and Al-Mg corrosion in MPC, CEM I, CEM IV and CEMI+50%SF.

#### 4.4.5 Steel corrosion in magnesium phosphate cements

Kim Le, Sylvie Delpech, Davide Rodrigues, Céline Cannes (CNRS)

No significant corrosion of steel is observed in presence of boric acid in the MPC formulation (Figure 16). This acid is then important both to retard the cement setting and to inhibit the steel corrosion. The Al/steel galvanic corrosion current is higher in MPC in presence of  $\text{H}_3\text{BO}_3$  than in absence of this acid. This current depends on the reactivity of Al in the medium since it is imposed by the Al oxidation. That means that Al is more corroded in MPC in presence of boric acid than in absence of this acid. During galvanic corrosion, the reduction of water to hydrogen is observed. The  $\text{H}_2$  volume produced by galvanic corrosion has been estimated from Zero Resistance Ammeter measurements at  $1.8\text{L}/\text{m}^2\text{Al}/\text{y}$  in MPC with  $\text{H}_3\text{BO}_3$  and  $0.5\text{L}/\text{m}^2\text{Al}/\text{y}$  in MPC without MPC, which are very low values compared to OPC, more than  $300\text{L}/\text{m}^2\text{Al}/\text{y}$  (Figure 17).

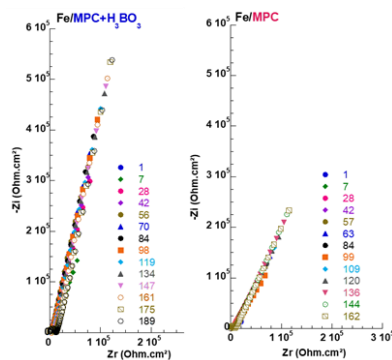


**Figure 16:** Nyquist diagrams of steel measured at OCP, from  $10^6$  to  $10^{-2}$  Hz in MPC and MPC +  $\text{H}_3\text{BO}_3$ .

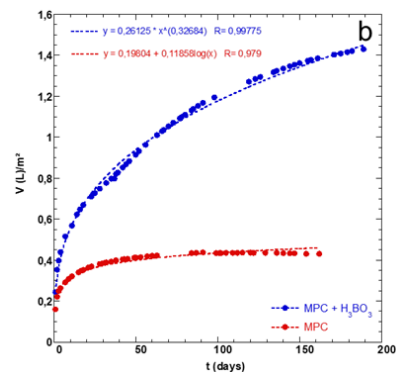


**Figure 17:**  $\text{H}_2$  volume produced by corrosion calculated from galvanic current in MPC and MPC +  $\text{H}_3\text{BO}_3$ .



#### 4.4.6 Be corrosion in magnesium phosphate cements

Sébastien Caes, Valdir de Souza, Bruno Kursten (SCK CEN)  
Andrey Bukaemskiy, Guido Deissmann, Giuseppe Modolo (FZJ)

At SCK CEN, the evaluation of the corrosion rate and mechanism of beryllium was studied by using S-200-F Be grade, corresponding to the grade used in the matrix of the Belgian Reactor 2 (BR2). Part of the samples were cut into pellets to allow the corrosion tests. The first tests were started in solution representative for the OPC pore solution. The first results obtained from the hydrogen concentration measurement gave a corrosion rate evolving around 5 to 10  $\mu\text{m}/\text{y}$ . This needs to be compared to the electrochemical tests. New tests will start in direct contact with OPC cement paste to study the effect of the matrix. Tests in solutions representative for MPC or in MPC pastes will also be started afterwards.

At FZJ, the Be corrosion was studied by gravimetry in alkaline solutions (pH 12.2 and 13.95), representative of OPC pore fluids (Figure 18). At pH 12.2, the corrosion rate is lower than 5  $\mu\text{m}/\text{y}$ , which is close to or below the detection limit. At pH 13.95, the corrosion is active. The initial corrosion rate is around 195  $\mu\text{m}/\text{y}$  and tends to a steady state around 135.2  $\mu\text{m}/\text{y}$  after 7 d. The Be surface was characterized by SEM after immersion in the alkaline solutions (Figure 19). After 7 d of immersion at pH 12.2, the stripes initially present on the Be surface are still observed and a few small corrosion pits appeared. After 10 d of immersion at pH 13.95, the stripes are less visible and more pits are observed and their surfaces are bigger than at pH 12.2.

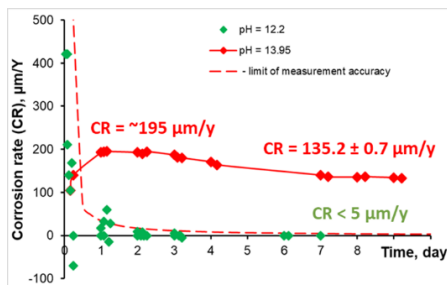


**Figure 18:** Variation of Be corrosion rate in alkaline solutions as a function of time.

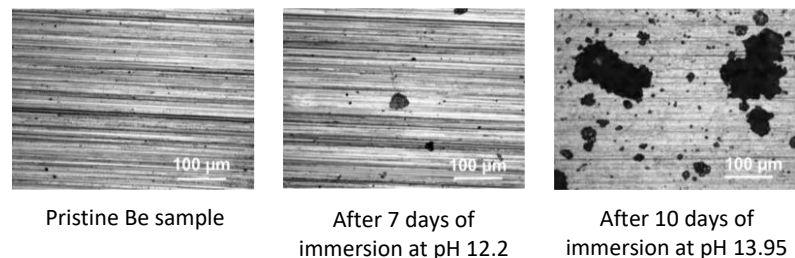


**Figure 19:** SEM image of Be surface before and after immersion in solution at pH 12.2 and 13.95.

## 5 Scientific progress Innovations in liquid organic waste treatment and conditioning (WP5)

### 5.1 Innovations in liquid organic waste treatment and conditioning – overview (WP5)

Maxime FOURNIER, David LAMBERTIN, Kahina HAMADACHE, CEA, France, [maxime.fournier@cea.fr](mailto:maxime.fournier@cea.fr),

#### Abstract

**Keywords:** direct conditioning, radioactive liquid organic wastes (RLOW), geopolymer

#### 1. Introduction

The PREDIS project targets the development and implementation of activities for pre-disposal treatment of metallic, solid organic, liquid organic and cemented waste streams other than nuclear fuel and high-level radioactive waste.

Work package five (WP5) of the PREDIS project is concerned with the treatment and conditioning of radioactive liquid organic wastes (RLOW). WP5 is developing options for direct conditioning in RLOW using innovative geopolymers and related alkali activated materials. The work is focused on improving waste loadings and waste-form properties with the aim of conditioning RLOW into a final waste-form that is compatible with waste acceptance criteria for (prolonged) storage and transport and final disposal.

A significant amount of Radioactive Liquid Organic Waste (RLOW) needs to be processed prior to storage and disposal. A group of representative Waste Management Organizations and Waste Producers classified RLOW and identified oils contaminated with alpha-emitters, organic solvents, scintillation cocktails and decontamination liquids, which can result from nuclear power plant operation, decommissioning and other industrial processes, as main constituents of this waste category.

19 European partners from 8 countries join forces to develop and implement geopolymers and related alkali-activated materials as innovative RLOW direct conditioning solution.

#### 2. Description of work and main findings

In 2021, the collection and review of waste, regulatory, scientific and technical data (Task 2) involving PREDIS stakeholders has enabled the description of RLOW inventories at the European level. High priority and high volume RLOW streams were identified to be the focus of the PREDIS experimental work. The four reference wastes are: oils, decontamination solvents, TBP/dodecane and scintillation cocktails. I

In late 2021, three reference geopolymer matrix formulations were identified as candidates for direct conditioning solutions for RLOW (Task 3). These formulations are respectively based on metakaolin (NNL), blast furnace slag (SCK CEN) and a mix of raw materials, namely metakaolin, blast furnace slag and fly ash (KIPT). At the beginning of the year, robustness and optimisation studies were initiated by groups of partners and are still ongoing. The aim is to develop geopolymer formulations that could be scalable to different countries in Europe by using local raw materials. The beginning of 2022 marks the start of the durability testing campaign (Task 4) under endogenous, aerated or leaching conditions. The partners will also study the behaviour of the binders under irradiation, the binding and leaching of radionuclides as well as the thermal behaviour and fire hazard. These tests will be carried out by groups of partners.

This year also brings the start of the Life Cycle Assessment (LCA) process. WP5 has developed a specific template to collect information for the LCA that will be carried out in WP2. It has been designed to capture the LCA information for the geopolymer processes that are studied in the WP5. As our processes are at laboratory scale, the objective will be to specify the materials used and waste-normalised quantities. WP5 has identified

several base cases involving the absorption and cementation of RLOW waste that allow us to compare our geopolymer techniques.

### **3. Summary**

Optimisation of the direct conditioning process, testing the performance of conditioning matrix - as well as technical, economic and environmental analysis are ongoing. They will allow to optimize, assess robustness and investigate upscale feasibility of the conditioning matrix formulations. Latest outcomes have defined the experimental guidelines and protocols, which have led to develop geopolymer matrix formulations that are currently being tested to incorporate RLOW. Indeed, formulations based on metakaolin, slags and mixes of raw materials have shown very promising results improving waste loadings and wasteform properties in comparison with traditional cementitious waste forms. This innovation is intended to provide a reliable solution for the direct conditioning of RLOW, allowing access to storage, transportation or disposal of this waste stream, while complying with technical, economic and safety requirements.

### **Acknowledgements**

This project has received funding from the Euratom research and training programme 2019-2020 under grant agreement No 945098.

## 5.2 Reference Formulations and Robustness Study Plan (Task 5.3)

Federica Pancotti, SOGIN, Italy, [pancotti@sogin.it](mailto:pancotti@sogin.it)

### Abstract

**Keywords:** direct conditioning, radioactive liquid organic wastes (RLOW), geopolymer, alkali-activated materials

### 1. Introduction

PREDIS WP5 aims to investigate, develop and assess direct conditioning solutions for Radioactive Liquid Organic Waste (RLOW) based on geopolymers and alkali-activated materials. Task T5.3 concerns the study of direct conditioning process of RLOW to:

- assess conditioning options and to select most promising reference formulations to be further studied and developed (T5.3.2)
- optimize and assess robustness of selected reference formulations (T5.3.3)
- further consolidate reference formulations from tests with real RLOW (T5.3.4)
- investigate feasibility of scale-up from exploratory pilot scale tests (T5.3.5)

This article presents the main findings of the partners involved in Task 5.3 (NUCLECO/SOGIN, NNL/USFD, CIEMAT, POLIMI, SCK-CEN, KIPT, RATEN, CEA-ECL) to this date with reference to the selection of the reference formulations to be further studied and developed (T5.3.2) and the plan for the Robustness Study (T5.3.3).

### 2. Main Findings and Future Plan

All partners of Task 5.3 have shown that different AAM formulations may be used for RLOW encapsulation, either based on metakaolin, or on BFS or volcanic tuff, or mixes of these alumino-silicate precursors. Alkaline activation is achieved either with NaOH, KOH or metasilicate (sodium or potassium based) and in some cases the need for surfactants was highlighted.

After a preliminary experimental phase, three reference families, based on Metakaolin, Blast Furnace Slag and mixture of different raw materials, were defined and tested for RLOW incorporation rates. The main parameters (aluminosilicate precursor(s), alkaline activator, water, filler, surfactant or other additives) were studied and optimized. The assessment of the conditioning options and the completion of the optimisation study led to the selection of the following three reference formulations to be further developed.

<p><b>1) NNL formulation – MK based</b></p> <p>➤ <b>Row material:</b></p> <ul style="list-style-type: none"> <li>Metamax® - RC: <math>\text{Al}_2\text{O}_3 = 43.99\%</math>, <math>\text{SiO}_2 = 51.48\%</math></li> </ul> <p>➤ <b>Activator:</b></p> <ul style="list-style-type: none"> <li>K silicate (K120): <math>\text{K}_2\text{O} = 21.3\text{ wt}\%</math>, <math>\text{SiO}_2 = 30.38\text{ wt}\%</math>, <math>\text{H}_2\text{O} = 48.32\text{ wt}\%</math></li> </ul> <p>➤ <b>Optimized formulation:</b></p> <ul style="list-style-type: none"> <li><math>\text{SiO}_2:\text{K}_2\text{O} = 1.2</math></li> <li><math>\text{K}_2\text{O}:\text{Al}_2\text{O}_3 = 1.2</math></li> <li><math>\text{H}_2\text{O}:\text{K}_2\text{O} = 13</math></li> </ul> <p>➤ <b>RLOW:</b></p> <ul style="list-style-type: none"> <li>Nevastane Oil (20% vol.)</li> </ul>	<p><b>2) SCK CEN formulation – BFS based</b></p> <p>➤ <b>Row materials:</b></p> <ul style="list-style-type: none"> <li>BFS = 46.5 wt% (<math>\text{Al}_2\text{O}_3 = 11.10\%</math>, <math>\text{SiO}_2 = 32.40\%</math>)</li> </ul> <p>• Sand = 28 wt%</p> <p>➤ <b>Activator:</b></p> <ul style="list-style-type: none"> <li><math>\text{Na}_2\text{O} \cdot 2\text{SiO}_2 \cdot x\text{H}_2\text{O} - 1.5\text{ wt}\%</math></li> <li>NaOH (10M) - 5.5 wt%</li> <li>Additional water - 18.4 wt%</li> </ul> <p>➤ <b>RLOW:</b></p> <ul style="list-style-type: none"> <li>Ionic liquid (Aliquat 336) - 9.9 wt. % <sup>(1)</sup></li> <li>TBP - 19.1 wt. %</li> </ul> <p>(1) Tween 80 surfactant used: 0.5 % and 0.95 % relative to the waste volume</p>	<p><b>3) KIPT formulation – MIX based</b></p> <p>➤ <b>Row materials:</b></p> <ul style="list-style-type: none"> <li>FA = 34 wt.% (<math>\text{Al}_2\text{O}_3 = 18\%</math>, <math>\text{SiO}_2 = 46.12\%</math>)</li> <li>BFS = 20 wt.% (<math>\text{Al}_2\text{O}_3 = 6.02\%</math>, <math>\text{SiO}_2 = 40.6\%</math>)</li> <li>MK = 14 wt.% (<math>\text{Al}_2\text{O}_3 = 35.50\%</math>, <math>\text{SiO}_2 = 51\%</math>)</li> </ul> <p>➤ <b>Activator:</b></p> <ul style="list-style-type: none"> <li><math>\text{K}_2\text{SiO}_3 = 11\text{ wt}\%</math></li> <li>KOH - 9 wt.%</li> <li>Water - 12 wt.%</li> </ul> <p>➤ <b>RLOW:</b></p> <ul style="list-style-type: none"> <li>ShellSpirax: from 10% to 40% vol <sup>(2)</sup></li> </ul> <p>(2) Castament FW 10 (solid Polyethylene glycol-based additive) used to improve several properties: 0.5 %</p>
--	---	---

To ensure conditioning materials robustness regarding waste, raw materials and process variability a detailed plan was developed and agreed between T5.3 partners.

In order to meet the goal of defining the “Optimised formulations for reference formulations (MS34)”, two partners per formulation will work in a two stage approach to test both the fresh paste properties (viscosity, setting time, etc.) and hardened matrix properties (bleeding, compressive strength, etc.) of the 3 reference formulations by varying:

- RLOW Type (TBP/Dodecane mixture, Scintillation Cocktail, low viscosity Oil, high viscosity Oil)
  - With fixed incorporation rate (for example 30 % volume (depending on the ROLW type)) and fixed raw materials, different RLOW will be tested
- Raw materials
  - With fixed incorporation rate (for example 30 % volume) and fixed RLOW, different raw materials will be tested depending on local availability
- Process parameters
  - With fixed incorporation rate (for example 30 % volume), fixed raw materials and fixed RLOW, the variability of the following parameters will be tested:
  - aluminosilicate source-to-activation source ratio (for example  $\pm 2$  %)
  - ROLW composition (e.g. TBP-dodecane ratio)
  - water-to-binders ratio (for example  $\pm 2$  %)
  - sand-to-water ratio (for example  $\pm 2$  %) (at fixed incorporation rate)
  - emulsifier, if needed (for example  $\pm 2$  %) (at fixed incorporation rate)

Due to the fact that a key technical bottleneck is related to RLOW emulsion properties and stability either in activation solution or in fresh grout, the possibly using surfactants will be further studied. CEA – ECL (in close collaboration with all the other partners) will work to improve the understanding of emulsification process and the influence on hardened materials properties and in the identification of the most suitable emulsifier (if needed).

### 3. Conclusions

Preliminary results showed that the three reference formulations based on Metakaolin, Blast Furnace Slag and mixture of different raw materials can result in a high ROLW incorporation rate (up to 30% vol). Optimisation and testing of the robustness of those reference formulations are ongoing. They will allow the investigation of reference formulations with real RLOW and the feasibility of direct conditioning process scale-up.

### Acknowledgements

This project has received funding from the Euratom research and training programme 2019-2020 under grant agreement No 945098.

### 5.3 Study of conditioning matrix performances – Status Update (Task 5.4)

The main objectives of the task 5.4 ‘Study of conditioning matrix performances’ are to study the conditioning matrix performances and behavior in relation with disposal, transport and prolonged storage requirements and specifications. In another term, it is about the study of the durability of the conditioning matrices for RLOW while assessing the disposability according to RLOW radiological features and targeted disposal facilities.

The sub-tasks will be performed on three reference formulations selected after Task 5.3 (Sub-task 5.3.2) in close collaboration between pools of partners.

During PREDIS Webinar on the fifth of May 2022, Professor John Provis (University of Sheffield) has defined a list of criteria describing what durability should respond to.

- Sufficient retention of binder mechanical performance with material ageing
- Sufficient resistance of binder to attack by relevant environmental factors
- Dimensional stability to prevent mechanically-induced damage to other aspects of multi-barrier system
- Release of immobilized/encapsulated wastes not exceeding acceptable levels
- Release of binder constituents (e.g. alkaline pore fluid) below the level that would cause chemical damage to other aspects of multi-barrier system

In order to attend those objectives, a selection of experimental protocols is done (deliverable from Task 5.4.1).

#### **CIEMAT:**

Using the pre-emulsion method with oil immobilization, 30% oil emulsion samples were mixed with the activator and prepared 24 h before the experiment. The emulsion was added to the Metamax and stirred for 10 min at high rpm. Different samples were prepared: two samples were prepared at room temperature and two others at 80°C. Mechanical performances seem to be better when no heat is applied.

#### **ECL:**

While it is not possible to have the same commercial alkaline activator, the effect of the alkaline potassium silicate solution was studied. Betol 5020T and Geosil 14517 having different silicate to potassium oxide molar ratios can provide the same results in compressive strength if the stoichiometry is adjusted (identical stoichiometry).

#### **CVRez:**

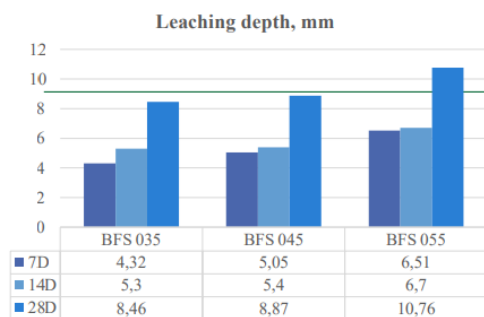
With shared samples CVRez can provide: mechanical static and dynamic tests: for compressive strength on cubes and cylinders, modulus of elasticity, leaching tests, water immersion test, bond structure, sample composition, XRD and SEM on powders

#### **ENEA:**

Preliminary compressive tests were performed on 22x22x16 cubic millimeter samples. The samples were cured for 28 days in atmospheric conditions. The maximal resistance to compression obtained was 117.67 MPa.

#### **SCK CEN:**

Leaching tests were performed on blast furnace slags mixes. Results show that the higher W/B ratio, the more susceptible are the samples to leaching. In addition, C-A-S-H seems to be the more vulnerable to be leached in the case of BFS compared to N-A-S-H in the case of geopolymers.



**IRSN** (in partnership with SCK CEN):

After accelerated carbonation, a characterization of degraded MK Na-based geopolymer show a 100  $\mu\text{m}$  of decrease of Na/Si atomic ratio close to the interface.

**UNIPi:**

Program of the study:

- Phase 1: Sample preparation
- Phase 2: Pre-test Phase control
- Phase 3: Thermal/fire test
- Phase 4: Post-test control
- Phase 5: Mechanical characterization



## 6 Scientific progress in Innovations in solid organic waste treatment and conditioning (WP6)

### 6.1 Physical and chemical characterization of thermally-treated IERs surrogates

Elena Torres, Luis Alberto Bahillo, CIEMAT, Spain, [elena.torres@ciemat.es](mailto:elena.torres@ciemat.es)  
 Raúl Fernández, Ana I. Ruiz, UAM, Spain, [raul.fernandez@ciemat.es](mailto:raul.fernandez@ciemat.es)

**Keywords:** thermally-treated, IERs, leaching, dopants, TOC

#### 1. Introduction

Large amounts of spent granular IERs are generated in water purifications systems of nuclear power plants. This type of waste is known to release hydrogen by radiolysis degradation, reactive species and complexing compounds due to its chemical composition (generally copolymers of styrene and divinylbenzene) [1]. So, the reduction of volume of this waste and its treatment to wasteforms suitable for long-term disposal is an issue of increasing concern. For safe storage and disposal, the spent IERs have been treated by several thermochemical methods to minimize volume and produce a chemical stable product, compatible with conditioning matrices in order to obtain a wasteform that fulfils relevant national WACs. Among these methods, incineration in excess of air has been frequently used [2].

This work aims to evaluate on one hand, the potential benefits of the immobilisation of thermally-treated IERs and on the other hand, the compatibility of the reconditioned waste with cement and geopolymer matrices formulated in task 6.4. by CSIC.

#### 2. Description of work and main findings

CIEMAT has continued working on the production of reconditioned waste for the delivery to the other two Spanish partners (UAM & CSIC) in WP 6. In parallel to this, progresses have been made in the evaluation of the physical and chemical stability of the thermally-treated waste in highly-alkaline environment.

##### 2.1 Preparation of thermally-treated IERs surrogates

Surrogates prepared for CIEMAT consist of a form of mixed Ionic Exchange Resins (IERs), that have been doped according to the specifications provided by two Spanish waste producers. For this project, a blend of Amberlite IRN-77 (cationic form) and IRN-78 (anionic form) in a 50/50 ratio is being used. These resins have been saturated with solutions containing boron and traces of Sr, Cs and activation products (Ag, Co, Cr, Zn, Fe). For pH adjustment, ammonia has been used.

For thermal treatment, a target temperature of 450°C has been chosen to minimize volatilization of Cesium and Boron. After thermal treatment, a black granulated product is obtained (Figure 1). These ashes are hygroscopic with average water content lower than 3%. Due to sulphonic groups present in the cationic exchange resins, exhibited a strong acidic behaviour in aqueous media. Table I shows the elemental composition of the ashes.

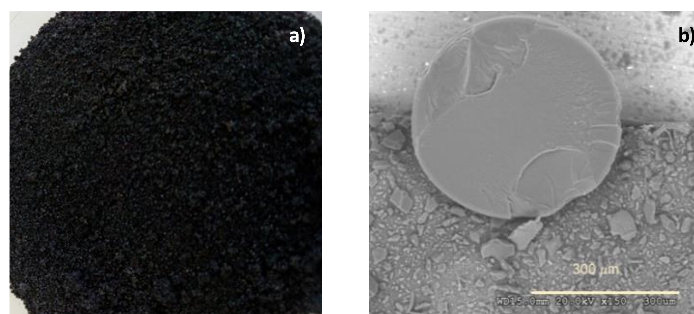


**Figure 1.** Thermally-treated IERs surrogates: a) photograph of the black powder obtained after incineration; b) Cross-section SEM image of one resin bead after treatment.



**Table 1.** Elemental analysis of thermally-treated IERs.

%C	%N	% H	% S
74±2	1,21±0,05	5,3±0,2	7,1±0,5

## 2.2 Leaching tests for thermally-treated IERs characterization

Two series of leaching tests were run in order to evaluate the chemical stability of doped IERs, before and after thermal treatment, in a highly-alkaline media as foreseen in a geopolymer or cement porewater. Tests were dismantled after 1 and 4 months and two leachants were used: deionized water (reference) and NaOH 1M.

Concentrations of leached elements after 4 months are low in both, deionized water and NaOH 1M (Figure 2). Boron is the prevalent leached dopant (~20 mg B/kg of waste). Traces of metallic elements and Sr were also detected in solution. Concentrations of cesium measured in solution in were negligible for both leachants.

Additional tests were run to evaluate potential advantages that thermal treatment can provide for long-term performance of the reconditioned wasteform. Both, doped IERs and thermally-treated waste exhibited similar acidic behaviour in both, water and NaOH 1M. However, in alkaline media, TOC measured for doped IERs was up to 3 times higher than treated waste. Likewise, dopants in solution are significantly higher for doped IERs (Figure 3). These data suggest that treated waste is more stable in alkaline media than doped IERs.

## 3. Way forward

CIEMAT workplan for next months includes the evaluation of the robustness of thermal treatment. Matrices formulations can be sensitive to the chemical composition of the incinerated waste. So, it is important to determine if this process can yield a chemically-homogeneous residue compatible with cement and geopolymer matrices formulated in task 6.4. by CSIC. Another matter of interest is the release of volatile dopants (i.e. B, Cs, ..) during thermal treatment that can jeopardize its future application. Thus, mass balance to evaluate the loss of volatile elements is programmed.

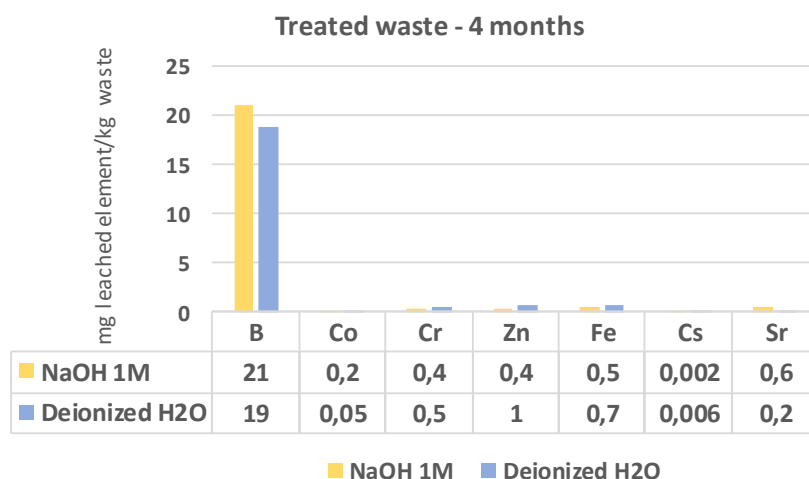


**Figure 2.** Concentrations of elements measured in solution in 4-month leaching tests in two leachants: deionized water and NaOH 1M (mg of leached element/kg waste).

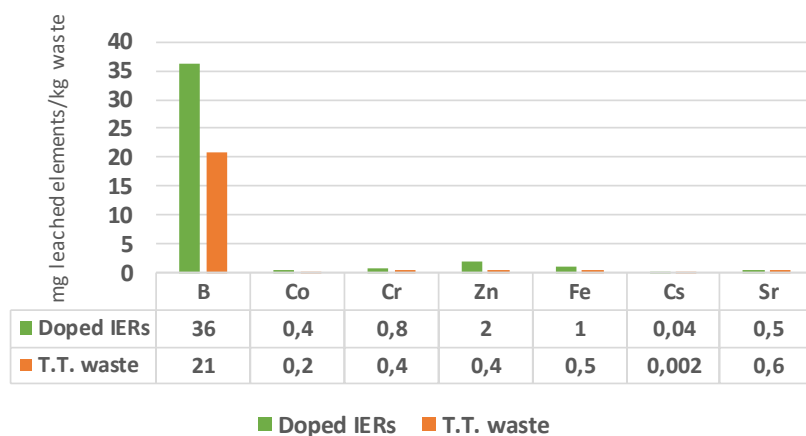


**Figure 3.** Concentrations measured in solution in 4-month leaching tests using NaOH 1M as leachant for doped resins and thermally-treated waste (mg of leached element/kg waste).

## Acknowledgements

CIEMAT would like to acknowledge ENRESA and waste producers, (ENDESA- ANAV & IBERDROLA – Cofrentes NPP) for their active collaboration in the materials supply, the definition of the waste streams and the tailoring of the chemistry for the IERs surrogates.

## References

- [1] B. Frasca, L. Griffault, J. Lefevre, C. Martin, M. Romero, Influence of thermal treatment on the disposability of spent ion exchange resins in a deep geological repository: a French case. IOP Conference Series: Materials Science and Engineering. 818. 012021.10.1088/1757-899X/818/1/01021, 2020.
- [2] M.I. Ojovan, G.A. Petrov, S.A. Dmitriev, B.G. Trusov, K.N. Semenov, V.I. Klimov, Thermochemical Treatment of Spent Ion Exchange Resins, IAEA-CSP—6/C, paper 49, 2001.

## 6.2 Characterization, densification and encapsulation of ashes from incineration of RSOW by IRIS process

*Hélène NONNET, Virginie ANSAULT*  
CEA, DES, ISEC, DE2D, Univ Montpellier, Marcoule, France  
*helene.nonnet@cea.fr*

**Keywords:** RSOW, ashes, compaction

### 1. Introduction

This paper summarizes the work carried out since the last workshop. A complete characterization of the ashes produced by the incineration process IRIS has been achieved. Studies on densification by granulation, pressing and thermal treatment, on one hand, and encapsulation by molten glass, on the other hand have started. In addition, several batches of IRIS ashes have been delivered to partners (USFD and Polimi) for HIP and geopolymer mortars conditioning feasibility.

### 2. Description of work and main findings

#### a. Chemical and structural characterizations of the ashes

The ashes considered in these studies come from the IRIS incineration pilot process (Installation for Research on Incineration of Solids) developed at CEA Marcoule for R&D support and devoted to the treatment of the organic waste contaminated by  $\alpha$ -emitting actinides from glove boxes in the nuclear industry. This pilot is working exclusively under inactive environment, and the ashes produced come from the incineration of a mix of different organic solids and IER resins. This leads to achieve a volume reduction of the waste to about a 30 factor. IRIS is a three-step process implemented in rotating kilns. The first step consists in oxidative pyrolysis at 550°C, producing pitch that is then processed in a calcining step at 900°C in oxygen-enriched atmosphere. The off-gases arising from the thermal treatments include a volatile hydrocarbon fraction that is oxidized at 1100°C in an afterburner. This multistep process has two advantages. The elimination of chlorine at low temperature in the pyrolyzer limits corrosion problems and allows operation with low gas flow, which also limits particle entrainment. Adding oxygen during the pyrolysis step oxidizes the heavy hydrocarbons that produce tars capable of forming deposits in the ducts. Forming during the pyrolysis step, the pitch drops into the calciner being a rotary kiln heated at 900°C. The pitch remains around 2 hours in this furnace and is transformed into ashes having a very low carbon content ( $< 1\%$ ). Before discharge to atmosphere, the gas stream is submitted to caustic scrubbing to eliminate the volatile acids. The material balance in the process is about as follow: a feeding rate of 4kg/h produces around 1550g/h of pitch, 111 g/h of ashes and 47g/h of dust. Although this technology limits corrosion, it does not completely prevent the production of metal chlorides [1].

The ashes produced have a high flying behaviour with a density of  $0.2 \text{ g.cm}^{-3}$  and their particle size is mainly centered between 0.1 to 1 mm [Figure 1].

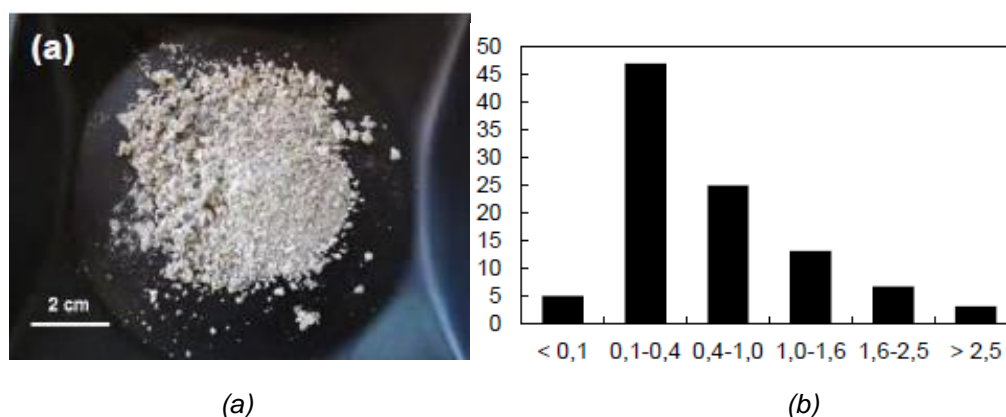


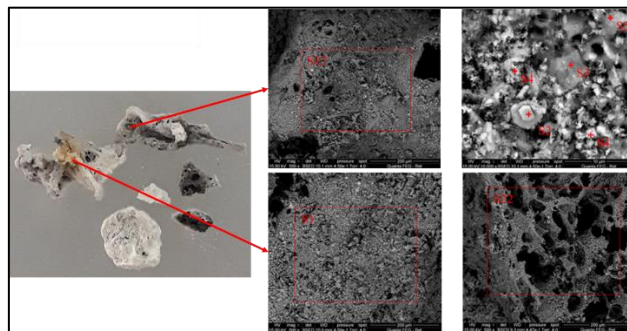
**Figure 1:** (a) IRIS ashes general morphology, (b) IRIS ashes granulometric class.

Elementary chemical characterisations have been done. The ashes are mainly composed of aluminium, silicon, calcium and zinc [Table 1].

**Table 1: Chemical analysis of the IRIS ashes.**

Component	%weight		Component	%w
C	0,200		Cl	1,74
F	0,005		SO <sub>3</sub>	1,41
Cl	1,744		BaO	0,15
S	0,566		Cr <sub>2</sub> O <sub>3</sub>	0,08
Ba	0,131		Al <sub>2</sub> O <sub>3</sub>	28,46
Cr	0,057		Fe <sub>2</sub> O <sub>3</sub>	0,63
Co	0,001		MgO	4,53
Cu	0,002		K <sub>2</sub> O	3,60
Sn	0,001		TiO <sub>2</sub>	0,69
Li	0,001		P <sub>2</sub> O <sub>5</sub>	3,24
Al	15,061		Na <sub>2</sub> O	0,95
Fe	0,441		CaO	13,55
Mg	2,732		SiO <sub>2</sub>	29,35
K	2,997		NiO	0,61
Ti	0,414		ZnO	7,17
P	1,830		Bi <sub>2</sub> O <sub>3</sub>	0,12
Na	0,705			
Ca	9,684			
Si	13,720			
Ni	0,481			
Pb	0,000			
Zn	5,763			
Bi	0,109			
Σ	56,644			
O (difference)	43,356			

SEM and structural characterizations have been done. The micro particles have a very porous aspect and are partially amorphous. The crystallized phase are composed of ringwoodite and anohrtite.


**Figure 2: SEM analysis of the IRIS ashes.**

#### b. Densification

The immobilization of the ashes waste is studied according to different routes, with the objective to get a densified monolith.

The first route is compaction. Ashes are shaped to get pellets obtained either starting from the raw ashes, either from a mix of ashes and glass as vitrification agent.

The pellets are then heat-treated to get a densified and sintered monolith.

The interest of an adjuvant made of sodium silicate has been evaluated.

Pellets of ten millimeters in diameter and weighing zero point five grams have been shaped, using a uniaxial press. Various pressure strength from sixty-four to two hundred megapascal have been tested. The best mechanical performances have been achieved with the two hundred pressed pellets [Figure 3].

Granulates have been shaped using a granulator mixer and many parameters as operating speed, granulation times and water addition have been evaluated. The best parameters have been defined to get quite homogeneous sizes of granulates but their mechanical strength are weak, making them very difficult to handle, and their mechanical performance are difficult to assess.

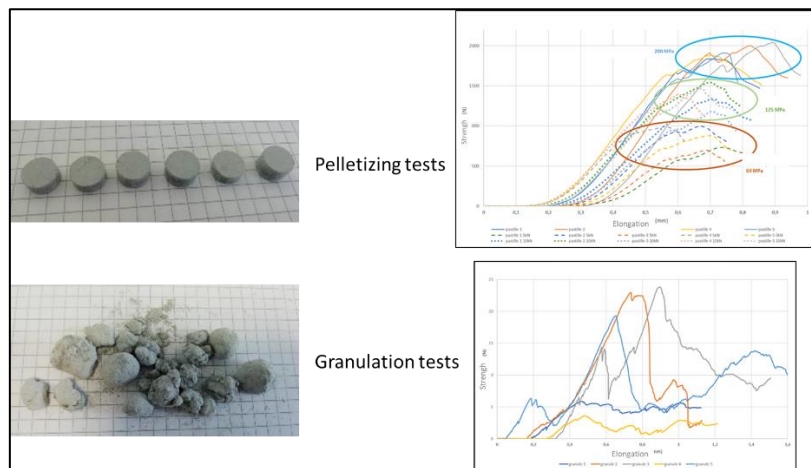


**Figure 3:** Mechanical characterizations of the pellets and granulates.

In a second step, these different shaped ashes have been heat treated in a classical lab furnace at eleven hundred degrees during three hours. For both shapes, a densified material has been achieved, with a significant densification factor, especially for the pellet **[Figure 4]**.

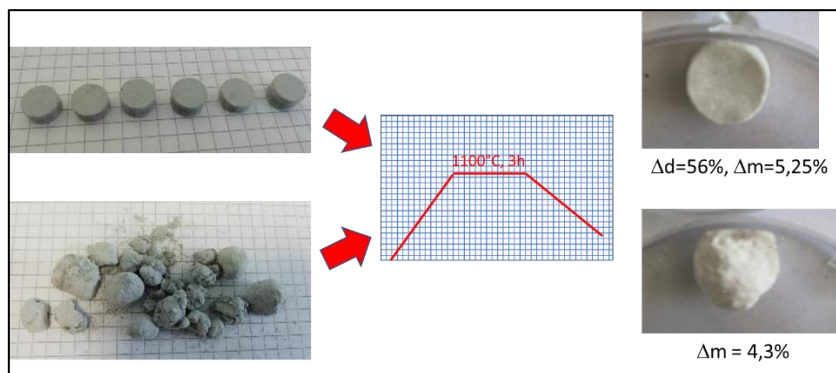


**Figure 4:** Thermal treatment of the pellets and granulates.

The next steps will be to realize microstructural analysis to understand the material transformations.

#### c. Encapsulation

The second route is the molten glass coating, using a glass in order to catch the ashes inside the glass. The idea here is to use low temperature melting glass, in order to avoid the volatilization of radionuclides and to get a monolithic form.

Specific glass frit made of sodium, silicon and boron having a very low melting temperature, has been carried out various morphologies both of the glass adjuvant and the ashes have been tested, as various mix ratio in order to assess the best way of shaping.

To date, more or less twenty screening tests by varying ratio waste to glass, material morphology and treatment temperature have been achieved. Visually, the best results in terms of homogeneity are reached with crushed glass and ash weight load up to 40% **[Figure 5]**. Above 40% of load, the ashes are not well coated and will not be retained by the matrix.

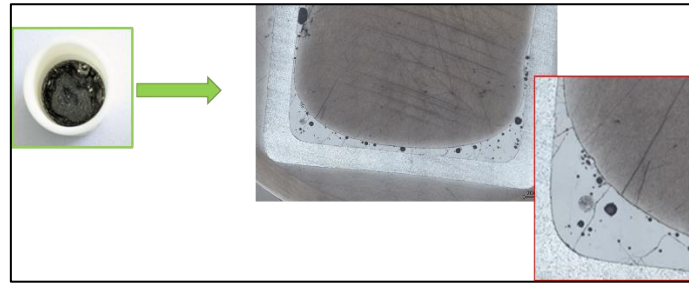


**Figure 5:** Optical observation of the molten glass coating monolith at 40% load.

### 3. Way forward

The compaction route with powder glass adjuvant followed by thermal treatment will be tested.

Then, the most promising samples will be characterized at microstructural scale, by SEM or optical analysis.

Feasibility demonstration of the coating route with CVRez waste in accordance with sub task 3.1 is also planned.

At least, leaching tests will be started on the best monolithic materials obtained from these feasibility demonstrations.

### Acknowledgements

I would like to acknowledge Virginie Ansault (CEA DES/ISEC/DE2D/SEVT/LDMC) who achieved the technical experimentations presented in this paper.

### References

- [1] Lemont F. Management of metal chlorides in high temperature processes--application to the nuclear wastes treatment. J Hazard Mater. 2012 Apr 30;213-214:38-45. doi: 10.1016/j.jhazmat.2012.01.038. Epub 2012 Feb 3. PMID: 22365141.

## 6.3 Synthesis, Stability and Physico-Chemical Characterisation of a Reconditioned Waste Form Relevant to Radioactive Wastes

Gianni F. Vettese<sup>1</sup>, Taavi Vierinen<sup>1</sup>, Tandr   Oey<sup>2</sup>, Matti Nieminen<sup>2</sup>, Jaana Laatikainen-Luntama<sup>2</sup>, Markku Leivo<sup>2</sup>, Tapio Vehmas<sup>2</sup>, Emmi Myllykyl  <sup>2</sup>, Gareth T. W. Law<sup>1</sup> & Suvi Lamminm  ki<sup>2</sup>

<sup>1</sup>The University of Helsinki, Radiochemistry Unit, Helsinki, Finland,

<sup>2</sup>VTT Technical Research Centre of Finland, Helsinki, Finland

Main contact: [gianni.vettese@helsinki.fi](mailto:gianni.vettese@helsinki.fi)

**Keywords:** Geopolymer, characterisation, leachability

### 1. Introduction

Low and Intermediate Level radioactive Waste (LILW) typically includes operational wastes (i.e., contaminated materials) and ion-exchange resins (IXR) used in the cleaning of process water at nuclear plants. Although LILW represents only about 1 % of the total radioactivity of waste, it represents more than 95 % of the total volume. Finland alone generates over 300 m<sup>3</sup> of LILW annually <sup>1</sup>. Generally IXR waste is immobilised in a solid matrix and contained in a steel drum, where it is held in interim storage until the final disposal concept is ready. LILW final disposal in Finland is via burial in geological disposal, with waste emplaced in rock caverns ~ 100 m below surface.

In this research, ion-exchange resins have been thermally treated via gasification (Figure 1) and immobilised in a novel metakaolin geopolymer by VTT <sup>2</sup>. Here, treatment enables substantially higher loading of the LILW (more than 90% volume reduction) into the geopolymer without loss of matrix strength or cohesion. Currently, the chemical stability of the geopolymer and the encapsulated contaminants remain unknown. Here, we share early results on the characterisation and leachability of a novel geopolymer.

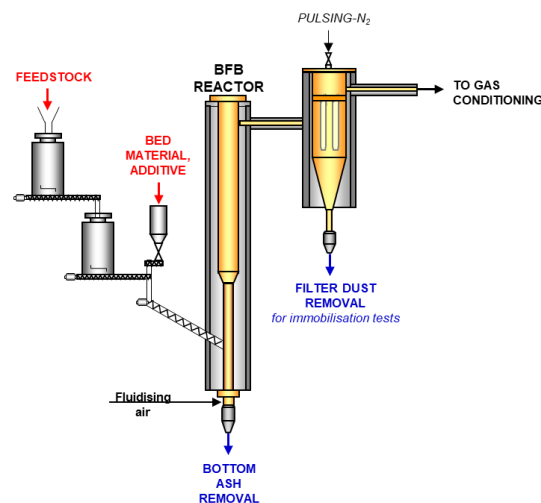


**Figure 6:** Schematic of the gasification process.

#### 1.1 Geopolymer Characterisation

The gasified ash represents 1% of the final geopolymer matrix and contains stable isotopes of Cs (200 mg/kg), Sr (20 mg/kg) Cr (3000 mg/kg), Co (40 mg/kg), and Ni (3000 mg/kg) representative of nuclear fission and activation products. Contaminants in ash are heterogeneously concentrated as dense agglomerations observable in electron imaging (Figure 2B). Geopolymer general structure is a  $\text{--Na/K-Al-Si(H)--}$  network, heterogeneous particles from ash are retained after encapsulation into the geopolymer matrix (Figure 2C).



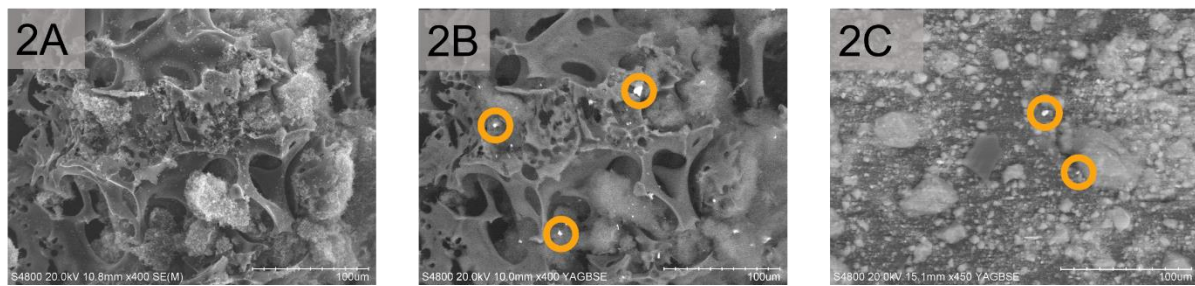


**Figure 7:** [A] Scanning Electron Microscopy (SEM) imaging of ion-exchange resin ash; [B] SEM-Back-Scattering Electron (BSE) image of ion-exchange resin ash; [C] ESEM-BSE of metakaolin geopolymers. Circles highlight dense agglomerations.

## 1.2 Geopolymer Leachability

During the final disposal of LILW, passing water will come into contact with concrete structures present in the facility creating a high ambient pH ( $\sim 12$ , CaOH buffered) rich solution that may leach the immobilised radionuclides from the geopolymer. Semi-dynamic leaching experiments assess the short- and long-term (1 month – 2 years) behaviour (see section 4) of the matrix and contaminants (Figures 3A-C). pH and conductivity remain stable at 12.5 and 8.5 mS/cm respectively. Na, Al, Si leach into solution on the scale of  $10^2$ - $10^3$  mg/kg, Ca and K are removed from solution into the geopolymer on the scale of  $10^1$ - $10^2$  mg/kg. Trace ( $10^{-3}$ - $10^{-1}$  mg/kg) amounts of Co, Cs, Cu, and Ni leach out of the geopolymer into the solution. Here, Sr and Cr are below the LOD (0.7 and 0.09  $\mu\text{g/kg}$ , respectively). Moreover, no colloids observed in leachate using dynamic light scattering or zetapotential analysis.

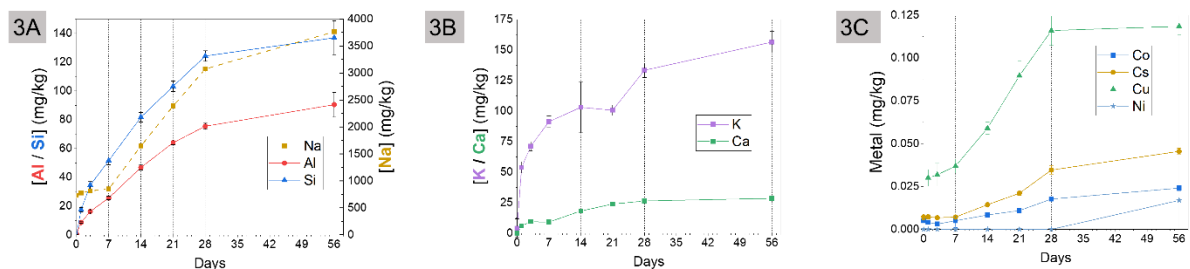


**Figure 8:** [A] Cumulative leaching of Al, Si, and Na; [B] Cumulative absorption of K and Ca; [C] Cumulative leaching of Co, Cs, Cu, and Ni.

## 1.3 Post-Mortem Analyses

Leached geopolymers are sacrificed, preserved, and dissected after 1 month, 6 months, 1 year and 2 years of leaching. Post-mortem analyses (XRD,  $\mu$ -CT, ESEM-EDX, EMPA &  $^{29}\text{Si}$  NMR) of the end points will yield information on the changing crystallinity and pore structure, evolution of the geopolymer matrix elements and trace contaminants.

## 2. Conclusions & Future Work

VTT has successfully developed a process to treat spent resins that significantly reduces the volume of resin to be disposed of and enables more efficient immobilization prior to disposal. Current experiments at The University of Helsinki assess the stability of the geopolymer when high pH leachate eventually passes through the stored waste. These first leaching tests have been running for 4 months as of 10/6/22 and are expected to last 24 months. Leached geopolymers are sacrificed and characterised after 1, 6, 12 and 24 months.

Soon we will receive a new set of geopolymers spiked with: i) higher ash loadings to assess the extremities of potential waste loading using thermal treatment; ii) elevated concentrations of Cs and stable actinide analogues Eu and Ce. Here, concentrations sufficiently high enough for nano-microscale analysis (XRF, XRD, and XAS) of local structure and bonding environments.



## Acknowledgements

This Project has received funding from the Euratom research and training programme 2019-2020 under grant agreement No 945098. SEM imaging and EDS measurements were done in ALD centre Finland research infrastructure.

## References

- (1) Kumpula, L.; Huhtanen, I.; Palander, S.; Ylä-Mella, M.; Kuhmonen, V. *Management of Spent Nuclear Fuel and Radioactive Waste in Finland*; 2021.
- (2) Vehmas, T.; Myllykylä, E.; Nieminen, M.; Laatikainen-Luntama, J.; Leivo, M.; Olin, M. Geopolymerisation of Gasified Ion-Exchange Resins, Mechanical Properties and Short-Term Leaching Studies. In *IOP Conference Series: Materials Science and Engineering*; Institute of Physics IOP, 2020; Vol. 818, p 012017.

## 6.4 Immobilization of the treated wastes by geopolymer or cement-based materials encapsulation

Maria Cruz Alonso, Agencia Estatal Consejo Superior de investigaciones Cientificas (CSIC), Spain, [mcalonso@ietcc.csic.es](mailto:mcalonso@ietcc.csic.es)

Francisca Puertas, Agencia Estatal Consejo Superior de investigaciones Cientificas (CSIC), Spain, [puertasf@ietcc.es](mailto:puertasf@ietcc.es)

Ines Garcia-Lodeiro, Agencia Estatal Consejo Superior de investigaciones Cientificas (CSIC), Spain, [iglodeiro@ietcc.csic.es](mailto:iglodeiro@ietcc.csic.es)

Pedro Perez-Cortes, Agencia Estatal Consejo Superior de investigaciones Cientificas (CSIC), Spain, [pedro.perez@ietcc.csic.es](mailto:pedro.perez@ietcc.csic.es)

**Keywords:** immobilization, geopolymer, cement, radioactive nuclear wastes

### 1. Introduction

This document describes the experimental work and compiles the main findings of the WP6 presented by CSIC at the 3rd PREDIS workshop that took place from April 25 to 28, 2022 at VTT in Espoo, Finland. Three different cementitious matrices based on geopolymer and cement, adapted for the immobilization of the two types of residues, were prepared and tested.

### 2. Description of work and main findings

- a. Task 6.4 Immobilization of the treated wastes by geopolymer or cement-based materials encapsulation

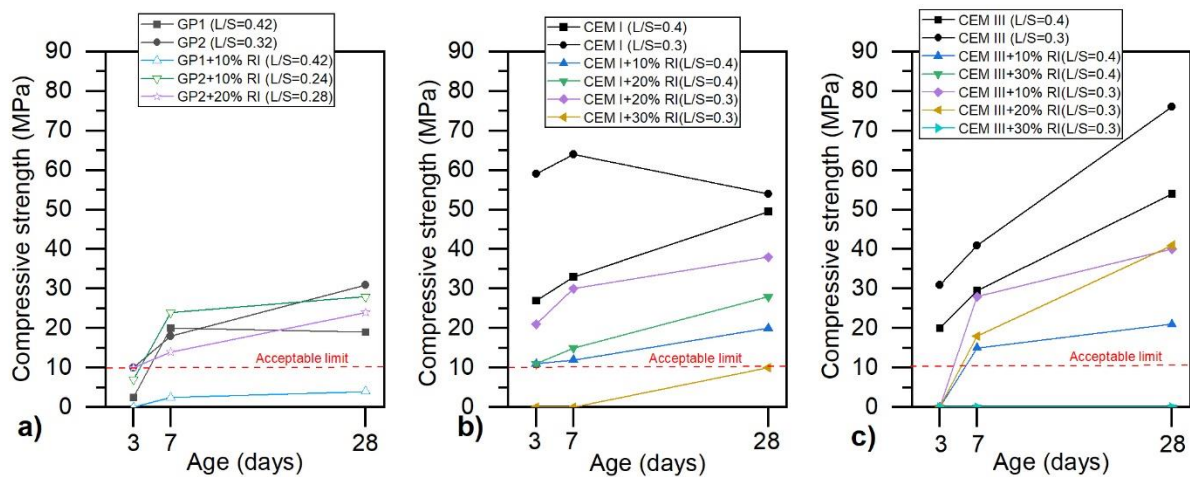
CSIC has been working on the design and development of geopolymer and cement matrices to immobilize two type of residues: a) thermally-treated ion-exchange resins (RI) supplied by CIEMAT and b) molten salt wastes (MS) supplied by CVRez. Table 1 describes the different systems that have been prepared and tested with several percentages of wastes. Pastes were prepared by mixing the solids with water, in which the liquid/solid ratio by mass (L/S) was adjusted to optimize the mechanical strength and achieve suitable fluidity. Prisms of 1\*1\*6 cm<sup>3</sup> were prepared and cured in the climatic chamber at 21°C and 99% RH until the testing ages.

**Table 2.** Cementitious systems used for the immobilization of the radioactive wastes.

System		Description/composition
Geopolymer based matrix	GP1	39%MK-36%BFS-25%NS/NH
	GP2	39%MK-36%BFS-25%NS/NH
Cement-based matrix	CEM I	CEM I 42.5 SR/MSR
	CEM III	CEM III/B 32.5 N/SR

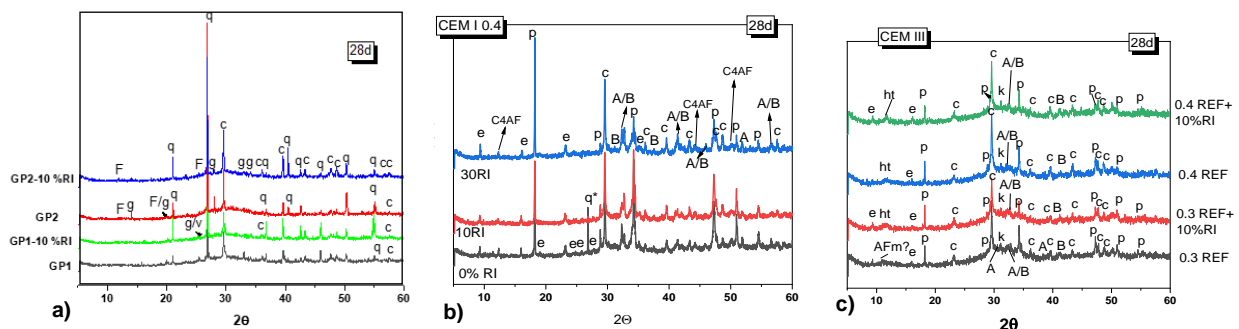
- i. Immobilization of the thermally-treated ion exchange resins (RI)

Figure 1 shows the compressive strengths of the geopolymers and cement-based cementitious systems, with and without the incorporation of the RI. GP-1 showed 28-day strength values of ~18 MPa and the incorporation of 10%RI had a negative effect, declining the strengths in more than 77 % (Fig. 1a). Based on this result, the GP system was improved, adjusting the l/s ratio and increasing the amount of activator (NS+HS) (GP-2 from Table 1). This adjustment favoured the progress of the reaction, densified the microstructure, increased in the mechanical strengths (~30 MPa at 28 days) and reduced the total porosity from ~30 % to ~ 25%. The incorporation of 10% and 20% of the RI in the GP-2 led to a 28-day compressive strength of ~28 MPa and ~24 MPa, respectively, satisfying the strength requirements (>10 MPa, [1]).



**Figure 9.** Compressive strength at 3, 7 y 28 days in pastes with and without the RI. a) Geopolymer based systems, b) CEM I based systems and c) CEM III based systems.

The two Portland cement-based systems with  $l/s$  of 0.4 performed a 28-day compressive strength of ~50 MPa; however, such values reduced substantially with the incorporation of RI (Fig. 1b and 1c), which correlated with an increase in the total porosity from ~20% to ~25% and an increase in the pore size. The use of  $l/s$  of 0.30 favored the compressive strength development in both cement-based systems. Although the incorporation of RI reduced the mechanical strength, values >30 MPa were achieved in both cement-based systems with 20%RI, satisfying the strength requirements [2]. Nonetheless, the incorporation of 30%RI was detrimental to the compressive strength development in both cement-based systems, affecting the hydration kinetics and delaying the setting process (pH in CEM III reduced from ~13 to ~8 when 30% of RI was incorporated, pH of RI=2.4).



**Figure 10.** XRD patterns at 28 days of samples with and without the RI a) GP1 and GP2, b) CEM I and c) CEM III Legend: q:quartz ( $\text{SiO}_2$ ), c: Calcite ( $\text{CaCO}_3$ ); v: vaterite ( $\text{CaCO}_3$ ), g: Gaylussite  $\text{Na}_2\text{Ca}(\text{CO}_3)_2 \cdot 5\text{H}_2\text{O}$ ; F: Na-Faujasite ( $\text{Na}_2\text{O} \cdot \text{Al}_2\text{O}_3 \cdot 2.1\text{SiO}_2 \cdot 6.7\text{H}_2\text{O}$ ), p: portlandite ( $\text{Ca}(\text{OH})_2$ ), e: ettringite  $/3\text{CaO} \cdot \text{Al}_2\text{O}_3 \cdot 3\text{CaSO}_4 \cdot 32\text{H}_2\text{O}$ , A: Alite ( $\text{C}_3\text{S}$ ), B: Belite ( $\text{C}_2\text{S}$ ),  $\text{C}_4\text{AF}$ : Ferritic phase.

The XRD analysis of the geopolymer and cement-based systems shows that the incorporation of RI did not affect the types of mineralogical phases detected (Fig. 2). In the geopolymers (GP1 and GP2, Fig. 2a), an amorphous hump, located between 24-36  $2\theta$ , associated with the condensation of the geopolymeric N-(C)-A-S-H gel [3] was identified; as secondary reaction products, different types of carbonates and small peaks of Na-faujasite were detected. In the cement-based systems, portlandite, ettringite and anhydrous clinker phases were identified while hydrotalcite was detected only in CEM III (Fig. 2b and 2c).

## ii. Immobilization of the molten salt wastes (MS)

Figure 3 shows the compressive strengths of the geopolymers and the cement-based cementitious systems, with and without the incorporation of the MS. Similarly as for the incorporation of the RI, GP-2 performed better than GP-1 when 10% of the MS was incorporated as GP-2+10%MS achieved up to ~45 MPa at 28 days, overpassing the mechanical strength of the reference (without MS) and the strength requirements for the immobilization of radioactive wastes [2] (Fig. 3a). In line with this, the total porosity in GP-2 reduced from 25 to 15% when 10% of MS was incorporated. Nonetheless, the incorporation of 30% of the MS in the GP-2 had

a deleterious effect as the samples broken after 7 days of curing, which can be related to the crystallization of gaylussite ( $\text{Na}_2\text{Ca}(\text{CO}_3)_2 \cdot 5\text{H}_2\text{O}$ ), pirsonnite ( $\text{Na}_2\text{Ca}(\text{CO}_3)_2 \cdot 2\text{H}_2\text{O}$ ), and thermonatrite ( $\text{Na}_2\text{CO}_3 \cdot \text{H}_2\text{O}$ ) (Fig. 4a).

The incorporation of 30% of the MS in the cement-based systems reduced the 28-day compressive strength in 84% for CEM I and 89% for CEM III; in both cases, with values below the strength requirements [2] (Fig. 3b). The decrease in the mechanical strength of the cement-based samples with 30%MS is related to a substantial increase in the total porosity (2-3 times relative to the references) and changes in the pore size distribution, increasing the volume of pores higher than 1  $\mu\text{m}$ . In addition, the incorporation of 30% MS in both cement-based systems promoted the formation of calcite and limited the formation of portlandite (Fig. 4b and 4c); gaylussite was also identified in CEM III+30%MS (Fig. 4c).

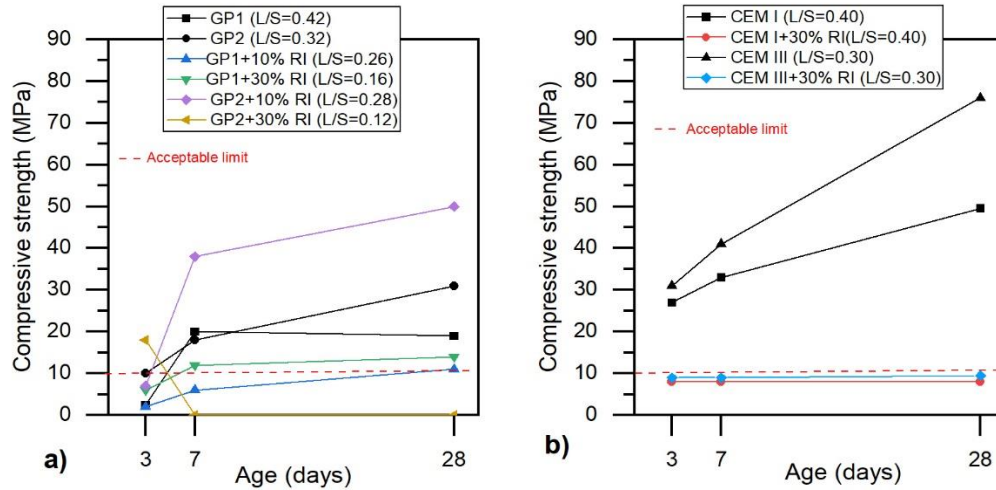


**Figure 11.** Compressive strength at 3, 7 y 28 days in pastes with and without the MS. a) Geopolymer based systems, and b) cement-based systems.

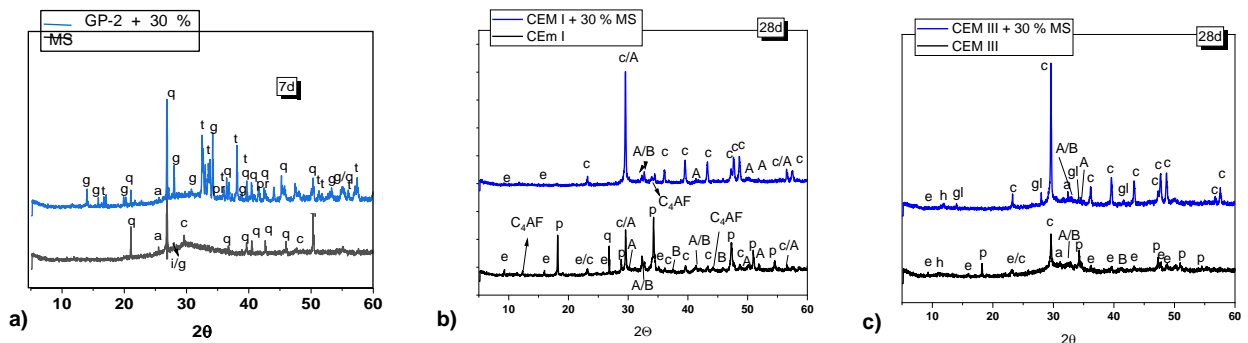


**Figure 12.** XRD patterns of samples with and without the MS a) GP-2, b) CEM I and c) CEM III Legend: q:quartz ( $\text{SiO}_2$ ), c: Calcite ( $\text{CaCO}_3$ ); g: Gaylussite  $\text{Na}_2\text{Ca}(\text{CO}_3)_2 \cdot 5\text{H}_2\text{O}$ ; t: thermonatrite ( $\text{Na}_2\text{CO}_3 \cdot \text{H}_2\text{O}$ ); pr: pirsonnite ( $\text{Na}_2\text{Ca}(\text{CO}_3)_2 \cdot 2\text{H}_2\text{O}$ ); p: portlandite ( $\text{Ca}(\text{OH})_2$ ), e: ettringite  $/3\text{CaO} \cdot \text{Al}_2\text{O}_3 \cdot 3\text{CaSO}_4 \cdot 32\text{H}_2\text{O}$ , A: Alite ( $\text{C}_3\text{S}$ ), B: Belite ( $\text{C}_2\text{S}$ ),  $\text{C}_4\text{AF}$ : Ferritic phase.

Studies by calorimetric conduction (ICC) show that the inclusion of MS changes the kinetic of hydration in the cement-based systems. After a short induction period, new peaks appeared in both systems, probably due to the precipitation of carbonates (Fig. 5a); this was accompanied by an increase in the pH value. The reduction of the total heat released in both cement-based samples with 30%MS (Fig. 5b) could be related to a dilution effect, but probably is also an indication that the cements are not being properly hydrated.

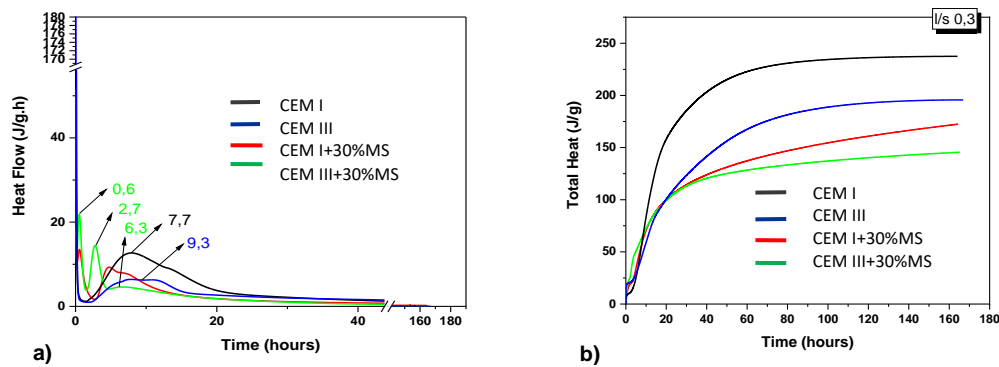


Figure 13. ICC in cement-based systems with and without the MS, a) heat flow b) total heat.

### 3. Way forward

- Tailoring of the geopolymer and cement-based cementitious matrices according to the waste features since different wastes require different geopolymer designs.
- Densify the cementitious materials (especially in geopolymer).
- Characterization of the waste-cementitious matrix interaction.
- Pre-treatment of the Molten Salts.  $\rightarrow \text{Na}_2\text{CO}_3 + \text{Ca}(\text{OH})_2 \text{ susp.} \rightarrow \text{CaCO}_3 + 2\text{Na}(\text{OH}) \text{ aq.}$

For the Task 6.6: “Physico-chemical characterization of the reconditioned waste form and stability testing”, prismatic specimens of  $1 \times 1 \times 6 \text{ cm}^3$  (prepared by CSIC and cured for 56 days at  $21^\circ\text{C}$  and 99% relative humidity) will be immersed into three different leaching media: a) synthetic cementitious water (CSIC), b) Cabril site water (CIEMAT), and deionized water (UAM). The characterization of solids includes mechanical strength (CSIC), micro-tomography (UAM), DRX (UAM/CSIC), porosity BET (CIEMAT), porosity MIP (CSIC), SEM (UAM/CSIC/CIEMAT) TG/DTA (CSIC/CIEMAT) RMN (CSIC). The analysis of the solutions includes pH, electrical conductivity, and elemental concentrations (CSIC/CIEMAT/UAM).

### References

- [1] Alonso, MC, García Calvo, JL, Petterson S; Cuñado MA; Vuorio M; Weber H.; Ueda H; Naito M. Development of an Accurate Methodology for Measure the Pore Fluid pH of Low-pH Cementitious Materials. Cement Based materials for nuclear waste storage. Edt. Springer. Edts.F. Bart, C. Cau-dit-Coumes, F Frizon and S. Lorente, p. 251-259, 2013.
- [2] ENRESA. Criterios de Aceptación de Unidades de Almacenamiento. Referencia 031-ES-IN-0002 rev. 1. Julio 2008.
- [3] I. García-Lodeiro, A. Fernández-Jiménez, A. Palomo, D.E. Macphee, Effect of calcium additions on N–A–S–H cementitious gels, Am. Ceram. Soc., 93 (7), p. 1934-1940, 2010.

## 6.5 Immobilization of spent salt from MSO process

*Vojtěch GALEK<sup>1</sup>, Anna ČERNÁ<sup>1</sup>, Petr PRAŽÁK<sup>1</sup>, Tomáš ČERNOUŠEK<sup>1</sup>, Martin VACEK<sup>1</sup>, Vojtěch BERGER<sup>2</sup>, Jan HADRAVA<sup>1</sup>*

<sup>1</sup>Research Centre Řež, Hlavní 130, Husinec-Řež, 250 68, Czech Republic, cvrez@cvrez.cz

<sup>2</sup>Czech Technical University in Prague, Jugoslávských partyzánů 1580/3, Prague 6 - Dejvice, 160 00, Czech Republic, cvut@cvut.cz  
Vojtech.galek@cvrez.cz

**Keywords:** Geopolymer, Molten Salt Oxidation, molten salt waste

### 1. Introduction

Organic waste is generated in every science field in the world. In nuclear facilities, the contaminated organic compounds are even more dangerous and must be safely disposed of. One type of organic waste is Ion Exchange Resins (IER). These organic granules are utilized in the nuclear industry to clarify and process water (1). These resins are used to remove unwanted impurities, such as radioactive and hazardous contaminants. Over time, the IER must be regenerated or replaced; when this happens, they must be properly disposed of (2). Direct immobilization of the IER is specific as high volume, and water swelling could damage the immobilization matrix. The volume reduction offers the possibility of immobilizing a lower amount of the IER with different conditions. The thermal decomposition of the IER is widely spread for the volume reduction processes, such as combustion. Still, due to the high CO<sub>2</sub> emissions, the other thermal processes could substitute the conventional ones. (3)

One of the promising thermal processes is the Molten Salt Oxidation (MSO). With molten alkaline carbonates, the acidic gases from the waste are captured within the salt and neutralized in the salt melt, forming corresponding stable salts. The non-combustible substances such as heavy metals and radionuclides are trapped in the molten salt. Some metals react with the alkali salts and form corresponding salts or metal oxides. (3,4).

### 2. Description of work and main findings

This work aimed to stabilize the spent salt from the MSO process with high content of alkaline carbonates in the geopolymer matrix. The physical and chemical properties of the geopolymer and spent salt were measured. The spent MSO salt was obtained during the decomposition of the 5 kg of IER (Purolite C100 H, DETO Brno, s.r.o.) in 25 kg of the Na<sub>2</sub>CO<sub>3</sub> (1<sup>st</sup> reactor) and 25 kg of Na<sub>2</sub>CO<sub>3</sub> (2<sup>nd</sup> reactor). The salt was taken and dried in up to moisture content of 20 wt.%. The dried salt was crushed to a fine powder and then dried up to 2.3 wt.% moisture content. The results of XRF semiquantitative chemical analysis are shown in table 1.

**Table 1:** The results of XRF analysis of the 2<sup>nd</sup> batch of spent MSO salt.

Component	Al <sub>2</sub> O <sub>3</sub>	Na <sub>2</sub> O	NiO	SiO <sub>2</sub>	MgO	Fe <sub>2</sub> O <sub>3</sub>	CaO	K <sub>2</sub> O	SO <sub>3</sub>
Mass, wt. %	6.24	84.50	0.23	6.17	0.25	0.23	0.14	1.66	0.19

CVRez used two batches of spent salt for the experiments. The first batch had a similar chemical composition as the spent salt but with different moisture content, which was determined to be 15 wt.%. So the only difference between the samples was the W/S ratio. Table 2 shows the geopolymer matrix's composition with a determined W/S ratio.

**Table 2:** The geopolymer matrix composition.

Batch Nm.	W/S ratio	Geopolymer (binder 10 wt.%) (g)	Waste load (wt.%)	Spent salt (g)	Geopolymer (g)	Activator (K <sub>2</sub> SiO <sub>3</sub> - 40 wt.%) (g)
1 <sup>st</sup> batch	0.63	170	5	85	802.78	642.22
	0.59	170	10	170	755.56	604.44
2 <sup>nd</sup> batch	0.61	170	5	85	802.78	642.22
	0.56	170	10	170	755.56	604.44



After synthesis, the mortar was put in each section of the mould. For the curing, the sealed bag option was chosen. The mould was covered with tin foil and put into a sealed plastic bag. This curing method provided the same conditions for each sample. The samples were left to cure for 28 days before they were opened and removed from the mould.

The results of mechanical testing of each waste load sample are shown in figure 1.

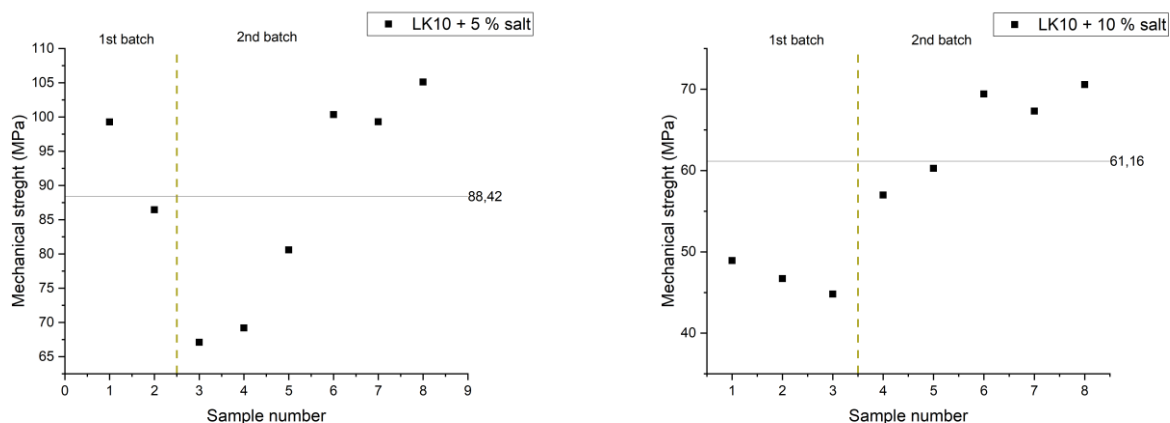


**Figure 14:** The results of the mechanical stress test for both waste load type matrices.

As shown in figure 1, the results differ highly with the lower waste loading, and the mechanical strength ranges from 66 MPa up to 105 MPa with an average of 88.42 MPa. In the 5 wt.%, the difference between the 1st and 2nd batch is not that substantial. For the 10 wt.% waste loading, the overall mechanical strength was lower, ranging from 44.81 MPa up to 70.55 MPa, averaging 61.16 MPa. The overall mechanical strength is high, which predicts good durability for some cases of unexpected mechanical damage. But the values differ significantly, so other experiments must be done to gain better statistics data.

The ultrasonic pulse velocity was measured with the same samples; the results are shown in figure 2.

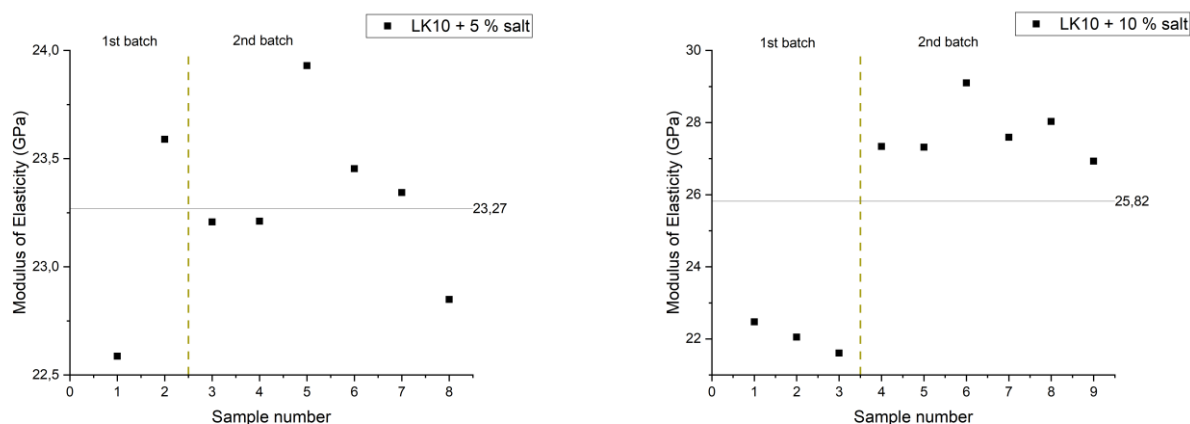


**Figure 15:** The results of the ultrasonic pulse velocity for both waste load type matrices.

For the 5 wt.% waste loads, the modulus of elasticity ranges from 22.6 GPa to 24 GPa, with an average of 23.27 GPa. These values mean that samples are homogenous in their bulk, corresponding to high mechanical strength and the uniformity of the bulk. On the other hand, the higher waste load, 10 wt.%, shows a big difference between the 1<sup>st</sup> and 2<sup>nd</sup> batch of spent salt. The first batch had a lower modulus of elasticity, which could be explained by higher moisture content and not completely stabilized bulk. The 2<sup>nd</sup> batch got an even higher modulus of elasticity than the lower waste load, which could mean evenly mixed geopolymers and complete inner reaction. The modulus of elasticity of the 10 wt.% waste loads ranged from 21.60 GPa to 29.10 GPa, with an average value of 25.82 GPa.

### 3. Summary

This work aimed to stabilize the spent MSO salt into the geopolymer matrix. With the experience gained through previous experiments, the group now aims for the geopolymer matrix's statistics with waste loading up to 25 wt.%. The results were aimed to obtain the proper chemical analysis of the spent salt and the moisture content, which determine the W/S ratio of the samples. The mechanical stress and ultrasonic pulse velocity analysis were performed to get the samples' physical properties. The future work is to prepare more samples to get more precise statistics of samples up to 25 wt.% waste loading. The recipe would need some update to change the W/S ratio for higher waste loading. The ongoing experiments are shrinkage and high moisture environment curing. The chemical analysis of the samples is in progress.

### Acknowledgements

This project has received funding from the Euratom research and training programme 2019-2020 under grant agreement No 945098.

### References

- [1] Yang, H. C., Cho, Y. J., Eun, H. C., Yoo, J. H., & Kim, J. H. (2005). Molten salt oxidation of ion-exchange resins doped with toxic metals and radioactive metal surrogates. *Journal of Nuclear Science and Technology*, 42(1), 123–129. <https://doi.org/10.1080/18811248.2005.9726371>
- [2] C. A. Cicero-Herman, et al., Commercial Ion-exchange Resin Vitrification in Borosilicate Glass, WSRC-MS-98-00392, Westinghouse Savannah River Co., 1–4 (1998).
- [3] Yao, Z., Li, J., & Zhao, X. (2011). Molten salt oxidation: A versatile and promising technology for the destruction of organic-containing wastes. *Chemosphere*, 84(9), 1167–1174. <https://doi.org/10.1016/j.chemosphere.2011.05.061>
- [4] Hsu, P. C., Foster, K. G., Ford, T. D., Wallman, P. H., Watkins, B. E., Pruneda, C. O., & Adamson, M. G. (2000). Treatment of solid wastes with molten salt oxidation. *Waste Management*, 20(5–6), 363–368. [https://doi.org/10.1016/S0956-053X\(99\)00338-4](https://doi.org/10.1016/S0956-053X(99)00338-4)

## 6.6 Treatment of surrogate ion exchange resin and conditioning of residues in a novel geopolymer matrix

*Eros Mossini, Andrea Santi, Francesco Galluccio, Gabriele Magugliani, Marco Giola,  
Elena Macerata, Enrico Padovani, Mario Mariani  
Politecnico di Milano (POLIMI), Italy  
[eros.mossini@polimi.it](mailto:eros.mossini@polimi.it)*

**Keywords:** Thermal treatment, wet-oxidation, encapsulation, tuff-based geopolymer

### 1. Introduction

Within the treatment of the radioactive solid organic waste (RSOW), aiming at reducing the waste volume and at the same time preventing the release of volatile contaminants, two different processes were addressed:

1. a dry oxidative (dry-ox) procedure, in which up to 15 g of nuclear-grade cationic IER were beforehand loaded with cations usually present in real waste and then incinerated in a muffle furnace at 800 °C;
2. a Fenton-like wet oxidative (wet-ox) process as a green alternative approach [1]. A focused optimization study allowed a first scale-up of the process from up to 200 g of cationic resin. Thereafter, the successful decomposition has led to the treatment of a mixed resin bed system composed of equal amounts of loaded strong cationic and anionic IERs as a more representative surrogate waste. A scale-up of the process up to 200 g is being pursued at POLIMI.

The ashes resulting from the dry oxidative process were characterized by Raman, IR, XRD, and elemental ICP-MS. It was demonstrated that sulphate salts were obtained, with no losses and without measurable organic contamination, and high mass and volume reductions were achieved.

The evolution of the wet oxidation process over time is representative of a very promising decomposition and mineralization of the organic matter, thereafter, confirmed by the preliminary characterization studies conducted.

Regarding the encapsulating matrix, POLIMI has focused its efforts on the development of a metakaolin-free geopolymer (GP), using volcanic tuff (VT) as a precursor due to its worldwide availability, low economic and environmental costs, high durability, satisfactory reactivity, and high cation exchange capacity (CEC). The addition of fly ash (FA) and blast-furnace slag (BFS) to the tuff powders increased the reactivity of the mixture, allowing geopolymerization reactions to occur at room temperature [2]. The CEC of VT proved to be higher than for MK, suggesting promising radionuclides retention in the VT-based GPs [3]. Moreover, the developed matrix proved satisfactory encapsulating behaviours, allowing the loading of different surrogate RSOW, such as IRIS ashes (CEA), dry-ox and wet-ox residues (POLIMI).

### 2. Description of work and main findings

#### Methods

##### Dry oxidative treatment

Dry oxidative processes were investigated at the scale of 15g batches, employing cationic nuclear-grade ion-exchange resins loaded with cations representative of fission and activation products, namely  $\text{Cs}^+$ ,  $\text{Sr}^{2+}$ ,  $\text{Co}^{2+}$ ,  $\text{Ni}^{2+}$ ,  $\text{Nd}^{3+}$ ,  $\text{Eu}^{3+}$ . The loading was performed for 1 h, afterwards the supernatant was removed and analysed via ICP-MS to assess the loading factor, while the resin underwent drying for 2 h at 90 °C and incineration in a muffle furnace at 800 °C for residence times up to 39 h. Characterisation of the residues was performed via XRD, Raman and IR spectroscopy.

##### Wet oxidative treatment

The process consists of an exothermic reaction of a catalyst and an oxidant by the production of reactive radicals that decompose organic matter. The presence of anionic resin entailed the addition of  $\text{CuSO}_4 \cdot 5\text{H}_2\text{O}$  to the  $\text{FeSO}_4 \cdot \text{H}_2\text{O}_2$  reaction system as co-catalyst to enhance the oxidation yield of the surrogate waste. The decomposition of a mixed resin bed was firstly performed by treating about 20 g of unloaded resins without any external heat supply in 3 hours. Thereafter, 100 g of a mixed resin bed system was prepared by loading same amounts of cationic and anionic resins (DuPont Amberlite IRN 77-78) with Cs, Co, Sr, Ni, I, Cl ions as representative of fission, activation and corrosion products.

The reaction temperature reaches a first peak of about 90 °C that can be related to cationic resin decomposition. Thereafter, a second peak at about 95 °C marks the beginning of the anionic resin degradation. The temperature remains constant for long, then it plummets when organic matter has been completely mineralized. Besides temperature, the colour shift of the resin mixture has been helpful to monitor the evolution of the treatment. Indeed, the orange solution gradually turns black in correspondence with the first temperature peak, then hazel-coloured and beyond yellow as the organic matter degrades within 8 hours.

Finally, the mineralized solution undergoes an evaporation process at controlled temperature of 70 °C in order to avoid volatile nuclide leakage, thereby obtaining a moist and brownish residue to be immobilized in a geopolymeric matrix.

A scale-up of the process from 100 g to 200 g of mixed resin bed has been recently managed in 12 hours at POLIMI.

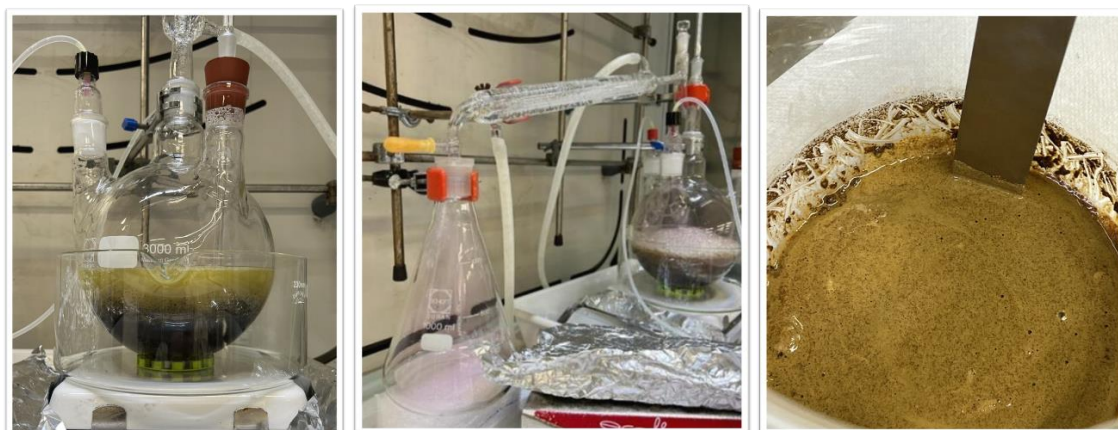


**Figure 1.** Wet oxidation in progress (left), pink coloured off-gas as first evidence of iodine release (middle), and the obtained brownish residue after the evaporation process (right).

#### Determination of the cation-exchange capacity of volcanic tuff

Cation Exchange Capacity (CEC) of the Volcanic Tuff (VT) was investigated in comparison with metakaolin (MK) by means of batch experiments. Several solutions containing known amounts of different cations ( $\text{Cs}^+$ ,  $\text{Sr}^{2+}$ ,  $\text{Co}^{2+}$ ,  $\text{Ni}^{2+}$ ,  $\text{Nd}^{3+}$ ,  $\text{Eu}^{3+}$ ), chosen as representatives of fission and activation products, were contacted with known amounts of VT and MK for few hours, to reach the thermodynamic equilibrium. Afterwards, the supernatant was separated by centrifugation and analysed via ICP-MS to assess the amount of non-exchanged cations.

#### Preparation of the tuff-based geopolymeric matrices

Weighed amounts of raw materials, additives, and activators were mixed to prepare the VT-based geopolymer (GP). The precursor mixture comprises fly ash (FA) and blast-furnace slag (BFS) provided by the KIPT. The activator is sodium hydroxide. Alumina was added to optimize the Si/Al stoichiometric ratio. Different formulations were prepared by varying the contents of raw materials. After casting in cylindrical moulds, curing was performed at room temperature in different configurations: mould, open air, dry chamber, water-saturated chamber. The resistance to compressive strength, water immersion (ANSI/ANS-16.1-2003 protocol), and thermal treatment (by TGA) were tested.

#### Loading of surrogate inactive waste into the matrix

Weighed amounts of surrogate waste were added to the freshly prepared VT-based grout, before its casting, and homogenized in the mixture. Ashes coming from the IRIS plant managed by the CEA were successfully encapsulated up to 20 %wt., while the residues from the wetox treatment were preliminary immobilized up to 40 wt% and evaluated by visual inspection.

## **Results**

#### Dry oxidative treatment

Single-cation and multi-cation incineration batches were carried out. According to the chemical behaviour of the loaded metal, different residues were obtained (see Figure 2):

- Cs- and Sr-loaded resins degraded into sulphates;
- Nd- and Eu-loaded resins degraded into oxide sulphates;
- Co- and Ni-loaded resins degraded into oxides.

XRD showed high crystallinity of the degraded material, while Raman and IR spectroscopies confirmed total organic degradation for batches incinerated for 39 h. Regarding mass reduction, factors up to 98 %wt. were derived for resin loading of 50 eq% of their capacity.

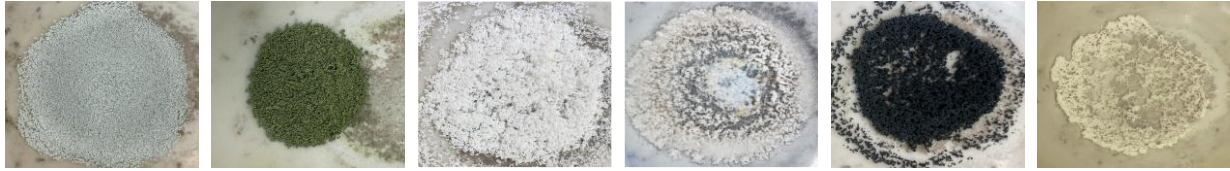


**Figure 2.** Residues from dry oxidative treatment. From left to right: Nd-, Co-, Eu-, Cs-, Co-, and Sr-loaded resins.

#### Wet oxidative treatment

The color shift of the resin mixture and the reaction temperature monitored over time point out that decomposition and mineralization of the organic matter happened. The left brownish residue obtained from the evaporation process resulted in a weight reduction rate of about 80% in all the three mixed resin bed systems (20 g, 100 g, 200 g). In addition, XRD analysis carried out on the left residue to identify obtained compounds mainly showed the presence of ammonium iron/copper sulfates. Nuclides distribution is being also evaluated via ICP-MS analysis that points out very promising retention of Cs, Co, Sr, Ni, while most of I and Cl are collected as off-gases downstream of the process in the arranged bubblers.

#### Cation-exchange capacity of volcanic tuff

CECs of VT and reference MK were computed as the exchanged cation equivalents per unit mass of material. Investigation was performed to understand and compare the interaction between these raw materials and the loaded waste. The values of VT proved to be higher than for MK for each of the six studied cations. Results showed that the highly zeolitized VT exhibits CEC one order of magnitude greater than that of MK for some cations, such as Cs<sup>+</sup> and trivalent lanthanides, while the gap is smaller for the other metals, namely cobalt, strontium, and nickel. Nevertheless, VT still exhibits the higher values. In addition, XRD of geopolymers highlighted the presence of zeolite peaks, proving their preservation during alkaline activation. Thus, the idea of employing highly zeolitized materials as GP precursors could feasibly improve waste-matrix interaction and radionuclides retention.

#### Geopolymerised waste forms

The addition of FA and BFS to the VT powders increased the reactivity of the precursors and allowed the hardening of the grouts. Six different formulations were tested by varying the amounts of raw materials and activator. An optimal one was identified according to the higher compressive strength (well above the WAC of 5 MPa at 28 days), and water-saturated chamber resulted to provide the best curing conditions. Besides satisfactory compressive strengths, water immersion tests, carried out for a total duration of 2 weeks, confirmed the stability of the matrix. The release rates of the main matrix constituents were measured and used to derive the leachability indices, which resulted far greater than the WAC of 6. Finally, preliminary evidence of thermal resistance was obtained by TGA.

Residues from wet oxidative treatment required efforts to be encapsulated within the VT-based geopolymer due to their extremely low pH, incompatible with the alkaline activation of the matrix. Preliminary immobilisations were achieved by compensating acidity with the further addition of activator. Such procedure allowed the encapsulation of the sludge up to 40 %wt., which was evaluated by visual inspection (see Figure 3). Regarding the ashes produced in the IRIS plant managed by the CEA, more detailed characterisation was performed. Compliance with WAC of both compression and water immersion was successfully proved for loadings up to 10 %wt., while assessments are still being carried out on samples 20 %wt. loaded.



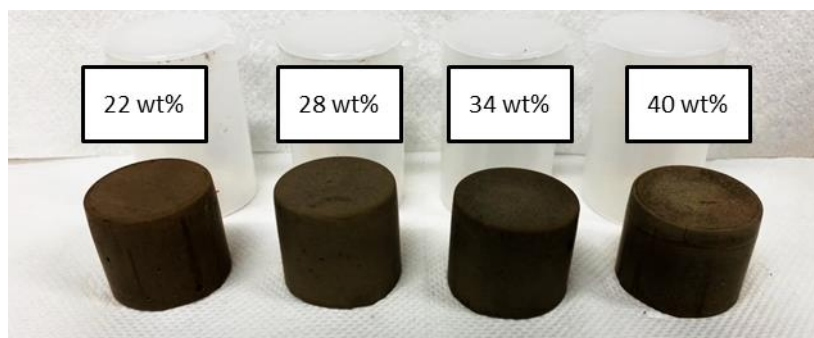


**Figure 3.** Preliminary waste forms obtained by encapsulating the sludge from wet oxidative treatments.

### 3. Conclusions

#### Dry and wet oxidative treatments

Despite the high mass reductions and the good stabilisation of the waste obtained using dry oxidative treatments, the high temperatures involved and the long residence times, together with the complex management of the gas streams, hamper the scale-up.

On the other side, wet oxidative process is a more sustainable approach due to low oxidation temperature (< 100 °C), cheap and non-toxic catalyst, and green oxidant. What is more, this kind of treatment shows low energetic costs, simple off-gas treatment, low risk of corrosion and potential volatilization of radionuclides. The weight reduction rates obtained so far are very promising and they move towards an impressive minimization of waste package volumes besides the gained physical and chemical stability of the matrix.

POLIMI research team is planning to complete characterization study by performing Chemical Oxygen Demand tests on aliquots of the resin mixture collected during the oxidative process in order to prove the complete degradation of organic matter in accordance with the XRD results. Furthermore, monitoring and collection of the off-gases (CO<sub>2</sub>, I and Cl) are being considered as one more proof of the organic matter degradation and to accomplish final closure of the process optimization study.

Finally, POLIMI outlook envisages an implementation of a more representative process scale-up to manage up to 1 kg of mixed resin bed by optimizing amounts of reagents and reaction time.

#### Geopolymerised waste forms

Information obtained by microstructural characterisation of the raw materials, with regard to zeolites, confirm the presence of a chemical barrier for the waste, in addition to the physical one provided by the matrix itself, when VT replaces MK in the grouts. Overall, the properties of the VT-based matrix are compliant with WAC and proved to be compatible with the surrogate RSOW investigated up to now, and further experimental work is required to understand the encapsulating behaviour towards other waste and to assess the properties of the waste within the final waste forms.

### Acknowledgements

This project has received funding from the Euratom research and training programme 2019-2020 under grant agreement No 945098.

### References

- [1] L. Xu, X. Meng, *et al.*, Dissolution and degradation of nuclear grade cationic exchange resin by Fenton oxidation combining experimental results and DFT calculations. *Chem. Eng. J.* **361**, p. 1511-1523, 2019.
- [2] W. Lee, *et al.*, Geopolymer technology for the solidification of simulated ion exchange resins with radionuclides. In: *Journal of Environmental Management*, **235**, p. 19–27, 2019.
- [3] W. Baek, S. Ha, S. Hong, *et al.*, Cation exchange of cesium and cation selectivity of natural zeolites: Chabazite, stilbite, and heulandite. *Microporous and Mesoporous Materials*, **264**, p. 159-166, 2018.



## 6.7 Immobilization of molten salt in alkali-activated and cement-based materials

*Lander Frederickx, Eduardo Ferreira, Quoc Tri Phung\**  
*Belgian Nuclear Research Center (SCK CEN), Belgium, \*quoc.tri.phung@sckcen.be*

### Abstract

In the context of PREDIS work package 6, the immobilization of a molten salt waste stream, received from CV Rez (Czechia) was investigated. The matrices investigated include alkali-activated (based on ground granulated blast furnace slag and metakaolin) and cementitious (blended system) binders. The molten salt was found to consist of hydrated sodium carbonate minerals. The direct immobilization of this salt produced materials which are especially sensitive to changes in humidity and temperature, which is undesirable for a waste form. Therefore, the sodium carbonate salts were reacted with  $\text{Ca(OH)}_2$  and  $\text{Ca(NO}_3)_2$  to form  $\text{CaCO}_3$ , which is insensitive to changes in temperature and humidity. The pretreated salt was then immobilized in the aforementioned matrices. In the case of alkali-activated binders, the  $\text{Ca(NO}_3)_2$  pretreated salt did not produce a stable waste form due to nitrate ions interfering with the geopolymerization process. The  $\text{Ca(OH)}_2$  pretreatment did produce waste forms with acceptable mechanical strengths. In the case of the cementitious binder, both the  $\text{Ca(OH)}_2$  and  $\text{Ca(NO}_3)_2$  pretreatments were found to produce materials with good mechanical strengths which are resistant to temperature and humidity changes. A remaining challenge involves the extent to which  $\text{CaCO}_3$  is formed in the pretreatment instead of the intermediary  $\text{Na}_2\text{Ca(CO}_3)_2 \cdot 5\text{H}_2\text{O}$  phase which is potentially unstable on the long term.

**Keywords:** cementitious materials, alkali-activated materials, geopolymer, sodium carbonate, molten salt, waste immobilization

### 1. Introduction

Solid radioactive waste, generated by several nuclear applications, must be conditioned in a stable matrix prior to storage and disposal. Among others, immobilization in an alkali-activated or cementitious matrix are being studied and implemented in many countries.

In work package 6 of PREDIS project, the immobilization of molten salt waste stream is investigated. The molten salt was received from CV Rez (Czechia) and the immobilization was done in two matrices: alkali activated and cementitious.

The molten salt is composed mainly of  $\text{Na}_2\text{CO}_3$ . Its presence has an positive effect on the use of alkali-activated materials using metakaolin precursor (Provis & Van Deventer, 2013). Besides that, the use of ground granulated blast furnace slag (BFS) as a precursor is well-known in the literature.

To immobilize the salt in cementitious materials, previous experience within SCK CEN waste and disposal group shows that a blended cement matrix could be used (Phung et al., 2021). A blended system with ordinary Portland cement (OPC), BFS, silica fume, lime and limestone filler was used.

The main goal of this project is to demonstrate the reliability of the mentioned binders for conditioning this residue. For that, a research plan was drafted to verify the matrix performance of conditioned waste over time according to several criteria and to improve the understanding of its behaviour.

### 2. Materials & Methods

#### Nature of molten salt

The molten salt, received from CV REZ (Czechia), was found to have a high water content at 56 wt%. The salt was air dried at room temperature for three weeks, after which the water content was reduced to 16 wt% (determined by oven drying at 200°C). The mineral composition of this air-dried salt consists of sodium carbonate in various hydration states: 77 wt.% thermonatrite ( $\text{Na}_2\text{CO}_3 \cdot \text{H}_2\text{O}$ ), 22 wt.% trona ( $\text{Na}_2\text{CO}_3 \cdot \text{NaHCO}_3 \cdot 2\text{H}_2\text{O}$ ) and 1 wt.% natron ( $\text{Na}_2\text{CO}_3 \cdot 5\text{H}_2\text{O}$ ).

### Immobilisation in alkali-activated materials

The precursors used for the immobilization in alkali-activated materials were metakaolin and ground granulated blast furnace slag. In the preparation of a reference, i.e. without molten salt, material, the precursor is mixed with an activating solution in a planetary mixer. After an initial mixing step, sand is added to create a mortar. The activating solution is prepared by dissolving a sodium disilicate ( $\text{Na}_2\text{O} \cdot 2\text{SiO}_2$ ) in a solution of 10M NaOH. Depending on the formulation, an amount of water is added to the activating solution as well.

In trials A1 and A2, the molten salt is added to the mixture after the initial mixing step of precursor and activating solution. In trial A3, the molten salt is reacted with  $\text{Ca}(\text{NO}_3)_2$ , after which  $\text{Na}_2\text{O} \cdot 2\text{SiO}_2$  and NaOH are added to the slurry. The slurry of salt and activating solution is then added to the precursor to prepare the alkali-activated material. Trial A4 was similar to trial A3 with the difference that  $\text{Ca}(\text{NO}_3)_2$  is replaced by  $\text{Ca}(\text{OH})_2$ .

Curing time and conditions were varied between trials to test the effect of humidity on the immobilized waste form (**Table 3**).

**Table 3:** Overview of the factors varied in the different trial tests for alkali-activated materials. A water/solid ratio is used instead of a water/binder ratio, as the pre-treatment of the molten salt generates NaOH, which acts as an activating molecule for the precursor, thereby making the calculation of the amount of binder unsure.

Trial	Precursor	Waste loading (wt%)	water/solid ratio	Pretreatment	Curing
A1	BFS	20, 30, 40	0.27, 0.22, 0.28	NA	14 days (sealed)
A1	MK	20, 30, 40	0.42, 0.36, 0.30	NA	14 days (sealed)
A2	MK	28, 32, 39, 36	0.70, 0.61, 0.66, 0.71	NA	7 days (sealed)
A3	MK	5, 6, 8, 9, 11	0.55, 0.52, 0.48, 0.50, 0.46	$\text{Ca}(\text{NO}_3)_2$	7 days (sealed)
A4	BFS	10, 15	0.33, 0.31	$\text{Ca}(\text{OH})_2$	28 days (sealed and/or humid)
A4	MK	10, 15	0.50, 0.46	$\text{Ca}(\text{OH})_2$	28 days (sealed and/or humid)

### Immobilisation in cement based materials

The immobilisation of the molten salt in a cement based materials was done using a blended system containing OPC, BFS, silica fume, lime and limestone filler. Trial mixes were performed to assess the feasibility of immobilising directly the molten salt in this blended system. For that, 3 recipes per trial were proposed, varying the waste loading and water/binder ratio. The varied factors for the first 2 trials are shown in **Table 4** (1<sup>st</sup> trial) and **Table 5** (2<sup>nd</sup> trial).

**Table 4:** Varied factors in the 1st trial to immobilise the molten salt in cement based materials

Trial C1	Waste loading (wt%)	water/binder ratio
M40	40	0.60
M30	30	0.60
M20	20	0.60

**Table 5:** Varied factors in the 2<sup>nd</sup> trial to immobilise the molten salt in cement based materials

Trial C2	Waste loading (wt%)	water/binder ratio
M-35-0.78	35	0.78
M-35-0.90	35	0.90
M-25-0.78	25	0.78

In the 1<sup>st</sup> trial mix, the samples were cured for 7 days in a curing cabinet, at 20 °C and with relative humidity higher than 95%. For the 2<sup>nd</sup> trial mix, the curing was adapted and the samples were left for 35 days in a sealed bag at 20 °C. After that, they were placed in the curing cabinet to check their stability under humid conditions.

With the results of this first trial (see Section below), it was decided to perform a pre-conditioning of the molten salt before the immobilisation (see below the method for pre-conditioning). Another 2 trials mixes were then performed, one with the salt pre-conditioned with Ca(NO<sub>3</sub>)<sub>2</sub> and another with the salt pre-conditioned with Ca(OH)<sub>2</sub>. The samples were moulded and cured both in humid environment (20 °C, R.H. > 95%) and in a sealed bag (20 °C). The varied factors for the first 2 trials are shown in **Table 6** (3<sup>rd</sup> trial) and **Table 7** (4<sup>th</sup> trial).

**Table 6:** Varied factors in the 1<sup>st</sup> trial to immobilise the molten salt in cement based materials

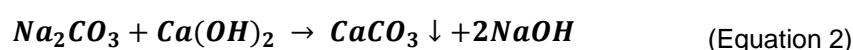
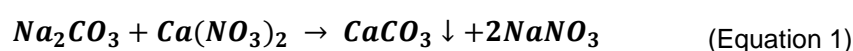
Trial C3	Waste loading (wt%)	water/binder ratio
CN-30-0.72	30	CN-30-0.72
CN-30-0.84	30	CN-30-0.84
CN-20-0.72	20	CN-20-0.72

**Table 7:** Varied factors in the 2<sup>nd</sup> trial to immobilise the molten salt in cement based materials

Trial C4	Waste loading (wt%)	water/binder ratio
CH-30-0.54	30	0.54
CH-30-0.66	30	0.66
CH-20-0.54	20	0.54

### Preconditioning of the molten salt

The hydration state of Na<sub>2</sub>CO<sub>3</sub>.xH<sub>2</sub>O in the molten salt was suspected to be strongly dependable on the humidity and temperature of the environment, thereby negatively affecting the mechanical properties of the immobilized waste form. Therefore, a preconditioning step was used in some trials to convert Na<sub>2</sub>CO<sub>3</sub> to a more stable form. A transformation with Ca(NO<sub>3</sub>)<sub>2</sub> was attempted in trials A3 and C3 (Equation 1) in order to form stable CaCO<sub>3</sub>, while Na<sup>+</sup> and NO<sub>3</sub><sup>-</sup> ions remain in solution. A transformation with Ca(OH)<sub>2</sub> was attempted in trials A4 and C4 (Equation 2) in order to form CaCO<sub>3</sub>, with Na<sup>+</sup> and OH<sup>-</sup> ions remaining in solution. In the case of alkali-activated materials, the formation of NaOH is potentially beneficial, as the strong base can act as an activator for the precursor, thereby limiting the amount of extra NaOH that needs to be added to the formulation.



### 3. Results

#### Immobilisation in alkali-activated matrix

The direct immobilization of molten salt, tested in trial A1, showed promising mechanical strengths. After 14 days of curing in a sealed bag, compressive strengths of BFS samples exceeded 10 MPa until 30% waste loading, while the strengths of the metakaolin samples even increased with increasing waste loading. The positive effect of the salt on the mechanical strength is due to  $\text{Na}_2\text{CO}_3$  acting as an activator for the metakaolin precursor (Provis & Van Deventer, 2013). Therefore, metakaolin was studied further in trial A2. As the setting of these materials was fast (under 15 minutes), the water/solid ratio was increased (from around 0.4 to 0.6) and the concentration of the activating solution decreased. An acceptable setting time ( $> 1$  hour) was achieved with a water/solid ratio of 0.71 and a waste loading of 36 wt.%. The compressive strengths of all tested materials were satisfactory, exceeding 14 MPa (**Figure 1**).

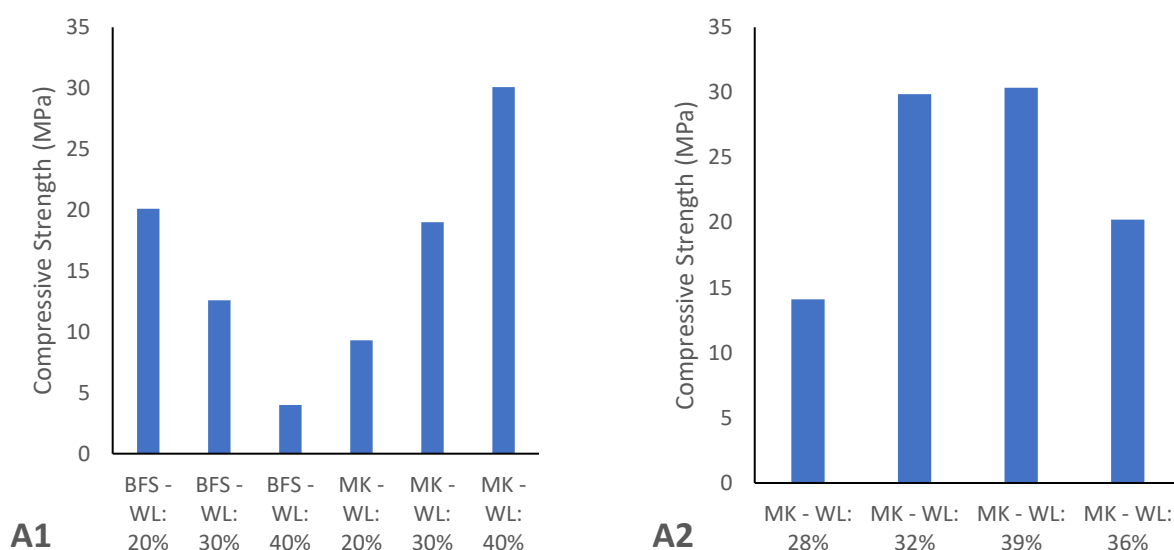


**Figure 1:** Compressive strengths of the waste forms synthesized in Trial A1 (left) and A2 (right).

The behaviour of the waste forms of trial A2 under variable humidity and temperature were tested by comparing sealed curing and curing under humid conditions, and by placing the waste form in an oven at 40 °C. The finding was that curing under humid conditions saw a significant expansion (2% after 10 days) and a drastic reduction of compressive strength from 21 to 2 MPa (**Figure 2**). While heating the waste form in the oven at 40°C saw the complete destruction of its structural integrity. These observations can be explained by the variable hydration states of  $\text{Na}_2\text{CO}_3$ . When mixed, the  $\text{Na}_2\text{CO}_3$  absorbs water to move to a highly hydrated state, after which it is fixed in the structure of the geopolymer. Upon heating, the hydrated  $\text{Na}_2\text{CO}_3$  expels its water, thereby having a deleterious effect on the integrity of the waste form. Likewise, prolonged exposure to humid conditions allows dehydrated or lowly hydrated states of  $\text{Na}_2\text{CO}_3$  to take up more water, thereby expanding the waste form and compromising its integrity.

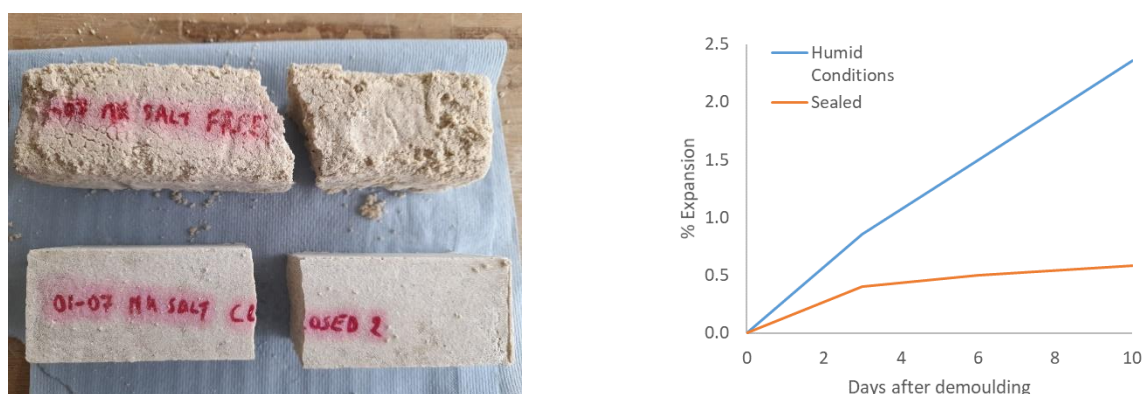


**Figure 2:** Comparison of the state of a metakaolin waste form from trial A2 cured under two different conditions (top: humid conditions, bottom: sealed). On the right the expansion of these samples during curing is shown.

Trials A3 and A4 attempted to combat these effects by preconditioning the salt with  $\text{Ca}(\text{NO}_3)_2$  and  $\text{Ca}(\text{OH})_2$  to form  $\text{CaCO}_3$ , which is insensitive to changes in humidity or temperature. Trial A3 was unsuccessful. While  $\text{CaCO}_3$  did form, the nitrate ions liberated in the process inhibit the geopolymerization process and thereby do not allow the formation of waste form with measurable mechanical strengths (Provis et al., 2008). Trial A4 was more successful. Waste forms with waste loadings of 10 and 15 wt.% achieved compressive strengths exceeding 10 MPa after 28 days of curing. Samples cured under different conditions (28 days sealed, 28 days under humid conditions, or 7 days sealed and 21 days of humid conditions) did not display differences in mechanical strengths, thereby confirming the successful transformation of the  $\text{Na}_2\text{CO}_3$ .

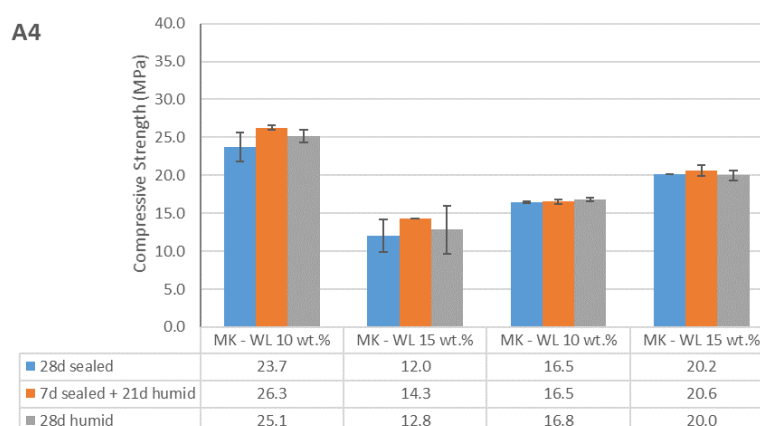


**Figure 3:** Compressive strengths of the waste forms synthesized and cured under different conditions in Trial A4.

### Immobilisation in cement based materials

The immobilisation of the molten salt directly in a cement based materials was done in the 1<sup>st</sup> and 2<sup>nd</sup> trial test. In the 1<sup>st</sup> trial, the samples were cast and left for cure inside a curing cabinet at 20 °C and relative humidity higher than 95 % for 7 days. After 7 days, it was possible to observe already some issues with the samples. **Figure 4** shows the pictures of the samples after the 1<sup>st</sup> trial. It is possible to observe that sample of M20 shows some bleeding, of M30 shows cracking and of M40 shows a loss of integrity.

**Table 6** shows the results of initial and final setting time, heat of hydration by isothermal calorimeter and compressive and flexural strength of the samples. It was possible to observe a too short setting time on all samples. The compressive and flexural strength was high for samples with only 7 days of cure. This shows that we could still change the recipe to solve the other problems observed.





**Figure 4:** Pictures of samples M20 (left), M30 (center) and M40 (right).

**Table 6:** Results of test with the samples from the 1st trial mix.

Trial C1 Sample	Initial setting time	Final setting time	Iso hydration heat	Compressive/flexural strength, MPa	
	(hh:mm)	(hh:mm)	J/ g sample	7d	14d
M20	00:32	01:24	114.70	24.9/5.0	34.0/7.3
M30	00:14	00:16	100.91	6.7/1.6	6.3/6.3
M40	00:20	00:28	93.41	-	-

In the 2<sup>nd</sup> trial, the method of cure was changed. The samples were cast and left for cure in a sealed bag for 35 days. They were then placed in the curing cabinet at 20 °C and relative humidity higher than 95 % for 7 days. **Table 7** shows the results of initial and final setting time, heat of hydration by isothermal calorimeter and compressive strength of the samples. It was possible to observe also a too short setting time on all samples, as seen in the 1<sup>st</sup> trial. The compressive strength was high for samples M35-0.78 and M35-0.90, but too low for the samples of M-25-0.78, even after 35 days of cure.

**Table 7:** Results of test with the samples from the 2<sup>nd</sup> trial mix.

Trial C2 Sample	Initial setting time	Final setting time	Iso hydration heat	Compressive strength, MPa	
	(hh:mm)	(hh:mm)	J/ g sample	7d	35d
M-25-0.78	00:46	01:04	93.65	51.3	50.7
M-35-0.78	00:50	01:09	60.07	43.6	46.0
M-35-0.90	00:55	01:17	61.39	4.9	6.6

**Figure 5** shows the pictures of the samples after they were placed in the curing cabinet for 7 days. It is possible to observe that samples of M35-0.78 and M35-0.90 presented a loss of integrity and the sample of M-25-0.78 shows some bleeding as well.



**Figure 5:** Pictures of samples M-35-0.78 (left), M-35-0.90 (center) and M-25-0.78 (right).



The 3<sup>rd</sup> trial mix was done with the molten salt pre-conditioned with  $\text{Ca}(\text{NO}_3)_2$ . **Table 8** shows the results of initial and final setting time, heat of hydration by isothermal calorimeter and compressive strength of the samples cured in humid conditions and in a sealed bag (for 7 and 35 days). It was possible to observe that the setting time was higher and in acceptable ranges. The compressive strength of all samples was very good after 7 and 35 days. No difference was found from samples cured in different conditions.

**Table 8:** Results of test with the samples from the 3<sup>rd</sup> trial mix.

Trial C3 Sample	Initial setting time	Final setting time	Iso hydration heat	Compressive strength, MPa		
	(hh:mm)	(hh:mm)	J/ g sample	7d, humid	7d, sealed	35d, sealed
CN-20-0.72	07:09	--	104.12	28.6	29.4	39.8
CN-30-0.72	31:59	--	107.09	6.5	7.9	16.7
CN-30-0.84	19:39	--	96.26	8.2	9.1	20.3

The 4<sup>th</sup> trial mix was done with the molten salt pre-conditioned with  $\text{Ca}(\text{OH})_2$ . **Table 9** shows the results of initial and final setting time, heat of hydration by isothermal calorimeter and compressive strength of the samples cured in humid conditions and in a sealed bag (for 35 days). It was possible to observe that the setting time was in acceptable ranges. The compressive strength of all samples was very good after 35 days. No difference was found from samples cured in different conditions.

**Figure 6** shows the pictures of the samples cured in a sealed bag for 35 days. It was not observed any structural damage in the samples during this period.

**Table 9:** Results of test with the samples from the 4<sup>th</sup> trial mix.

Trial C4 Sample	Initial setting time	Final setting time	Iso hydration heat	Compressive/flexural strength, MPa	
	(hh:mm)	(hh:mm)	J/ g sample	35d, humid	35d, sealed
CH-20-0.54	03:05	06:18	105.29	15.6 / 3.6	15.6 / 3.5
CH-30-0.66	03:21	07:52	92.67	10.4 / 2.3	10.4 / 2.3
CH-30-0.54	01:49	04:48	97.01	15.6 / 3.6	15.6 / 3.5

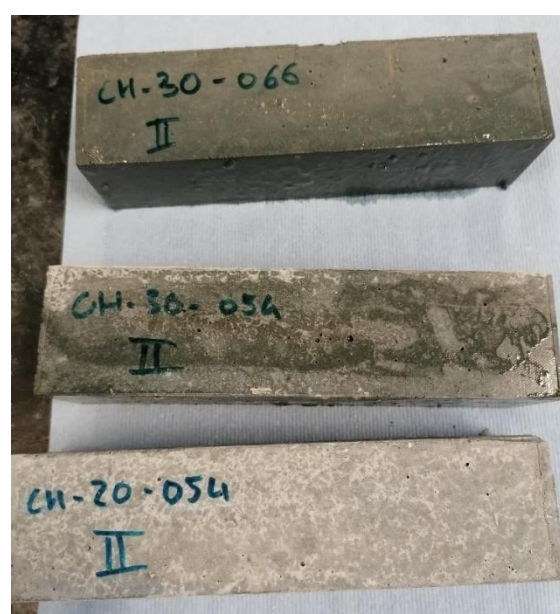


**Figure 6:** Pictures of samples CH-30-0.66 (top), CH-30-0.54 (centre) and CH-20-0.54 (bottom).

## 4. Conclusions

The immobilization of molten salt was found to require a pretreatment step to convert  $\text{Na}_2\text{CO}_3$  to  $\text{CaCO}_3$ , as the former has a significant negative impact on the structural integrity of a waste form exposed to variable temperatures or humidities. In the case of alkali-activated materials, a treatment with  $\text{Ca}(\text{OH})_2$  proved to be successful, while the nitrates ions liberated by  $\text{Ca}(\text{NO}_3)_2$  in the alternative route interfere with the geopolymerization process. In the case of blended cemented matrix, the treatment with both  $\text{Ca}(\text{OH})_2$  and  $\text{Ca}(\text{NO}_3)_2$  proved to be successful, with waste forms showing good mechanical strength and stability under humid conditions.

A remaining problem is the efficiency of the transformation of  $\text{Na}_2\text{CO}_3$  to  $\text{CaCO}_3$  after reaction with  $\text{Ca}(\text{OH})_2$ . Preliminary XRD analyses of the immobilized waste forms have shown the formation of an intermediary gaylussite ( $\text{Na}_2\text{Ca}(\text{CO}_3)_2 \cdot 5\text{H}_2\text{O}$ ) phase instead of  $\text{CaCO}_3$ . As gaylussite is potentially unstable on the long term, reverting to  $\text{Na}_2\text{CO}_3$  and  $\text{CaCO}_3$  with associated volume changes, it should be investigated how the pretreatment step can be optimized to directly form  $\text{CaCO}_3$  instead.

## Acknowledgements

This work has received funding from the European Union's Horizon 2020 research and innovation programme for Nuclear Fission and Radiation Protection Research (Call NFRP-2019-2020) under grant agreement No. 945098 (PREDIS).

## References

- Phung, Q. T., Ferreira, E., Seetharam, S., Govaerts, J., & Valcke, E. (2021). Understanding hydration heat of mortars containing supplementary cementitious materials with potential to immobilize heavy metal containing waste. *Cement and Concrete Composites*, 115, 103859.
- Provis, J. L., & Van Deventer, J. S. (2013). *Alkali activated materials: state-of-the-art report, RILEM TC 224-AAM* (Vol. 13). Springer Science & Business Media.
- Provis, J. L., Walls, P. A., & van Deventer, J. S. (2008). Geopolymerisation kinetics. 3. Effects of Cs and Sr salts. *Chemical engineering science*, 63(18), 4480-4489.

## 6.8 Thermal treatment & wasteform durability at the University of Sheffield (USFD)

Sam Walling, University of Sheffield (USFD), UK, [s.walling@sheffield.ac.uk](mailto:s.walling@sheffield.ac.uk)  
 Claire Corkhill, University of Sheffield (USFD), UK

**Keywords:** Densification, HIP, thermal, durability

### 1. Introduction

At the University of Sheffield (USFD), we have been investigating the thermal treatment of wastes via Fenton wet oxidation and Hot Isostatic Pressing (HIP). Principally, Fenton wet oxidation is being utilised for the thermal treatment of spent mixed bed cation-anion organic ion exchange resins. HIP is being utilised as a secondary thermal process, densifying existing simulant ashes or sludges from various processes (the wet oxidation residues, and IRIS ashes supplied by CEA within this work package)

Selected densified wasteforms (produced via HIP) are currently being assessed for aqueous durability, using a cementitious based leachate in common with other work package partners. Further densified wasteforms are due to be produced in the near future, with the aim of optimising the usage of HIP for Fenton wet oxidation sludges.

### 2. Work plan and current progress

Our workflow within PREDIS is focussed towards three principal objectives:

1. Production and assessment of Fenton wet oxidation wastes
2. Densification via HIP of various ashes and sludges
3. Densified wasteform durability assessment using a common leaching method

The first strand of this, Fenton wet oxidation, is nearly finished. This process was utilised to destroy organic ion exchange resins via oxidation utilising hydrogen peroxide and an aqueous metal catalyst. We have optimised our processing conditions based on a mixed iron / copper catalyst, and determined the composition of the resulting sludges after successful treatment of both as-received, and simulant active organic ion exchange resins. A simulant material has been sourced for usage in HIP processing, due to the very small volume of waste generated by the wet oxidation rig at USFD. This simulant material is largely a copper oxide / iron oxide based powdered material, and will allow substantial wasteform development without continued wet oxidation rig operation to generate wastes, this will also facilitate the scale-up of HIP wasteforms being undertaken by the National Nuclear Laboratory (UK).

Densification of received ash and sludge materials via HIP has been a great success to date. Recent work predominantly focussed on the optimisation of the HIP wasteforms and characterisation of the HIPed IRIS ashes, which were supplied by CEA within this work package. Figure 1 demonstrates a representative HIPed IRIS ash, with the formation of a solid monolithic product contained within a steel canister after the application of heat and pressure. The wasteform properties have been tailored via the use of additives and grinding, to produce products with varying crystalline and glassy phases. Produced wasteforms have all be subjected to laboratory characterisation, with attention paid to both the bulk properties and to any corrosion/interactions between the wasteform and the internal HIP can wall. Overall, the addition of minor quantities of sodium tetraborate appears sufficient to produce a suitable glass-ceramic material with minimal adverse canister-wasteform interactions, though other additives utilised also formed solid waste products.



**Figure 1.** HIP treatment of IRIS ashes at USFD from left to right: can packing, welding, crimping, thermal treatment (1250 °C), and sectioning open the can.

The durability of selected HIPed wasteforms are currently being assessed via an aqueous durability test, using a common methodology between work package partners. This is a semi-dynamic solution replacement test with an alkaline cementitious-based leaching liquid, performed at or near ambient temperatures. In order to assess the long-term durability of HIP wasteforms, the successful HIPed IRIS ash products were selected. Small cubed samples were sectioned from the HIP canisters, carefully removing all exterior faces so that only the bulk material was utilised for leaching, as depicted in Figure 2.

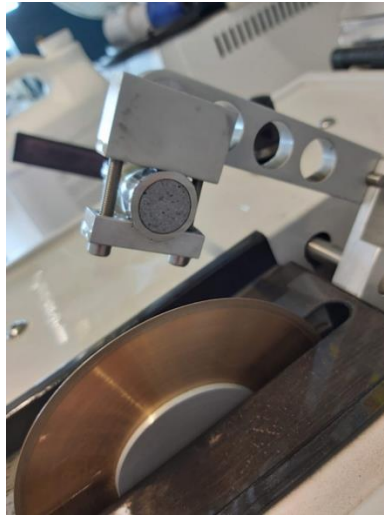


**Figure 2.** Preparation of monolithic samples for leach testing, removal of the HIP can from the solid product before further size reducing to cubes.

Samples for leaching are periodically sampled, with leachate replaced on a timescale agreed between partners. Resulting leachate is stored prior to ICP analysis to determine the total quantity of leached elements, with several sacrificial samples due to be removed (at set time points) to determine any effect on porosity, and if any alteration products have formed on the surface of these cubes.

### 3. Summary

Significant progress towards the desired objectives of this work package has been completed, with clear achievements in both simulant waste characterisation (Fenton wet oxidation), and in the successful HIP of IRIS ashes. The immediate future will entail several sintering trials for simulant Fenton wet oxidation sludges, culminating in HIP trials and ultimately, larger scale HIP trials. The overall aim of producing a solid, densified product from these sludges, achieving substantial waste volume reduction. Further characterisation and assessment of HIP IRIS ashes will be undertaken, alongside continued long-term leach testing to assess the wasteform durability.

### Acknowledgements

The authors are grateful for funding received from the European Union's Horizon 2020 research and innovation programme under grant agreement No 945098 (PREDIS), and UKRI / EPSRC under grant agreement EP/S032959/1. This research utilised the HADES/MIDAS and PLEIADES national nuclear user facilities at the University of Sheffield, established with financial support from EPSRC and BEIS, under grant numbers EP/T011424/1 and EP/V035215/1.

## 6.9 Physico-Chemical characterisation of reconditioned waste form and stability testing

Elena Torres Alvarez, Esther Marugán, Centro de Investigaciones Energéticas, Medioambientales y Tecnológicas (CIEMAT), Spain, [elena.torres@ciemat.es](mailto:elena.torres@ciemat.es)

María Cruz Alonso, Inés García-Lodeiro, Francisca Puertas, Pedro Pérez, Instituto de Ciencias de la Construcción Eduardo Torroja (IETcc, CSIC), Spain, [mcalonso@ietcc.csic.es](mailto:mcalonso@ietcc.csic.es)

Raúl Fernández, Ana Isabel Ruiz, Mikel Dieguez, Universidad Autónoma de Madrid (UAM), Spain, [raul.fernandez@uam.es](mailto:raul.fernandez@uam.es)

**Keywords:** leaching, X-ray micro-tomography, doped ion exchange resins

### 1. Introduction

Leaching tests can be used for the evaluation of the confinement ability of conditioning matrices. Also, they can be used for tracking leaching process of matrix elements, what allows determining its stability in the leaching solution.

CSIC, CIEMAT and UAM have agreed to perform a number of leaching experiments under different exposed conditions. CSIC will manufacture cement probes of  $1 \times 1 \times 6$  cm<sup>3</sup> dimensions with and without the incorporation of a 20 wt.% of thermally treated ion exchange resins (tt-IERs) in selected matrices of CEM I, CEM III and one-part geopolymer, according to the formulation given in Table 1.

**Table 1.** Dosage of selected matrices for the fabrication of specimens for testing in task 6.6.

Components mass	Reference matrices			Matrices with the waste RI		
	One-part Geopolymer	CEM I	CEM III	One-part Geopolymer	CEM I	CEM III
Metakaolin (g)	39.10	--	--	31.28	--	--
Slag (g)	36.36	--	--	29.09	--	--
Solid Na <sub>2</sub> SiO <sub>3</sub> (g)	18.18	--	--	14.54	--	--
Solid NaOH (g)	6.36	--	--	5.09	--	--
CEM I 42.5 SR/MSR (g)	--	100.00	--	--	80.00	--
CEM III/B 32.5 N/SR(g)	--	--	100.00	--	--	80.00
Waste RI (g)	--	--	--	20.00	20.00	20.00
Water (g)	30.00	30.00	30.00	30.00	30.00	30.00

### 2. Description of work and main findings

A complete set of characterization of the aqueous and solid phases is foreseen. X-ray micro-tomography will only be performed in selected samples due to the excessive time-consuming procedure of the analyses of samples and data. Nevertheless, a preliminary test was performed on two samples with and without tt-IERs. Characterization of waste form properties performed by X-ray micro-tomography at the initial state (CEM III+20% tt-IER after 28 days of curing time) is presented here as an example (Figures 1 and 2). The analysis of data confirms a homogenous distribution of the resin within the matrix. The load of tt-IERs could also be confirmed numerically as a volume fraction. A small volume < 2 % corresponds to air void trapped in the cement matrix.



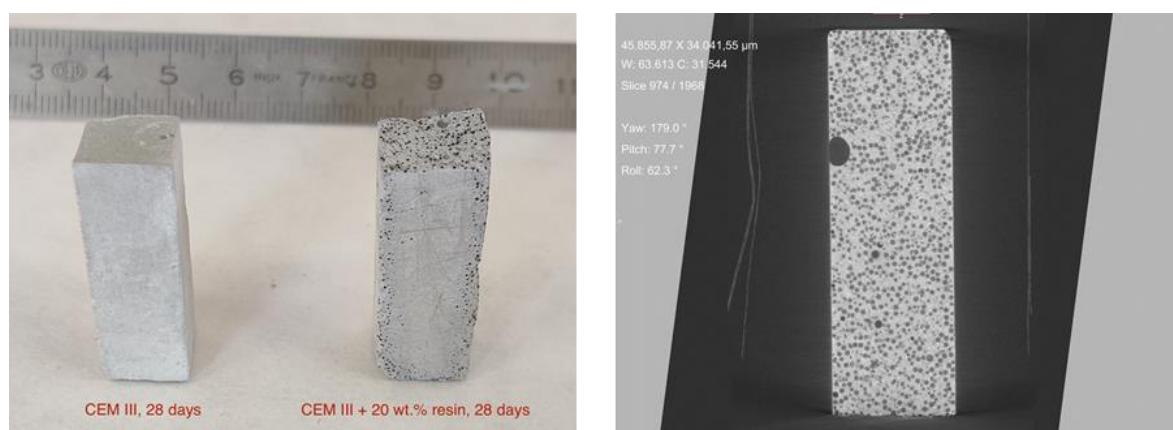


**Figure 1.** (left) Prismatic specimens (1x1x6 cm) of CEM III and CEM III loaded with a 20 wt.% of thermally-treated IERs.

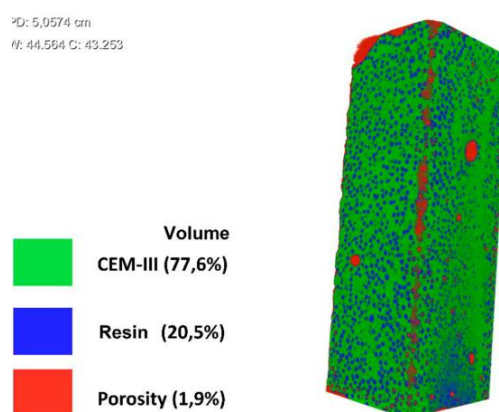


**Figure 2.** Porosity calculation in a CEM III prismatic specimen loaded with a 20 wt% of treated IERs.

### 3. Way forward

The experimental programme, already started, will produce a total number of 288 samples. Each group will perform 96 leaching experiments using a synthetic cementitious water (CSIC), on-site water from El Cabril (Spanish disposal facility for low and intermediate-level radioactive waste, CIEMAT) and deionised water (UAM). The experiments will be performed for different time, from 3 to 24 months, as expressed in Table 2. Four replicates will be used for each leaching experiment.

**Table 2.** Variables considered in the common leaching test programme defined by CIEMAT, CSIC and UAM.

Conditioning matrices	Waste loading (wt%)	Duration (months)	Leaching solutions
CEM I	0 - 20	3, 6, 12 and 24	Synthetic cementitious water (CSIC)
CEM III			Water sampled in disposal platform in El Cabril LILW facility (CIEMAT)
Geopolymer			Deionized water (UAM)

An exhaustive characterisation of both, the solid and aqueous phases, has been programmed by the 3 groups, including all the analytical techniques shown in Table 3.



**Table 3.** Analytical techniques for the pre-leaching and post-mortem characterization of solid and leaching solutions.

	Solid characterization	Leachant analysis
According to leaching protocol [1]	DRX (UAM, CSIC)	Monitoring (pH, E <sub>h</sub> , EC)
	BET (CIEMAT)	Elemental analysis (ICP-OES / ICP-MS)
	MIP (CIEMAT, CSIC)	Indicators of matrix degradation: Al, Si, Ca, Na, K
	SEM (UAM/CSIC/CIEMAT)	Immobilised elements: B, Co, Cr, Ni, Zn, Fe, Ag, Cs, Sr
Additional to leaching protocol	TG-DSC (CSIC)	TOC (CIEMAT)
	FTIR (CIEMAT, CSIC)	
	Micro-CT (UAM)	
	Mechanical resistance (CSIC)	

## References

- [1] E. Myllykylä, E. (2021). Milestone 39. Definition of the leaching procedure for the short-term experiments and the long-term durability experiments. PREDIS internal report. 7 pp.

## 6.10 Leaching tests with HIPed ashes

*Karine Ferrand, Borja Gonzalez, Karel Lemmens  
SCK CEN, Belgium  
karine.ferrand@scken.be*

### Abstract

SCK CEN is investigating the chemical durability of HIPed ashes by performing leaching tests. The ashes, which are surrogates of solid organic wastes and ionic exchange resins, were provided by CEA. Their elemental composition was determined by ICP. The University of Sheffield prepared HIPed samples by first mixing 95 wt.% ashes with 5 wt.%  $\text{Na}_2\text{B}_4\text{O}_7$  in stainless steel cans. Then, the welded cans were heated to 300 °C for ~12 hours under vacuum, and sealed. Afterwards, they were HIPed at 250 °C and 100 MPa for 2 hours. Two cans were sent to SCK CEN to carry out short- and long-term semi-dynamic leaching tests, following the reference protocol described in the Milestone 39. Before starting the tests, the unaltered HIPed samples were characterised by SEM-EDX and XRD, confirming that after HIPing a glass-ceramic material was produced. The HIPed samples are altered at 22 °C under anaerobic conditions with an alkaline solution at pH 12.7, which contains 2800 mg/L of K, 18 mg/L of Ca, and 1080 mg/L of  $\text{SO}_4^{2-}$ . pH and elemental concentrations were measured in the leachates collected over 2 months. Preliminary results showed that pH was constant at the reference pH value of 12.7 and K, Ca and  $\text{SO}_4^{2-}$  concentrations were similar to those measured in the initial leaching solution.  $\text{Cl}^-$  concentrations were below the detection limit. Similar silicon concentrations were determined by ICP/MS and UV/Visible spectrophotometry, suggesting that there were no polymeric silicon species in the leachates. Many elements initially present in the ashes were not detected or were not measurable by ICP/MS. The treatment of the data available for a few elements is ongoing.

**Keywords:** Intermediate and Low Level Waste (ILLW), HIPed ashes, glass-ceramic, chemical durability, short- and long-term leaching tests, high pH medium, Milestone 39.

### 1. Introduction

Within the PREDIS project (WP6 - task 6.6), SCK CEN is studying the chemical durability of HIPed ashes by performing short- and long-term leaching tests, following the reference protocol described in the Milestone 39. The ashes, which are surrogates of solid organic wastes and ionic exchange resins, were provided by CEA, and two HIPed cans were prepared at the University of Sheffield. First, 95 wt.% ashes were mixed with 5 wt.%  $\text{Na}_2\text{B}_4\text{O}_7$  in stainless steel cans. Then, the welded cans were heated to 300 °C for ~12 hours under vacuum, and sealed. Afterwards, they were HIPed at 250 °C and 100 MPa for 2 hours.

### 2. Description of work and main findings

From two rods (without stainless steel can), 5 mm cubes were prepared by using a Minitom machine and Isocut fluid as cooling fluid. Then, the cubes were cleaned with ethanol, and dried overnight at 50 °C. Before starting the leaching tests, the unaltered HIPed samples were characterized by SEM-EDX and XRD. The SEM pictures showed the presence of crystalline phases, identified as calcium chloride phosphate or calcium chloride phosphate oxide, and magnesium aluminium oxide by XRD. This confirms that after HIPing a glass-ceramic material is produced.

Short- and long-term semi-dynamic leaching tests are performed according to the reference protocol defined by all partners and described in the Milestone 39. The HIPed samples are leached in a glove box under Ar at  $22 \pm 2$  °C using a high pH solution ( $12.7 \pm 0.2$ ) containing potassium, calcium and sulphates. The sample surface area to solution volume is fixed to  $10 \text{ m}^{-1}$  by using 15 mL of leaching solution with a 5 mm cube. Regularly, the solution is refreshed to prevent the accumulation of the elements released by the HIPed sample, which leads to a decrease of the affinity, and thus to a decrease of the dissolution rate. Table 1 shows the test matrix and the schedule of the leaching tests with HIPed samples coming from two cans (can 1 in Exp.1, 3, 5 and 7 and can 2 in Exp. 2, 4 and 6). pH is measured and the elemental concentrations are measured by ICP/MS, IC. The concentrations of the monomeric Si concentration is also determined by UV/Visible spectrophotometry.

Preliminary results after 2 months showed that pH is constant at the reference pH value of 12.7, and potassium, calcium and sulphate concentrations are similar to those measured in the initial leaching solution. Chloride concentration is below the detection limit. Similar silicon concentrations are determined by ICP/MS and UV/Visible, suggesting that there are no polymeric Si species in the leachates. Many elements initially present

in the ashes are not detected or are not measurable by ICP/MS. The treatment of the data available for a few elements is ongoing. Similar data are found for HIPed samples coming from different cans.

The HIPed samples altered for 3 months, 1 and 2 years will be characterized by SEM and XRD.

**Table 1:** Test matrix and schedule of the semi-dynamic leaching tests conducted following the reference protocol.

SA/V	10 m <sup>-1</sup>
pH	12.7
T	22 °C
Cubic sample	5 mm
Volume of solution	15 mL

Test container		Duration									
		M1				M2	M3	M4	M5	M6	M7
		7d	14d	21d	28d						
Exp. 1	Exp. 2	2022-01-17	2022-01-24	2022-01-31	2022-02-07	2022-03-10	2022-04-11				
Exp. 3	Exp. 4						2022-04-11	2022-05-10	2022-06-10	2022-07-11	2022-08-10
Exp. 5	Exp. 6										
Exp. 7		2022-01-17	2022-01-24	2022-01-31	2022-02-07	2022-03-10	2022-04-11	2022-05-10	2022-06-10	2022-07-11	2022-08-10
		M8	M9	M10	M11	M12	M14	M16	M18	M24	
Exp. 1	Exp. 2										
Exp. 3	Exp. 4	2022-09-09	2022-10-10	2022-11-10	2022-12-09	2023-01-10					
Exp. 5	Exp. 6					2023-01-10	2023-03-10	2023-05-10	2023-07-10	2024-01-10	
Exp. 7		2022-09-09	2022-10-10	2022-11-10	2022-12-09	2023-01-10	2023-03-10	2023-05-10	2023-07-10	2024-01-10	
Renewal and analysis of the solution											
Stop and analysis of the solution + surface analysis											
Renewal of the solution (no analysis)											

### 3. Summary

The tests are running for two years, so many samples still need to be collected; samples are taken according to the durations indicated in the reference protocol. The chemical durability of the HIPed samples will be compared to that found by the University of Sheffield, as they are using the same type of samples, and also to those obtained for other waste forms developed for solid organic low and intermediate level waste (e.g. geopolymers).

## 7 Scientific progress of Innovations in cemented waste handling and predisposal storage (WP7)

### 7.1 Radiation detection tools for radwaste characterization & monitoring

*Paolo Finocchiaro, INFN Laboratori Nazionali del Sud, Catania, Italy, [finocchiaro@lns.infn.it](mailto:finocchiaro@lns.infn.it)  
Mauro Romoli, INFN Sezione di Napoli, Napoli, Italy, [romoli@na.infn.it](mailto:romoli@na.infn.it)*

#### Abstract

In the framework of WP7, that deals with innovations in cemented waste handling and pre-disposal storage, the subtask WP7.3 takes care to identify, evaluate and develop various methods for non-destructive evaluation (NDE), quality assurance and inspection of packages. Additionally, the impact of the developed monitoring technologies is being demonstrated under storage conditions. In particular the INFN section of Naples (INFN-NA) and the Laboratori Nazionali del Sud (INFN-LNS) have developed gamma and neutron radiation detectors suitable for the external monitoring of radwaste drums, in particular but not exclusively cemented radwaste. A compact, low power electronics, featuring wireless connection, is going to be completed. Detector tests using the newly developed front-end and data acquisition electronics prototypes are foreseen by autumn 2022 with laboratory radioactive sources at LNS, followed by tests with sources in a cemented mock-up drum currently being developed at UJV Prague. Preliminary simulations suggest that such an external monitoring should be capable of detecting counting changes or asymmetries occurring in the medium term, indicating an internal modification of the matrix and/or the onset of a crack.

**Keywords:** SciFi gamma detector, scintillating fiber, SiPM, SiLiF neutron detector,  $^6\text{LiF}$ , silicon detector, wireless data acquisition.

#### 1. Introduction

In the framework of radioactive waste management the practice so far has been to store the radwaste drums following their initial characterization, the main radiological monitoring consisting in an overall set of few ambient radiation detectors and periodic manual checks done by operators. The proposed system for online real-time monitoring consists of an array of many radiation sensors to be deployed all around a number of radioactive waste drums, in order to collect counting-rate data in real time. A continuous automatic monitoring of the radwaste drums represents an added value in terms of safety and security, and the availability of continuous streams of counting-rate data around each drum would be a comfortable tool toward the transparency, which now more than ever is a relevant topic of the nuclear industry. As an evolution of the proof-of-principle systems discussed in [0-0], the detectors described here could become part of a prototype system to be installed in a radwaste storage site to prove its effectiveness.

The radiological monitoring of radwaste must be based on the measurement of gamma-rays and neutrons because these are penetrating and thus more easily detectable out of the drums. In view of a possible mass deployment, the sensors must be reasonably low-cost and configurable in a modular and scalable fashion, so that one can tailor the system to small, medium, and large-scale storage configurations. Such a monitoring system should be based on detectors which can be easily installed and/or reassembled in different geometrical configurations therefore being mechanically very simple.

This paper shortly describes the SciFi gamma ray counters and the SiLiF thermal neutron counters that are proposed in the framework of the PREDIS project.

#### 2. The SciFi gamma ray counter

If facing the development of gamma ray monitoring detectors, for a possible mass deployment around radwaste drums, the following requirements apply:

- the sensor must be simple and robust;
- spectroscopic features are not required, the sensor can be a simple counter;
- the intrinsic detection efficiency can be low, as the sensor can measure for long time spans;
- low efficiency also implies the capability to stand in high radiation fluxes without being saturated;
- the sensor should possibly be spatially extended to cover a wide region of a drum;
- it should be based, as much as possible, on commercially available technology;

- it should be reasonably inexpensive.

The SciFi counter [0] is based on a scintillating optical fiber, with each end coupled to a Silicon Photo Multiplier (SiPM photodetector) which is sensitive even to single photons. Whenever a gamma ray interacts with the fiber it produces a fast flash of light (few ns), and a fraction of this light is trapped and propagates along the fiber (few photons). It is detected by the SiPM, with an intrinsic amplification of  $10^6$ , and imposing the left & right coincidence suppresses the residual random noise. An on-purpose front-end, analog-to-digital conversion and data acquisition electronics is currently being developed, featuring wireless data transmission to the main control computer. The main features of the SciFi counter, whose structure and operating principle are sketched in **Figure 16**, are the following:

- the sensor, in a version 80 cm long, spans the full drum size;
- it can be easily replaced in case of failure or improvement;
- the behavior has been fully simulated (GEANT4);
- it has  $\approx$ uniform detection efficiency vs the impinging gamma energy;
- 10-year old prototypes are still working fine.

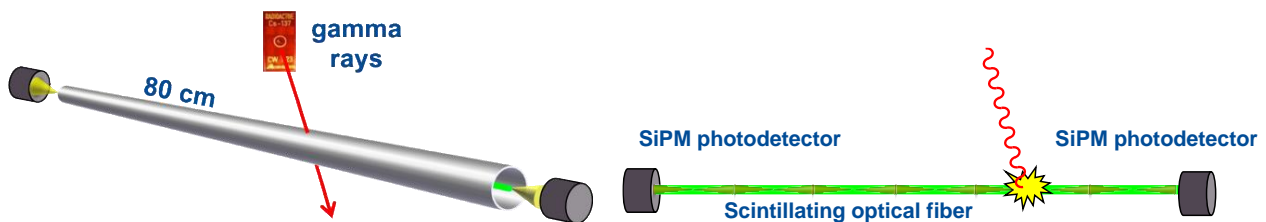


**Figure 16.** Structure and operating principle of the SciFi gamma ray counter.

#### 4. The SiLiF neutron counter

In order to be used for a network of neutron monitors around drums the main requirements for a sensor are:

- detection efficiency;
- reasonably low cost;
- mechanical robustness;
- operation at low voltage;
- use, as much as possible, of commercially available components.

The SiLiF neutron counter is based on a solid state silicon detector coupled to a thin layer of a neutron converter material ( $^6\text{LiF}$ ), which upon capture of a low energy neutron produces an alpha particle and a triton that can be detected in the silicon [0]. As compared to the well known thermal neutron detectors, namely  $^3\text{He}$  gas tubes at high pressure and voltage and whose price has been increasing and whose availability has been decreasing in the last decades, the SiLiF technology allows to achieve comparable performances at about one order of magnitude lower prices. The main features of the SiLiF counter, whose structure and operating principle are sketched in **Figure 17**, are:

- solid state (double sided silicon diode +  $^6\text{LiF}$ );
- lower cost technology, cheaper than  $^3\text{He}$ ;
- low operating voltage (25-50 V)
- compactness, robustness;
- good detection efficiency (5%)
- optimum gamma discrimination ( $<10^{-7}$ )

As the SiLiF is basically sensitive to thermal neutrons, a polyethylene moderator has been conceived, its performances simulated and then built. The final assembly of a SiLiF sensor is shown in **Figure 18**

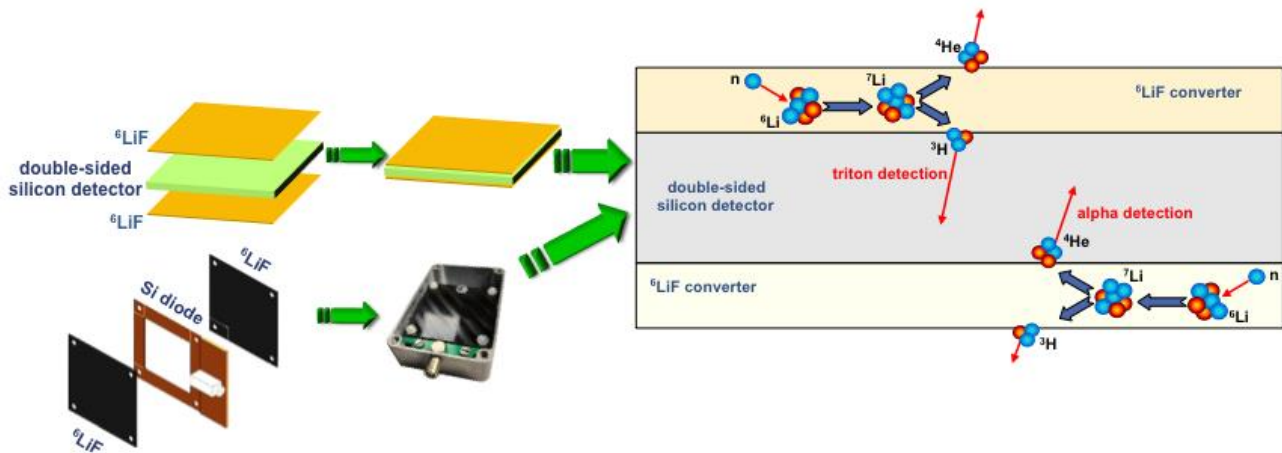


**Figure 17.** Structure and operating principle of the SiLiF neutron counter.



**Figure 18.** Left: sketch of the SiLiF detector (in yellow) and its arrangement inside the moderator (in grey). Center: a SiLiF hosted in a half moderator. Right: final assembly of a SiLiF.

### 3. The smart front-end and read-out electronics

The front-end and data acquisition electronics currently being developed to handle the above mentioned sensors consists of two boards, namely G and N boards for gamma and neutron sensors respectively, hosted as piggyback on the W motherboard. Each W+G+N board assembly will handle a SciFi+SiLiF sensor pair. A drawing of the prototype W board and a photo of the G-board are shown in **Figure 19**, and a simplified sketch illustrating the operational configuration is shown in **Figure 20**. The electronics has the following main features:

- low cost;
- low power consumption;
- modularity;
- scalability;
- compactness;
- reconfigurability due to its on-board microcontroller;
- GPS, temperature sensors, external sensors;
- SD memory card;
- stand-by sleep mode with remote wake-up;
- easy remote set-up and control;
- wired and/or wireless connections.



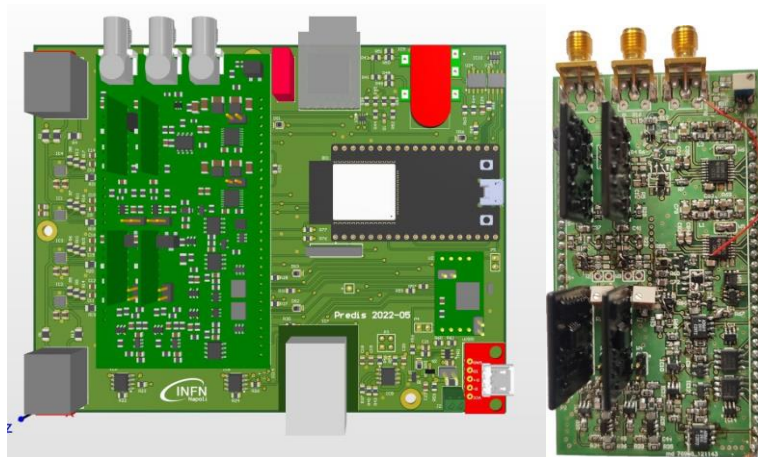


**Figure 19.** Front-end and data acquisition electronics. Left: design of the W-board. Right: the G-board.

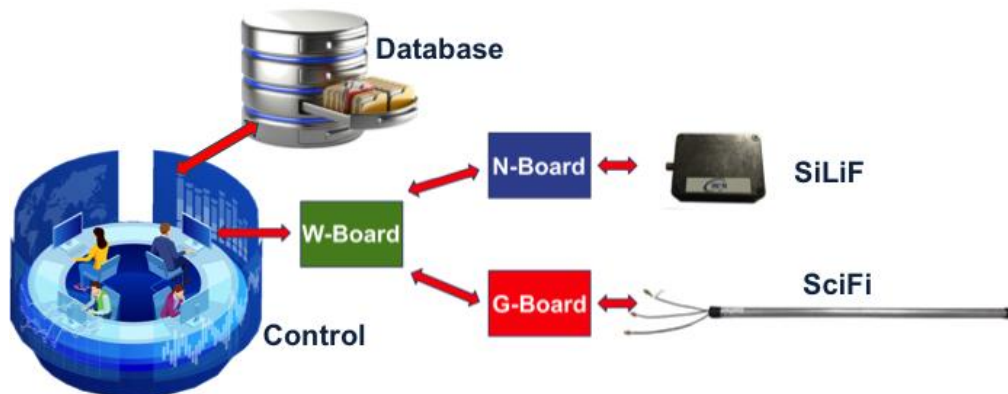


**Figure 20.** A simplified sketch illustrating the operational configuration of the monitoring system.

## 4. Discussion

Both SciFi and SiLiF technologies to detect gamma rays and thermal neutrons have been extensively tested and have shown quite promising performance in view of a possible solution for the radwaste drum monitoring. The electronics being currently finalized was designed on the basis of the experience acquired during the tests done in the previous years with the proposed detectors and traditional electronics. The capability to detect possible cracks in the concrete matrix by means of the proposed monitor detectors was the subject of a preliminary simulation done with the FLUKA code [0]. A steel cylinder was simulated, 1 cm thick, 29 cm radius, 80 cm high, filled with portland concrete. The thickness was purposefully exaggerated with respect to the 3 mm usual one. A smaller inner concrete cylinder, 15 cm radius, 40 cm high, was assumed to contain also  $^{137}\text{Cs}$  or  $^{240}\text{Pu}$  homogeneously distributed, respectively emitting 662 keV gamma rays ( $10^6/\text{s}$ ) or spontaneous fission high energy neutrons ( $10^5/\text{s}$ ). A missing part of the concrete, 1cm x 15cm x 30cm filled with air, was meant to simulate a crack. As a result a slight counting rate asymmetry appears around the crack, both for gamma rays and neutrons, indicating that the proposed detectors should be able to detect it.

In order to perform some more realistic tests, in the coming months a mock-up cemented drum is going to be built by UJV (Prague), according to the preliminary scheme of **Figure 21**, that will make possible to insert radioactive sources in different positions and emulate a few different cracks. Four SiLiF+SciFi pairs of detectors will be installed around the drum using a lightweight aluminum frame assembled using modular Bosch Rexroth profiles, as shown in **Figure 22**.

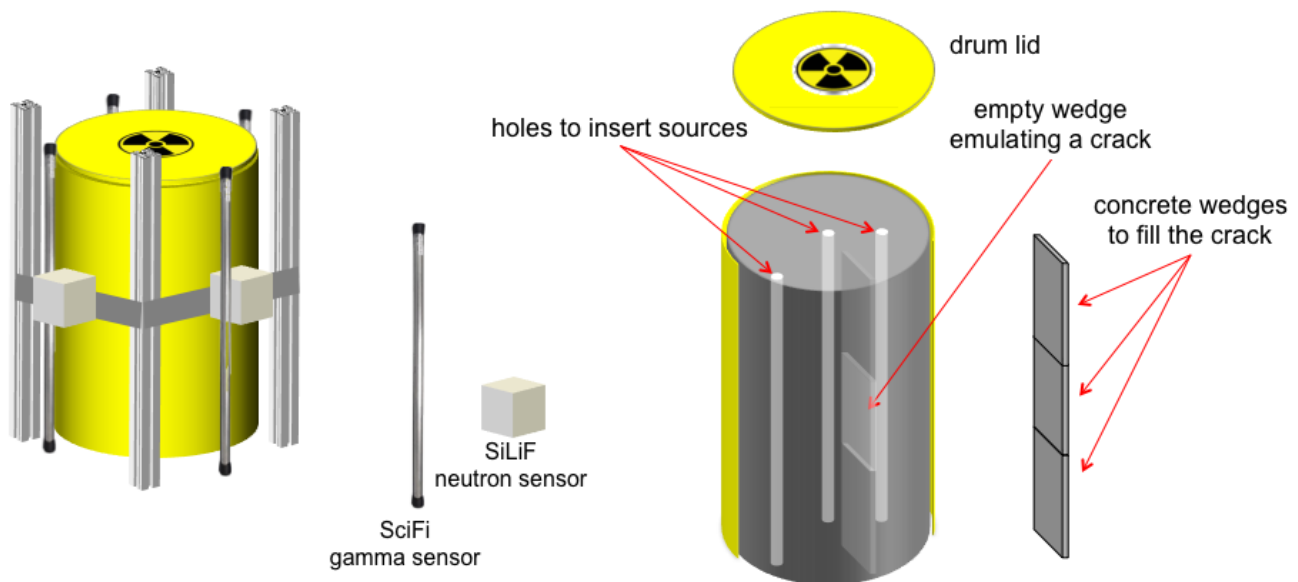


**Figure 21.** Preliminary sketch of a mock-up cemented drum that is going to be built by UJV (Prague). It will make possible to insert radioactive sources at various heights and positions and emulate a few different cracks.



**Figure 22.** The lightweight aluminum frame to support the SiLiF and SciFi sensors around the mock-up drum, assembled using modular Bosch Rexroth profiles.

## 5. Conclusions

Our activity so far performed in WP7 aims at developing new external radiological monitoring technologies to demonstrate store and package quality assurance. Two sensor types, SciFi for gamma rays and SiLiF for neutrons, are quite promising to monitor radwaste drums, in particular but not exclusively cemented radwaste. A compact, low power electronics, featuring wireless connection, is going to be completed. During 2022 the sensors, and their electronics currently being finalized, will be tested with laboratory radioactive sources at LNS. Afterword tests with sources in a cemented mock-up drum currently being developed at UJV will be done in Prague. New simulations will be performed with the final geometry of the cemented mock-up, to help evaluating the foreseen sensitivity of the monitoring system to assess the integrity of radwaste drums.

## Acknowledgements

We thank Paolo Di Meo and Antonio Pandalone of the SER electronics laboratory of INFN Napoli for their endeavor in the design and development of the electronic boards.

## References

1. L. Cosentino, Q. Ducasse, M. Giuffrida, S. Lo Meo, F. Longhitano, C. Marchetta, A. Massara, A. Pappalardo, G. Passaro, S. Russo, P. Finocchiaro, SiLiF Neutron Counters to Monitor Nuclear Materials in the MICADO Project. *Sensors* 2021, 21, 2630, doi:10.3390/s21082630.
2. L. Cosentino, M. Giuffrida, S. Lo Meo, F. Longhitano, A. Pappalardo, G. Passaro, P. Finocchiaro, Gamma-Ray Counters to Monitor Radioactive Waste Packages in the MICADO Project. *Instruments* 2021, 5, 19. DOI:10.3390/instruments5020019.
3. P. Finocchiaro, DMNR: A new concept for real-time online monitoring of short and medium term radioactive waste. In *Radioactive Waste: Sources, Types and Management*; Nova Science Publishers: New York, NY, USA, 2011; pp. 1–40.
4. P. Finocchiaro, Radioactive Waste: A System for Online Monitoring and Data Availability. *Nucl. Phys. News* 2014, 24, 34.
5. L. Cosentino, C. Calì, G. De Luca, G. Guardo, P. Litrico, A. Pappalardo, M. Piscopo, C. Scirè; S. Scirè; G. Vecchio, E. Botta, P. Finocchiaro, Real-Time Online Monitoring of Radwaste Storage: A Proof-of-Principle Test Prototype. *IEEE Trans. Nucl. Sci.* 2012, 59, 1426–1431.
6. P. Finocchiaro, M. Ripani, Radioactive Waste Monitoring: Opportunities from New Technologies. In *Proceedings of the IAEA International Conference on Physical Protection of Nuclear Material and Nuclear Facilities*, IAEA-CN-254/117, Vienna, Austria, 13–17 November 2017.
7. A. Fasso, A. Ferrari, J. Ranft, P.R. Sala, FLUKA: A Multi-Particle Transport Code; CERN Technical Report No. INFN/TC\_05/11; CERN-2005-10; 2005.

## 7.2 First test of the detection of metal bodies in concrete matrix using the INFN Padova Muon Tomography apparatus

*Paolo Andreetto, INFN Padova, Via Marzolo 8, Padova, Italy*

*Paolo Checchia, INFN Padova, Via Marzolo 8, Padova, Italy*

*Enrico Conti, INFN Padova, Via Marzolo 8, Padova, Italy, email: [enrico.conti@pd.infn.it](mailto:enrico.conti@pd.infn.it)*

*Franco Gonella, INFN Padova, Via Marzolo 8, Padova, Italy*

**Keywords:** Muon Tomography; cemented drums; metallic waste; detection and visualization

Muon Tomography is a powerful technique to detect and visualize dense and heavy materials hidden inside a less dense medium. It is the case, for example, of metal pieces (with density similar or greater than iron) cemented in a concrete drum, as radiative waste confinement.

Muon Tomography exploits the natural flux of cosmic ray muons. Muons are highly penetrating particles which can traverse large amount of dense material without being absorbed. On the opposite, they are deflected (by the Coulombian multiple scattering) from their initial trajectory and that deflection is the measured quantity that allow us to reconstruct the density map of the body.

In INFN Padova we have developed an apparatus composed by two drift wire chambers (spare Muon chambers of the CERN CMS experiment) which define a useful inspection volume of almost 5 m<sup>3</sup> (see Fig.1).

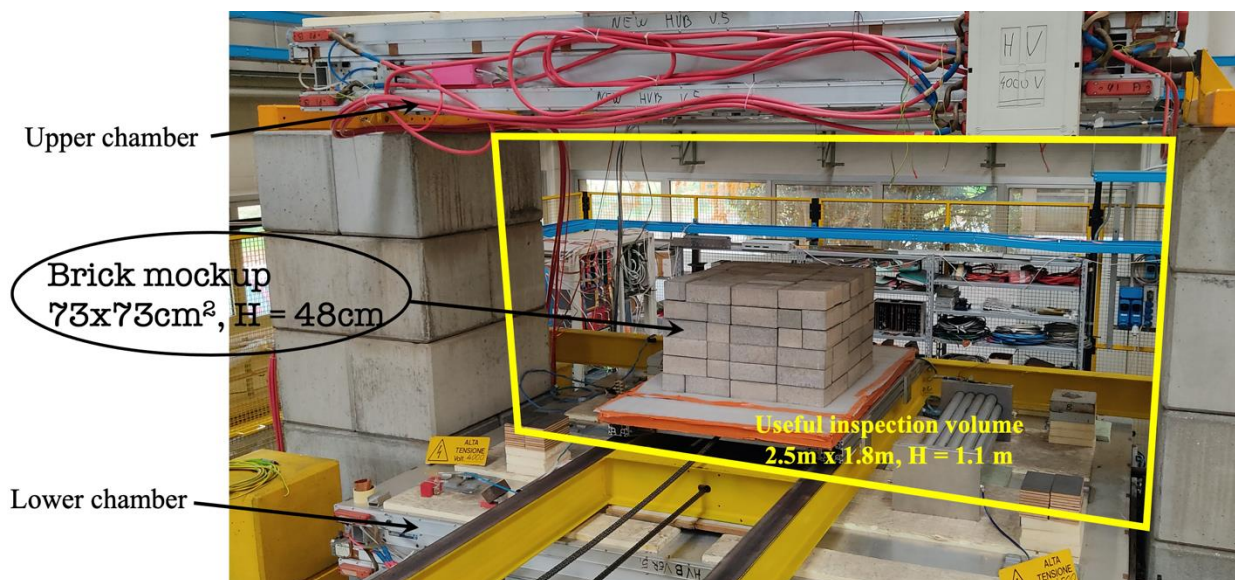


**Fig.1.** Photo of the INFN Padova experimental apparatus for Muon Tomography. The concrete cuboid used for the test is also present.

As preliminary test of the technique for detecting and visualizing metal piece in a concrete matrix, we made some concrete bricks, about 1 l volume, with metal pieces embedded in, with different shape, dimension, and material (hereafter “special bricks”). Metals were iron, stainless steel, lead, and tungsten.

Using pure concrete bricks, we built a concrete cuboid of dimension 73x73x48 cm<sup>3</sup> (total volume 0.26 m<sup>3</sup>) placing the special bricks in random, but known, positions in the brick matrix. A total of 9 metal pieces were hidden, with dimensions down to 1-2 cm. The goal of the test was to detect the presence of the metal pieces, and visualize them in the correct place.

We collect data for a time equivalent to 116 hours (4.8 days) continuative data taking.

A 3D offline reconstruction of the data was performed using the analysis techniques that the INFN Padova group has developed since long time (see for example [1] and references therein). An example of the result of the data analysis is shown in Fig.2.

The result was positive. All piece could be detected, although a few of them with a low signal-to-noise ratio. In particular, the higher density metals (lead and tungsten) are easily detected and visualized, while discovery and discrimination power for stainless steel and iron bodies is limited by the statistics (i.e., acquisition time). It

is to note that the apparatus is not optimized for the vertical coordinate, which is determined with a lower resolution than the horizontal plane.

This test confirms the effectiveness of Muon Tomography technique to inspect cemented drums, to identify and visualize high-density and high-atomic number bodies, down to dimensions of 1-2 cm.

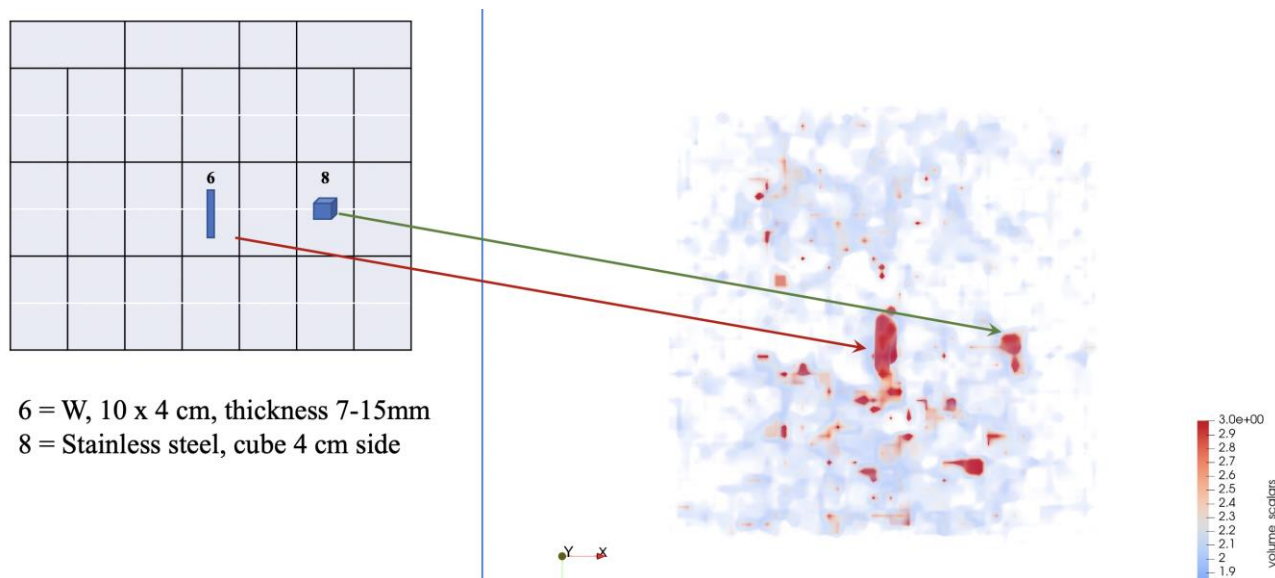


**Fig.2.** An example of the result of the offline data analysis.

On the right side, in false colour, the intensity of the signal in the horizontal plane for a selected slice of the concrete cuboid, equal to the brick height: red = high signal; cyan = low signal; white = no signal.

On the left side, a sketch of the position of the tungsten and stainless steel pieces, which are clearly detected and correctly displayed by the Muon Tomography.

## References

- [1] P. Checchia et al., “INFN muon tomography demonstrator: past and recent results with an eye to near-future activities”, (2018) Phil. Trans. R. Soc. A377: 20180065  
<http://doi.org/10.1098/rsta.2018.0065>



## 7.3 Demonstration and implementation of monitoring technologies

*Yasmine HELAL, Orano, France, [Yasmine.helal@orano.group](mailto:Yasmine.helal@orano.group)  
 Sabah BEN LAGHA, Orano, France, [sabah.ben\\_lagha@orano.group](mailto:sabah.ben_lagha@orano.group)  
 Coralie ChAPUZET, France, [coralie.chapuzet@orano.group](mailto:coralie.chapuzet@orano.group)*

### Abstract

During the PREDIS Workshop, we have presented the progress related to task 7.6 and explored the options in regards with conducting the demonstration test. This option related first to the package/ mock-up which will be the main subject of the test, second to the location of the demonstration test and finally to the technologies that will be selected based on the comparative table.

**Keywords:** Demonstration, Mock-up, Technologies, Comparative table

### 1. Introduction

This document describes the task 7.6 demonstration work, which is prepared with three major components:

- Firstly, select the technologies to be tested using the comparative table and it's follow up work.
- Secondly, identify different packages options for the demonstration work.
- Lastly, identify the location of the test

### 2. Description of work and main findings

#### • The comparative table

The comparative table has been sent to all WP7 partners. As a reminder, this table is based on a list of criteria which will be considered to compare all non destructive technologies developed in WP7.3

Among this list, it's important to mention: Technical performance, Safety/security, Cost and planning (including procurement, fabrication, exploitation and dismantling), Operability. The comparative table will give us first information on each technology and will be revised and updated in 2023 to integrate new developments related to technologies.

#### • Mock-up / Real waste package

We have identified three packages options for the demonstration test:

- End-User (E.U) Old Mock-up: 27 years Magnox mock-up (non-radioactive)
- Two Mock-up created by UJV as part of task 7.3 (non-radioactive and radioactivity simulation)
- UJV Real waste package (double skin package).

#### • Test Location / Possible options regarding test location:

Demonstration task should be held in a realistic environment, it could either be real storage or a non active environment. In case, we will hold the demonstration task in a non active environment, a comparison with a real storage must be carried on to identify similarities and differences. So, we will collect information from End-User real storage and compare these real storage facilities with non active test environment.

A storage template which summarizes the main characteristics describing the End-User storage. Each E.U. partner will fill in this template depending on their storage facilities.

This template will be considered for the selection of the demonstration test location.

The Storage template has been sent To WP7 End-users (Orano, UJV, SOGIN) and to a non-active environment test location owners (NNL, UJV, Orano).



### **3. Conclusion**

The preparatory steps for the demonstration test in work package 7, task 6 are well advanced. The planning is ahead of schedule and decisions about the final demonstration including used technologies, relevant waste packages and the test location itself are expected to be well in time.